DESIGN, CONSTRUCTION AND TESTING OF A NEW APPARATUS FOR VAPOR LIQUID EQUILIBRIUM STUDIES AT LOW PRESSURES

By

AMIT G. SURA

Bachelor of Engineering

University of Bombay

Bombay, India

1988

Submitted to the Faculty of the
Graduate College of the
Oklahoma State University
in partial fulfillment of
the requirements for
the degree of
MASTER OF SCIENCE
July, 1991

DESIGN, CONSTRUCTION AND TESTING OF A NEW APPARATUS FOR VAPOR LIQUID EQUILIBRIUM STUDIES AT LOW PRESSURES

Thesis Approved:

Robert S. Robinson, Jr.

Thesis Adviser

K. A. M. Gasem

Roland H. Johannes

Norman N. Durham

Dean of the Graduate College

PREFACE

A new apparatus was designed, constructed and tested for vapor-liquid equilibrium studies at low pressures. This complemented the existing facilities for phase equilibrium studies in the School of Chemical Engineering at Oklahoma State University. Initial measurements on three binary mixtures yielded data which met thermodynamic consistency requirements.

I wish to express my sincere gratitude to the individuals who assisted me in this project and during my course work at Oklahoma State University. In particular, I wish to thank my advisors, Dr. Robert L. Robinson Jr. and Dr. Khaled A.M.Gasem, for their intelligent guidance, inspiration, and invaluable aid. I am also grateful to Dr. Arland H. Johannes for serving on my committee.

Financial aid for the course of this study has been gratefully received from the U.S. Department of Energy.

Special thanks are due to my parents, grandparents, Mrs. & Mr. O M. Desai, and uncle, Mr. Kirit Desai, for their constant support, moral encouragement, and understanding.

TABLE OF CONTENTS

LIST OF TABLES

Table Page

LIST OF FIGURES

Figure Page

Figure Page

LIST OF SYMBOLS

Symbol

A1, A2, A3	Antoine equation constants
B	Second virial coefficient
B_{ij}	Second virial cross coefficient
$\bar{B}_i$	Partial virial second coeffcient
f	Fugacity
H	Enthalpy
P	Total pressure
P_i^{sat}	Vapor pressure of component "i"
P_c	Critical pressure
R	Universal gas constant
T	Temperature
T_c	Critical temperature
V	Volume
x	Mole fraction in liquid phase
y	Mole fraction in vapor phase
A(1,2), A(2,1)	Wilson parameters
Z	Compressibility factor
w	Acentric factor

Greek Symbols

γ	Activity coefficient
ø	Fugacity coefficient

ϕ^s	Fugacity coefficient of the pure component at its vapor pressure
μ	Chemical potential

Subscripts

1	Component one
2	Component two
i	Component "i"

Superscripts

E	Excess property
L	Liquid phase property
V	Vapor phase property
sat	Saturation property

CHAPTER I

INTRODUCTION

Vapor-liquid equilibrium data are necessary not only for design of phase separation equipment, but also for developing new methods and theories for describing such data. Even though extensive vapor-liquid equilibrium data exist in the literature, the direct measurement of vapor-liquid equilibrium remains an important source of information concerning the equilibrium properties of fluid mixtures. This is due, in part, to the dubious reliability of much of the existing literature data. In addition, available data may cover pressure and or temperature ranges different from those desired.

In general, when a process for the separation of mixtures of chemicals is to be designed, high accuracy vapor-liquid equilibrium data are indispensable, and in most cases new, reliable and accurate experimental measurements are justified. Measurements on systems composed of substances of known purity in an apparatus capable of producing accurate and reliable measurements often lead to results of high reliability more quickly than the evaluation of available literature data.

The experimental measurement of vapor-liquid equilibrium

has occupied many investigators over the decades. Few scientific fields have produced so many variations of devices for measuring a single property. In spite of this large amount of effort, time and ingenuity, the resulting experimental data have often been disappointing.

In the School of Chemical Engineering at Oklahoma State University, facilities for vapor-liquid equilibrium studies at high pressures exist, but no apparatus designed specifically for low pressure studies is available. Hence, the purpose of this work was to design, construct and test a vapor-liquid equilibrium apparatus to produce thermodynamically consistent data for low pressure (ambient and below) systems. Such an apparatus would provide a valuable complement to the existing capabilities for phase equilibrium studies in the School.

Initial measurements in the new apparatus were made on binary systems formed among the constituents n-hexane, methylcyclohexane and toluene. Binary mixtures of these compounds exhibit molecular interactions between the important hydrocarbon types: alkanes, cycloalkanes and aromatics. Also, many investigators (including the principal advisor for this project) have studied vapor-liquid equilibrium in the above-mentioned systems. Further, these substances have moderate volatilities, are available at high purities, and accurate analysis of phase compositions using the simple principle of refractometry is possible. All these factors were taken into consideration in making the

selection of the above-mentioned compounds for testing the new experimental device.

The following sections of this work describe the design, construction, operation and evaluation of the new low pressure vapor-liquid equilibrium facility.

CHAPTER II

LITERATURE REVIEW

Vapor-Liquid Equilibrium Apparatus

The number of available methods and apparatuses for measurement of vapor-liquid equilibrium is large, and to choose the most appropriate technique is a difficult task. Fortunately, the works of Hala (17) and Malanowski (24) provide excellent descriptions of experimental procedures available for the determination of vapor-liquid equilibria at moderate pressures by circulation methods. Vapor phase circulation and vapor and liquid phase recirculation methods are considered, and critical evaluations are given in those reference works.

The common principle of all circulation methods is the continuous separation of the vapor phase from the liquid phase under steady-state conditions, measurement of the thermodynamic parameters determining the equilibrium state, and then recombination and recirculation of the vapor and liquid streams. In a properly designed still, this technique can give true equilibrium liquid and vapor compositions.

The modified Swietoslawski ebulliometer (as perfected by Malanowski) is an example of a modern dynamic circulation apparatus of good design; Malanowski (33) has developed two

designs. One allows sampling to determine the equilibrium liquid and vapor compositions, x and y (thus providing, with T and P, complete data sets). Another simpler apparatus has no such sampling provisions; in this case, equilibrium liquid compositions are determined from overall compositions via material balance and equilibrium equations. The data set (P, T, x) in this case is incomplete. The former case, in which all the parameters are known, provides adequate information to facilitate testing the data for thermodynamic consistency.

The design of Malanowski and coworkers fulfils the conditions required for a properly designed recirculating still (17, 24). The Malanowski design is shown in Figure 1. Advantages of Malanowski's design are stated to be the following; (1) stable hydrodynamic and thermal conditions under pressures from 200 to 1000 mm Hg and from room temperature to 500 K, and (2) the compositions of the liquid and vapor streams leaving the equilibrium chamber remain constant (within the accuracy of composition measurements) until the streams have passed through the sample chambers, and they correspond to thermodynamicaly consistent values of pressure and temperature (within the accuracy of temperature measurements and pressure stability).

The still in Figure 1 operates as follows. The mixture boils in an electrically heated container, H_1. Powdered glass is sintered on the inside walls of this container, providing nucleation sites to obtain steady boiling. The vapor generated provides gas lift via a Cotrell pump, W, and

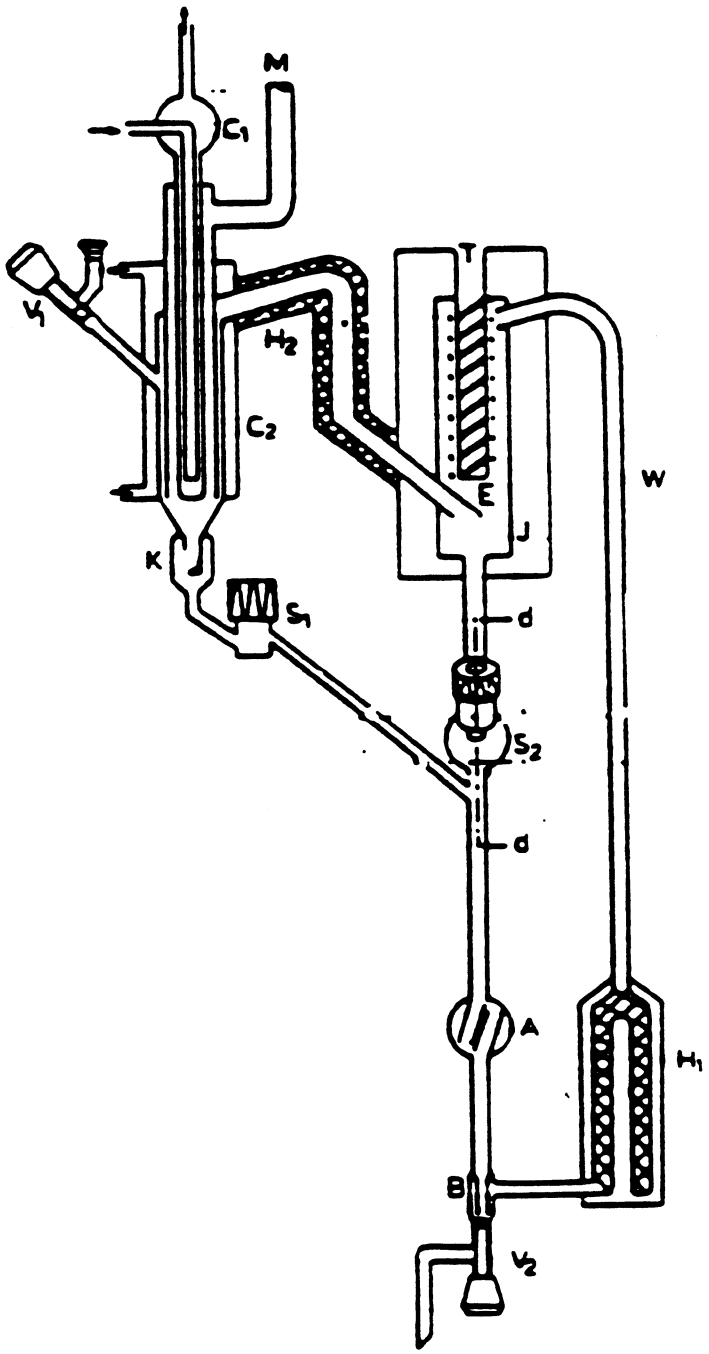

Figure 1. Malanowski Vapor-Liquid Equilibrium Still (33)

the continuous stream, consisting of vapor and superheated liquid, is delivered into the equilibrium chamber, E. This stream empties onto a thermometer well, T. The equilibrium chamber is placed inside a vacuum jacket, J, in order to minimize heat losses. The liquid and vapor streams separate in the equilibrium chamber, E. The vapor stream leaves E through a large bore tube leading to a condenser, where it is totally condensed. This large bore is heated by heater, H_2, to slightly above the equilibrium temperature to prevent partial condensation and refluxing, which may affect the composition of the condensate leaving the condensers, C_1 and C_2. This heating is unnecessary when vapor condensate samples are not withdrawn. The vapor is totally condensed, and the condensate cooled in the condenser. The condensate then flows through a drop counter, K, and condensate container, S_1, to a mixing chamber, A, where it is mixed with the liquid flowing from the equilibrium chamber, E, via the liquid container, S_2. Good mixing is very important to minimize boiling temperature fluctuations. The still is equipped with two mixing devices, A and B. The mixed stream of uniform composition reenters the heated chamber, H_1, where it is partly evaporated, thus completing the recirculation cycle.

Thermodynamics of Phase Equilibrium

The thermodynamic treatment of multicomponent phase equilibria is based on the concept of the chemical potential

(29). Two phases are in thermodynamic equilibrium when the temperature and pressure of one phase are equal to that of the other and when the chemical potential of each component is identical in the two phases.

For engineering purposes, the chemical potential is an awkward quantity. A physically more meaningful quantity, equivalent to chemical potential, can be obtained by simple transformation; the result of this transformation is a quantity called fugacity, which has units of pressure. For convenience, it is easy to think of the fugacity as a thermodynamic pressure since, in a mixture of ideal gases, the fugacity of a component is equal to its partial pressure. In real mixtures, the fugacity is sometimes viewed as a partial pressure, corrected for nonideal behavior.

For vapor (superscript V) and a liquid (superscript L) phases, at the same temperature, the equation of equilibrium for each component i, is expressed in terms of the fugacity f_i (29):

$$f_i^V = f_i^L \qquad (2\text{-}1)$$

The fugacities in Equation 1 are related to experimentally accessible quantities x, y, T, P (as explained below), where x = mole fraction in the liquid phase,

y = mole fraction in the vapor phase,

T = absolute temperature, assumed to be same for both phases,

P = total pressure, assumed to be same for both phases.

The desired relationship between fugacities and experimentally measured quantities is facilitated by the use of two auxiliary functions, namely the fugacity coefficient, ϕ_i, which relates the vapor phase fugacity f_i^V to the mole fraction, y_i, and to the total pressure, P, and the activity coefficient, γ_i, which relates the liquid phase fugacity, f_i^L, to the mole fraction, x_i, and to a standard state fugacity, f_i^{oL}.

$$\phi_i \equiv f_i^V / y_i P \qquad (2\text{-}2)$$

$$\gamma_i \equiv f_i^L / x_i f^{oL} \qquad (2\text{-}3)$$

From Equations 1-3, the equation of equilibrium for any component i becomes,

$$\phi_i y_i P = \gamma_i x_i f_i^{oL} \qquad (2\text{-}4)$$

Details regarding the fugacity coefficient and activity coefficient are given below.

The Fugacity Coefficient

The fugacity of a component in a vapor phase is usually related to the volumetric properties of that phase through the use of an equation of state. At low or moderate pressures, a suitable equation of state is the virial equation truncated after the second term (1).

$$Z = Pv/RT = 1 + BP/RT \qquad (2\text{-}5)$$

where v is the molar volume, P is the total pressure, T is

the absolute temperature and R is the gas constant; B is the second virial coefficient which depends on temperature and composition but is independent of pressure. For a system containing m components, the composition dependence of B is given by

$$B = \sum_{i=1}^{m} \sum_{j=1}^{m} y_i y_j B_{ij} \qquad (2\text{-}6)$$

where $B_{ij} = B_{ji}$ and y is the mole fraction. For a binary mixture,

$$B = y_1^2 B_{11} + 2y_1 y_2 B_{12} + y_2^2 B_{22} \qquad (2\text{-}7)$$

where B_{ij} depends only on the temperature and on the identity of components i and j. In this work, the second virial coefficient for pure component, B_{ii}, and cross coefficient, B_{ij}, were estimated using the correlation of Tsonopoulos (41).

The fugacity coefficient, ϕ_i, may be calculated from the thermodynamic relation (1)

$$\ln \phi_i = \int_0^P \frac{\bar{Z_i} - 1}{P} dp \qquad (2\text{-}8)$$

where,

$$\bar{Z_i} = P\bar{v_i}/RT = 1 + P\bar{B_i}/RT \qquad (2\text{-}9)$$

where $\bar{B_i}$ is the partial molar virial coefficient, and the expression for $\bar{B_i}$ is (1)

$$\bar{B}_i \equiv \left[\frac{\partial(nB)}{\partial n_i}\right]_{T,n_j} \qquad (2\text{-}10)$$

$$= -B + 2\sum_i y_j B_{ij}$$

When Equations 6, 9 and 10 are substituted into Equation 8, we obtain,

$$\ln \phi_i = \left[2\sum_j^m y_j B_{ij} - B\right] P/RT \qquad (2\text{-}11)$$

Equation 11, applicable at low or moderate pressures, is used in this work to describe the behavior of the vapor mixtures.

The Activity Coefficient

In a liquid mixture, activity coefficients are directly related to the molar excess Gibbs energy, g^E, by the relation (29)

$$g^E = RT \sum_i x_i \cdot \ln \gamma_i \qquad (2\text{-}12)$$

A mathematical model for γ_i, preferably based on molecular considerations, can provide a convenient method for expressing g^E as a function of x. There are many activity coefficient functions proposed in literature. Systems of the type studied in this work can be adequately represented by two parameter equations, such as those of Van Laar, Wilson, etc. (1, 29).

The Wilson model has been shown in the literature (12) to fit data well for systems of the type studied in the present work; hence, the Wilson model was used extensively in this study.

For a binary mixture, the Wilson and Van Laar equations for correlation of liquid phase activity coefficients are:

Wilson:

$$\ln \gamma_1 = -\ln (x_1 + A_{12} x_2) + x_2 \left[\frac{A_{12}}{x_1 + A_{12} x_2} - \frac{A_{21}}{x_2 + A_{21} x_1} \right] \qquad (2\text{-}13)$$

$$\ln \gamma_2 = -\ln (x_2 + A_{21} x_1) - x_1 \left[\frac{A_{12}}{x_1 + A_{12} x_2} - \frac{A_{21}}{x_2 + A_{21} x_1} \right] \qquad (2\text{-}14)$$

Van Laar:

$$\ln \gamma_1 = \frac{A_{12}}{\left[1 + \frac{x_1 A_{12}}{x_2 A_{21}} \right]^2} \qquad (2\text{-}15)$$

$$\ln \gamma_2 = \frac{A_{21}}{\left[1 + \frac{x_2 A_{21}}{x_1 A_{12}} \right]^2} \qquad (2\text{-}16)$$

The activity coefficient is completely defined only if the standard-state fugacity is specified clearly. The choice of standard state for f_i^{0L} is dictated by convenience. In this work, f_i^{0L} is taken as the fugacity of pure component

i at the same temperature and pressure as that of the solution.

The standard state fugacity can be written as (29),

$$f_i^{0L} = P_i^{sat}\phi_i^{s} \exp \int_{p_i^{sat}}^{p} (V_i^{L}/RT)\, dp \qquad (2\text{-}17)$$

where ϕ_i^{s} is the fugacity coefficient of the pure component at its vapor pressure, P_i^{sat} is the vapor pressure, and V_i^{L} is the liquid molar volume of the pure component. The integral term is negligible at low pressures and was ignored in our calculations.

From Equation 4, the following equation can be written

$$Py_i = \frac{x_i \gamma_i f_i^{0L}}{\phi_i} \qquad (2\text{-}18)$$

For a binary mixture, by summing Equation 2-18 for components 1 and 2, the following expression is obtained:

$$\frac{x_1 \gamma_1 f_1^{0L}}{\phi_1} + \frac{x_2 \gamma_2 f_2^{0L}}{\phi_2} = P \qquad (2\text{-}19)$$

Reliable estimates of the parameters in an activity coefficient correlation (e.g., A_{12} and A_{21} in the Wilson equation) can be obtained from a series of vapor-liquid equilibrium data (T, P, x and y). Because the number of data points exceeds the number of parameters to be estimated, the equilibrium equations are not satisfied for all experimental measurements. The optimum parameters are therefore found by satisfying some statistical criterion. For this work, least-

squares fit to bubble point pressure was used to determine the parameters for the liquid models used. The application of the techniques described above appears in Chapter V.

CHAPTER III

EXPERIMENTAL APPARATUS

In order to develop a reliable apparatus for accurate vapor-liquid equilibrium measurements at low pressure, the ebulliometer of Malanowski et al. (33) was modified in this work. The major components, along with the arrangement of the apparatus, are described below.

Arrangement of Apparatus

Figure 2 shows an overall schematic diagram of the experimental setup. The equilibrium still was clamped to an aluminum frame and connected through the condenser to a manifold. A platinum resistance thermometer was inserted into the separation chamber of the still through a threaded fitting with an "O" ring seal.

The regulated pressure supply line of a pressure controller was connected to the manifold. The pressure supply and the vacuum supply were also connected to the controller. A recorder was connected to the thermometer readout unit at the rear panel. A heating tape was wound around the reboiler, with heat input controlled by a variac. A magnetic stirrer was placed below the holding chamber upstream of the reboiler and the other was clamped to the

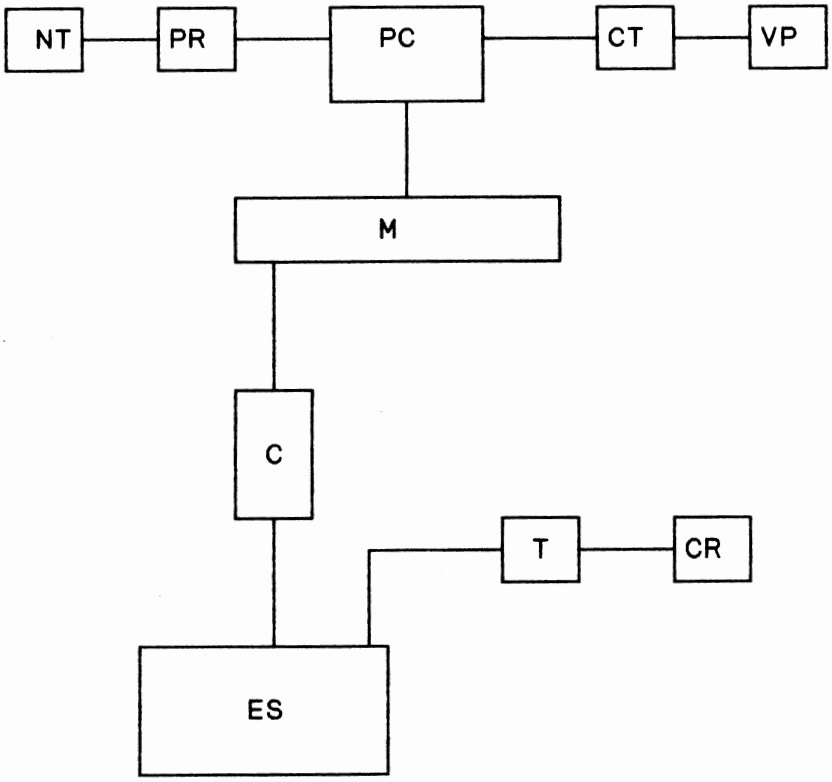

NT - NITROGEN TANK
PR - PRESSURE REGULATOR
PC - PRESSURE CONTROLLER
CT - COLD TRAP
VP - VACUUM PUMP
M - MANIFOLD
C - CONDENSER
ES - EQUILIBRIUM STILL
T - THERMOMETER
CR - CHART RECORDER

Figure 2. Overall Sketch of Experimental Setup

aluminum frame and positioned below the vapor sampling port.

Equilibrium Still

Equilibrium was attained in an all glass equilibrium still with circulation of both vapor and liquid phases. Figure 3 shows the still, as modified. General features of the still are based on the Malanowski design. However, the design used in the present study differs from Malanowski's (discussed in the previous section and illustrated in Figure 1) in several respects, including the following.

1. The thermowell was removed and direct contact of the equilibrium mixture with the thermometer was used in this study since it was observed that with different conducting oils in the thermowell (used as a conducting medium between the equilibrium chamber and the thermometer) led to differences in the observed temperature at a fixed controlling pressure; hence, direct contact of the equilibrium mixture with the thermometer, B, was used in this study.
2. The volume of the vapor sampling chamber was reduced from 25 cc to approximately 10 cc, so that the hold-up time of vapor condensate is shortened, and hence the time to reach steady state was decreased to approximately 12-15 minutes for the apparatus used in this study.
3. Capillary tubing was used for the return line for vapor condensate, further reducing the hold-up of condensate.
4. A separation cup, G, with splash guard, H, was introduced,

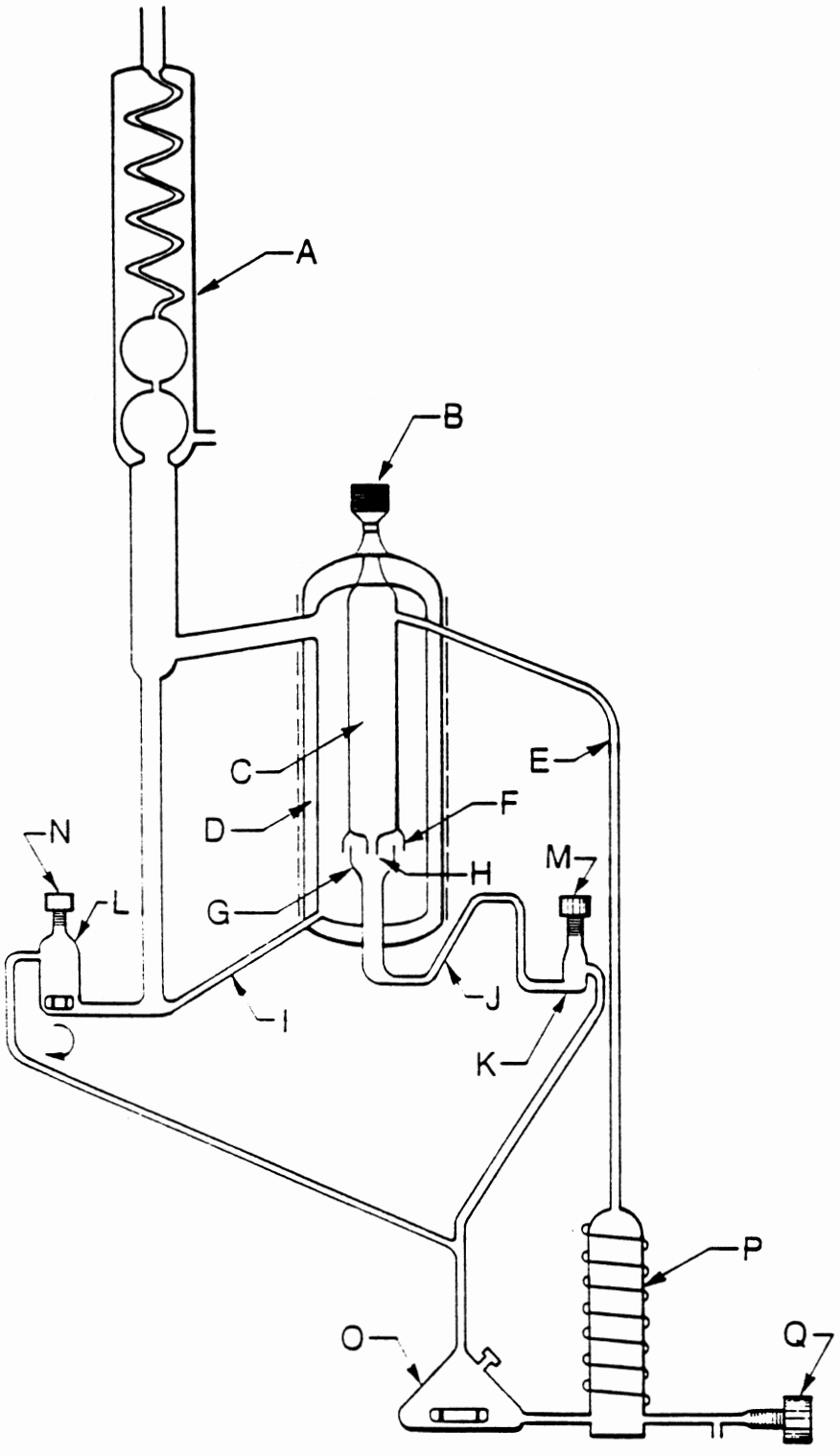

Figure 3. Modified Vapor-Liquid Equilibrium Still

This gives intimate contact of liquid and vapor during separation. The function of splash guard, as the name implies, is to prevent any vapor which might condense on the outer surface of C from dripping into the liquid in cup G.

5. The vapor outlet to the condenser was moved from the bottom to the top of the equilibrium chamber. Thus, the vapors, while passing to the condenser, bathed the outside of the phase separation chamber, C, and reduced heat losses from C by keeping the outer wall of C at the equilibrium temperature.
6. A tube, I, was introduced to provide a means for any vapor which might be partially condensed on the inner wall of D or outer wall of C from collecting in the bottom of the equilibrium chamber.
7. The vapor sample chamber, L, was provided with a stirrer to insure uniform composition of the mixed condensate streams from the condenser and from tube, I. (The liquid sample chamber, K, did not require a stirrer since it is fed by a single stream and the flow rate of recirculating liquid is much higher than that of vapor condensate.
8. A holding chamber, O, with a magnetic stirrer, was introduced so that the recombined condensed vapor and liquid streams were thoroughly mixed before being fed to the reboiler, P.
9. External heating was used since it was found to produce smoother boiling than did internal heating.

The condenser in this design has two spherical enlargements in the lower section where 80 to 90 percent of the condensation takes place.

Dimensions of the equilibrium still are as follows:

Equilibrium still: Height = 24 in., Diameter = 12 in.

Equilibrium Chamber: Height = 10 in., Diameter = 3.4 in.

Boiler: Height = 5 in., Diameter = 1 in.

Cotrell tube: Height = 13 in.,

Diameter = 7mm o.d, 5 mm i.d

Liquid Return leg: Length = 9 in.,

Diameter = 8 mm o.d, 5 mm i.d

Vapor condensate return leg:

Length = 7 in.,

Diameter = 6 mm o.d, 2 mm i.d

Liquid sampling chamber:

Height = 0.8 in.,

Diameter = 14 mm

Vapor sampling chamber: Height = 0.8 in,

Diameter = 25 mm

Condenser: Jacket Height = 13 in.

Jacket Diameter = 35 mm

The condenser as well as equilibrium still was assembled by the scientific glass blower, Mr. Tom Denton, of the OSU Chemistry Shop.

Platinum Resistance Thermometer

The temperature of the equilibrium mixture was measured

in the disengagement zone using an Hart Scientific thermometer (Model 1506) with matching resistance temperature detector (RTD), Model 5614.

The resistance temperature detector is 12 in. long and 0.25 in. o.d.. The element is constructed of reference grade platinum wire (99.999 % pure) for excellent stability. The wire is wound in a coil and placed in a mandrel where it is uniformly supported in a strain free manner to eliminate hystersis. The mandrel is surrounded by a SS316 sheath for rigidity. The temperature range of the thermometer is -183°C to 480°C with a resistance stability of ±0.01°C at 0.00°C. For stability of the readings, the probe immersion should be between 4 inch and 10 inch. In this work an immersion of approximately 6 inches was used.

The thermometer measures resistance and displays temperature with high resolution and speed. The accuracy of the digital thermometer is ± 0.005°C over the range -180°C to 650°C; however, the system error was ± 0.03°C with the probe used in this work. The instrument has a repeatability of ± 0.005°C at ambient operating temperatures of 10°C to 40°C.

Dual input channels for two-probe work, minimum and maximum temperature recall, and analog output are standard features of the thermometer display unit. Front panel buttons allow the user to select from five digital read out scales (°C, °F, K, R or Ohms), thus eliminating the need for conversion tables; however, only the celcius scale was used

in this work. Front panel switching also allows the user to select probe 1 and probe 2 for differential thermometry applications; however, only the probe 1 or probe 2 mode was used in this work.

The resolution is 0.001 on all scales at 1 second sample intervals, 0.0001 on all scales at 5 or 10 second intervals and 0.00001 all scales at 100 second sample intervals. The medium resolution of 0.0001 with 10 second sample time was used in this work.

The thermometer was checked by measuring the ice point temperature, which was observed to be 0.01 °C. Further, the boiling point distilled water was also measured and observed to be 99.99°C.

Pressure Controller

A Texas Instrument Precision Pressure Test Set (Model 156) was used to control the pressure. This unit is capable of both reading and regulating pressure. The operation of the unit is based upon a fused quartz Bourdon capsule. In the Model 156, an absolute pressure Bourdon capsule is installed.

There are three different modes of operation available: Manual Gage, Servo Gage, and Servo Control. In the present study, only the Servo Control mode was used. In this mode, the counter reading is manually adjusted to correspond to the desired controlled pressure. The error signal from the amplifier drives a pressure regulator. The regulator output

pressure line is connected to the Bourdon capsule and the Regulated Pressure Output fitting.

The plumbing of the Test Set contains three fittings. The first fitting was connected to about 0.25 ft of stainless steel tubing and then through a vacuum hose to a vacuum pump. The second fitting was connected in a similar manner to the pressure supply source. The third fitting was connected directly to the Bourdon capsule and contained the regulated pressure. This fitting was connected to the manifold (which is described later in this section).

The pressure supply can be dry air, nitrogen or equivalent inert gas. In the present work, chromatographic nitrogen was used, as it is of very high purity (99.995%). The pressure at the pressure supply source should be set at 1.2 times the desired regulated pressure, using a pressure regulator at the output of the gas tank. The pressure range of the test set is 0 to 1000 mm Hg and the control accuracy, i.e., the regulated pressure output versus counter reading is 0.002% of full scale (or 0.02 mm Hg in the present case).

The Test Set is capable of providing output signals at the rear panel for recording purposes, but this feature of the Test Set was not used in the present work.

The pressure set was calibrated against a newly calibrated Pressure Test set from Texas Instrument Inc.; details are given in Appendix A.

Vacuum Pump

A Sargent-Welch Duo Seal vacuum pump (Model 1400) was used. The vacuum pump was connected to a cold trap which was in turn connected to the vacuum supply port of the pressure controller. In the cold trap, ice was used as a safety measure, in case the cooling water supply to the condenser was turned off, the ice trap will keep vapor from the equilibrium cell from entering the pressure regulator (and hence the Bourdon capsule). The vacuum pump was necessary to regulate pressures by bleeding nitrogen from the assembly.

Manifold

The equilibrium still was connected through the condenser to a manifold using sealed glass ball joints, "O" ring seals, and pinch clamps. The regulated pressure was connected to the top of the manifold through a needle valve. The glass manifold has a diameter of a 3 in. and a length of 18 in. The manifold was used to provide a large volume which dampened pressure fluctuations.

Refractometer

All samples were analyzed using a Bausch & Lomb refractive index meter (Model 33-45-03, Series 945) on which scale readings can be made to two decimal places (XX.XX). The readings were reproducible to ±0.01. The refractometer plates were maintained at 25.00 ±0.05°C using a water bath

with an Haake temperature controller (Model FP). The range of the refractometer used was 1.32975 to 1.63448 with corresponding scale readings of 0.00 to 72.00 for sodium lamp. The accuracy of reading is of the order of 0.00003 refractive index units.

Chart Recorder

A Houston Instrument OmniScribe Model D5000 recorder was used to record the measured temperatures. On the front, it has three control knobs to position the recorder pen to a desired zero position, a five-position rotary switch to select the full scale voltage range, a two-position toggle switch to raise and lower the pen, and a chart speed selector, calibrated in cm/min and inch/min. Speed could be varied from 0.042 cm/min to 25 cm/min. The speed of 0.25 cm/min was used. Temperature fluctuations as small as 0.001°C could be seen clearly in the recorder output.

Heat Input

Heat was supplied to the reboiler by a heating tape from Thermolyne Corporation (width 1 in., length 4 ft., 418 watts, 120 volts, Catalog Number BOO101040) which was wrapped around the reboiler, and the amount of heat input was controlled by a variac. The heating tape was wrapped beginning about one inch above the base of the reboiler, since it was observed that, if wrapping was below that point, the heated mixture would flow backward into the line connecting the mixing

chamber to the reboiler. The above precaution prevented this back mixing.

Sampling

Sampling was done with two 1.0 cc hypodermic gas tight syringes (Hamilton Gas Tight Syringe, Catalog Number 1001LTSN, 81314). Samples were taken by insertion of the syringes in the sample ports. The septa used on the ports for sampling were rubber on one side and teflon on the other, with teflon facing the hot side to prevent any reaction with hot organic fluids. The septa were purchased from Supelco, Inc. (Catalog Number 2-2731).

Chemicals

All chemicals used were purchased from Aldrich Chemical Company. The manufacturers specifications were:

Hydrocarbon	Purity (mole %)
n-Hexane	99 +
Methylcyclohexane	99 +
Toluene	99.9 +

No further purification of the hydrocarbons was attempted.

Magnetic Stirrer

Two Cole-Palmer Micro-V magnetic stirrers (Model 4805-00) were used. One was used for mixing the liquid and vapor condensate after the two streams were combined in the

holding chamber. The other was placed below the vapor sampling port to insure uniform composition of the mixed condensate streams.

CHAPTER IV

EXPERIMENTAL PROCEDURE

All necessary steps for carrying out the vapor-liquid equilibrium investigation using the apparatus described in Chapter III are given below.

Prior to the vapor-liquid equilibria measurements, the relationship between composition and refractive index for each binary system was determined. This was done by preparing mixtures of known composition and determining their refractive index readings. Samples were prepared in 5 cc vials and an analytical balance was used to determine the weight of each component in the vials. Mixtures at composition intervals of approximately 0.1 mole fraction were prepared by first weighing an empty vial and cap, followed by addition of component one and weighing the vial and cap along with component one, after which the second component was added and the vial containing the mixture was weighed. Weights were recorded to the nearest 0.00001 gm. From the above observations, the weight fractions were determined. The refractive index readings of the samples were determined twice to insure accuracy (once in decreasing order and then in increasing order of composition). From the weight fractions, the mole fractions were calculated, and the

composition as a function of refractometer reading was established. Appendix B gives the details of these measurements and analysis of the resulting data.

A cubic equation was fitted to each composition-refractometer reading data set; the resulting relations for composition as a function of refractometer reading gave root-mean-square errors in calculated compositions for different mixtures of approximately 0.001 mole fraction.

Before the equilibrium still was filled, it was dried by aspirator, then rinsed with the pure component to be charged to the still. The condenser was also rinsed with the pure component. The still was then filled and clamped to the aluminum frame. A nitrogen blanket was put over it immediately to minimize contact between the chemicals and air. A charge of approximately 150 cc of a pure component was used to begin a run. The amount of liquid was maintained such that, during operation, the level in the tube I (Figure 3) was just below the bottom of the vacuum jacket.

For isobaric runs, the pressure regulator was set to the desired pressure and, once the pressure stabilized, the reboiler was heated and the condenser water was turned on. The heat was then adjusted so that approximately sixty drops per minute were observed through the drop rate counter. This corresponds to a steady state in which an incremental change in the energy applied to the boiler did not cause a change in the observed temperature (based on measurements with the equilibrium still used in this study). The drop rate counter

(as mentioned above) was used to check the amount of heat input to the reboiler.

Once a steady temperature was observed, the recorder was turned on and fluctuations in the temperature were continuously monitored. For the pure components, these fluctuations were typically on the order of ± 0.01°C.

The still containing the pure first component was allowed to operate for approximately forty to sixty minutes with the temperature, drop rate and pressure checked and noted at ten minutes interval. About twenty minutes thereafter, 0.15-0.20 cc sample were withdrawn from the liquid and vapor sampling ports in the same order and analyzed. Operation was allowed to continue for another fifteen minutes, and duplicate samples were analyzed. If for some reason the analysis of the second sample did not agree with the first to within the accuracy of the refractometer, another fifteen minute period was allowed and a third set of samples was taken. For a pure component, the liquid and vapor sample should yield the same refractive index. For this study, pure component liquid and vapor sample yielded the same refractive index within the experimental uncertainity of the refractometer used.

Once agreement was observed, a measured quantity of the charge was removed from the still, and an equal quantity of the second component was added. The still was again allowed to operate until steady state was reached; this was determined by monitoring the temperature. Typically the time

required for attaining steady state after addition of the second component was about fifteen to twenty minutes. For each overall composition in the still, the monitored temperature should remain constant at a given pressure, since this will indicate that the stream delivered by the Cotrell pump is of constant composition and that no concentration fluctuations (indicated by the observable variations of temperature) occur. The temperature deviations for the mixtures studied were observed to be about ±0.02°C. The sampling of the mixtures was done in the same manner as pure substances, but in the case of mixtures the vapor and liquid samples yield different refractive indices.

This procedure was repeated until the liquid became an almost equimolar mixture. The still was then shut down, cleaned, recharged with the second pure component and the above procedure repeated, adding the first component to the still as samples were removed. Operations were again stopped when the liquid sample became approximately equimolar. For each system studied, care was taken to ensure that there was overlap of the runs from the opposite ends of the composition range (i.e., one or two data points from the second run overlapped, in liquid mole fraction, those from the first run). This provided a valuable check on the compatibility of the two runs for a given system.

Each run took approximately fifteen hours. Sample analysis by refractometry was very rapid. After withdrawing a sample, the syringe was covered by a cool wet paper so that

the sample was cooled to prevent evaporation when it was injected into the refractometer. Between samples, the refractometer plates were wiped with Kimwipe tissues and allowed to dry.

For isothermal study, the pressure was adjusted so that the required equilibrium temperature was obtained. This required a trial-and-error procedure, and two or three adjustments were usually required before the equilibrium temperature was sufficiently close to the desired value (± 0.02°C). In all systems studied, the temperature reached steady state in approximately fifteen minutes.

Shut Down Procedure

The order in which the apparatus was shut down at the end of a run was as to turn off (in order):

1. Recorder
2. Heater
3. Stirrer
4. Vacuum Pump
5. Pressure Regulator
6. Nitrogen tank
7. Cooling system
8. Temperature probe

CHAPTER V

THERMODYNAMIC CONSISTENCY TESTS

Careful evaluation of experimental vapor-liquid equilibrium data is required to satisfy two types of users. On one hand, a person doing design or correlation work needs to identify the best data available for a system of interest, plus some overall quality rating for each of the best data sets, so that the appropriate safety factors can be used to compensate for probable error. On the other hand, a person developing an experimental apparatus needs access to accurate data at some common test conditions so that the data can be used to verify the accuracy of the equipment and techniques. The most commonly used evaluation procedures are discussed in this chapter.

Thermodynamic consistency tests for vapor-liquid equilibrium measurements are based on the Gibbs-Duhem equation, and much has been written in the literature about various applications of this equation (32). Although no method exists which will permit experimental data to be termed as unquestionably correct, the Gibbs-Duhem equation provides a means to detect incorrect data.

The Gibbs-Duhem Equation

The Gibbs-Duhem equation relates the partial molar properties of the components in a mixture to one another. In its most general form, the equation is valid for a property which depends on the pressure, temperature and composition of the mixture. It is most frequently applied to the excess Gibbs free energy because of the direct relationship this quantity has with the activity coefficient. The equation may be written (1):

$$-\frac{H^E}{RT^2}\,dT + \frac{V^E}{RT}\,dP - \Sigma x_i\, d\left(\frac{\mu^E{}_i}{RT}\right) = 0 \qquad (5\text{-}1)$$

The derivation by Van Ness (1) is reproduced in Appendix E. The excess chemical potential $\mu^E{}_i$ is related to the activity coefficient by the relationship

$$\mu_i{}^E = RT \ln \gamma_i \qquad (5\text{-}2)$$

For the isothermal case, Equation 5-1, written for one mole, becomes,

$$\Sigma\, x_i\, d\ln\gamma_i = v^E/RT\, dP \qquad (5\text{-}3)$$

where

$$v^E = v - \sum_i x_i\, v_i \qquad (5\text{-}4)$$

v being the molar volume of the mixture, and v_i being the molar volume of a pure liquid. Equation 5-3 is a rigorous

expression of the Gibbs-Duhem equation at constant temperature in a conveniently applicable form. The use of this equation requires data on excess volume, which limits the utility of the equation. At low pressures the right hand side of Equation 5-3 is negligible (see Appendix G), hence

$$\Sigma\ x_i\ d\ln \gamma_i = 0 \qquad (5\text{-}5)$$

Integrating Equation 5-5 gives

$$\int_0^1 \ln (\gamma_1/\gamma_2)\ dx_1 = 0 \qquad (5\text{-}6)$$

Similarly for the isobaric case, Equation 5-1 becomes

$$\Sigma\ x_i d\ln\gamma_i = \frac{-H^E}{RT^2}\ dT \qquad (5\text{-}7)$$

where H^E is excess heat of liquid mixture. This is a rigorous expression of the Gibbs-Duhem equation at constant pressure. Excess heat of the liquid mixture is neglected for our data (see Appendix G). Hence at constant temperature and pressure the above assumptions leads to the following equation

$$\int_0^1 \ln (\gamma_1/\gamma_2)\ dx_1 = 0 \qquad (5\text{-}9)$$

Thermodynamic Consistency Using the Gibbs-Duhem Equation

The most common among the many different relations devised to test data are (1) the differential test (slope

test), (2) the integral test (area test), and (3) the prediction test.

The Differential Test

In the differential (slope) test, $\ln\gamma_1$ and $\ln\gamma_2$ (or γ_1 and γ_2) are plotted against x_1. The slopes are then read from the plots and introduced into a modified form of Equation 5-5 to see if the data satisfy the equation.

The advantage of this test is that it is very simple. On the other hand, accurate determination of the slope of the curve at various points is difficult.

The Integral Test

From the above discussion, at constant temperature or pressure, the following approximate relation may be written:

$$\int_0^1 \ln(\gamma_1/\gamma_2)\, dx_1 = 0 \qquad (5\text{-}10)$$

The above equation forms the basis of integral test in which $\ln(\gamma_1/\gamma_2)$ is plotted against x_1 and, for the data to be consistent, the net area under this curve must be zero. Like the differential test, the integral test is also a graphical test. However, the fact that this test is based on the ratios of the activity coefficients causes it to be a consistency test in a restricted sense, because the only data needed to construct the plot are x and y values and the ratio P_2^{sat}/P_1^{sat}. That is,

$$\frac{\gamma_1}{\gamma_2} = \frac{Py_1/P_1^{sat}x_1}{Py_2/P_2^{sat}x_2} \qquad (5\text{-}11)$$

Thus, the pressure cancels from the ratio (except for the limiting values P_1^{sat} and P_2^{sat}). In other words, any errors in pressure cancel out when the activity coefficient ratio is taken. Thus, the test may fail to indicate error even when the pressure data are incorrect. A plot of $\ln(\gamma_1/\gamma_2)$ versus x_1 is sensitive to scatter in the x-y data, but it will show nothing about the internal consistency of the pressure data.

Predictive Tests

These tests probably provide the most direct way of evaluating the thermodynamic consistency of the data. They have the following characteristics:

(1) The experimental vapor-liquid equilibrium data must include pressure, temperature, liquid and vapor compositions (at constant temperature or at constant pressure)

(2) Any three of the measured quantities and Equation 2-18 are used to predict the fourth

(3) The predicted values are compared with the experimental values of this fourth variable.

When all four variables are measured, the data set contains redundant information, and thermodynamics provides a means to test the internal consistency of this redudant measurement. There are different procedures which may be used to reduce a set of P-x-y or T-x-y data for isothermal or

isobaric conditions, respectively, to a correlation for the liquid phase activity coefficients.

Model Test

This test involves analysis of deviations of the experimental data from predicted values using selected models (e.g., the virial equation of state for vapor phase and Wilson model for liquid phase).

Four plots commonly used to access the deviations for a set of vapor-liquid equilibrium data are, (Pcalc - Pexp)-x_1 (for isothermal data) or (Tcalc - Texp)-x_1 (for isobaric data); (ycalc - yexp)-x_1 ; γ_1, γ_2-x_1 and $\ln(\gamma_1/\gamma_2)$ -x_1.

Models for activity coefficients are specifically designed to obey the Gibbs-Duhem equation; hence, if the data fit such a model (within the experimental uncertainity of the data) they may be said to be consistent. If they do not fit the model they may be consistent or inconsistent. Also, consistency with the Gibbs-Duhem equation does not prove unequivocally that the data are correct. In addition, these tests cannot indicate the cause for data being in error.

The last of the three tests described above is used in this study to evaluate the experimental data, and a discussion follows in the next section.

CHAPTER VI

RESULTS AND DISCUSSION

Experimental Results

To test the operation of the new facility, measurements were made on binary systems formed among the constituents n-hexane, methylcyclohexane and toluene. One isotherm and one isobar were measured for each of the binary mixtures formed among the above-mentioned constituents.

Once the data were collected, they were subjected to tests described in the previous section. From the results of these tests, the quality of the data was assessed with respect to precision and thermodynamic consistency and, hence, the adequacy of the equilibrium facility was determined.

Before studying the vapor-liquid equilibrium for the binary systems, tests of the equipment were conducted by measuring the vapor pressure of water. Results are given in Table 1.

TABLE 1

VAPOR PRESSURE OF WATER

Pressure	Temperature °C		
mm Hg	Observed	Literature(7)	Difference
760	99.99	100.00	-0.01
700	97.71	97.72	-0.01
650	95.67	95.67	0.00
600	93.50	93.51	-0.01
550	91.17	91.18	-0.01
500	88.67	88.67	0.00
450	85.94	85.94	0.00

(7) Boublik, T., Fried, V., and Hala, E., "The Vapor Pressures of Pure Substances", Elsevier, New York, (1984).

From the above observations, calibrations of the pressure regulator and temperature sensor were confirmed, and study of the organic substances was begun.

Pure substance behavior was next checked by measuring the normal boiling points (Table 2) and vapor pressures (Table 3) of the organic chemicals.

TABLE 2

NORMAL BOILING POINTS OF PURE SUBSTANCES

Compound	Temperature, °C		
	Observed	Literature(13)	Difference
n-Hexane	68.65	68.73	-0.08
Methylcyclohexane	100.67	100.94	-0.27
Toluene	110.57	110.63	-0.06

(13) Engineering Sciences Data, ESDU International Plc. London (1987).

TABLE 3

VAPOR PRESSURES OF PURE SUBSTANCES

Compound	Vapor Pressure, mm Hg		
	Observed	Literature(7)	Difference
	AT 70 °C		
n-Hexane	792.89	790.60	2.29
Methylcyclohexane	292.30	289.79	2.51
Toluene	204.12	203.74	0.38
	AT 90 °C		
Methylcyclohexane	556.82	552.30	4.52
Toluene	407.29	406.73	0.56

(7) Boublik, T., Fried, V., and Hala, E., "The Vapor Pressures of Pure Substances", Elsevier, New York, (1984).

These differences in the pure substance properties may be due to impurities in pure compounds. To verify the purities, refractive index measurements were performed, as reported in Table 4.

TABLE 4

REFRACTIVE INDICES OF PURE SUBSTANCES

Compound	Refractive index		
	Observed	Literature(39)	Difference
n-Hexane	1.3724	1.3722	0.0002
Methylcyclohexane	1.4207	1.4206	0.0001
Toluene	1.4941	1.4941	0.0000*

* Toluene, being of high purity, was used as a basis for calibration of refractometer

(39) Timmermans J., "Physico-Chemical Constants of Pure Organic Compounds", Elsevier, New York (1950).

All refractive index measurements in this work were done at 25 °C, using a sodium vapor lamp.

The discrepancies observed in the normal boiling points and vapor pressures of the pure compounds from literature values may be attributed to impurity in these compounds.

Following measurements on the pure substances, study was begun on mixtures. Results are presented in Tables 5-10.

TABLE 5

VAPOR-LIQUID EQUILIBRIUM DATA FOR METHYLCYCLOHEXANE (1) + TOLUENE (2) AT 760 mm Hg

Temperature °C	Liquid Mole Fraction x_1	Vapor Mole Fraction y_1
110.53	0.0000	0.0000
109.78	0.0340	0.0545
108.77	0.0855	0.1275
107.75	0.1415	0.2010
106.90	0.1935	0.2630
106.17	0.2420	0.3175
105.50	0.2915	0.3705
104.92	0.3385	0.4175
104.43	0.3815	0.4580
103.11	0.5220	0.5840
102.69	0.5725	0.6290
102.25	0.6335	0.6800
101.85	0.6975	0.7330
101.46	0.7670	0.7930
101.12	0.8430	0.8585
100.78	0.9415	0.9455
100.64	1.0000	1.0000

TABLE 6

VAPOR LIQUID EQUILIBRIUM FOR METHYLCYCLOHEXANE (1) + TOLUENE (2) AT 90°C

Pressure mm Hg	Liquid Mole Fraction x_1	Vapor Mole Fraction y_1
407.29	0.0000	0.0000
419.23	0.0395	0.0655
440.13	0.1145	0.1760
454.51	0.1745	0.2505
466.81	0.2290	0.3150
478.88	0.2890	0.3775
487.81	0.3355	0.4240
504.15	0.4365	0.5175
511.89	0.4895	0.5645
518.76	0.5405	0.6080
526.01	0.5990	0.6570
533.17	0.6645	0.7110
541.88	0.7565	0.7865
547.88	0.8350	0.8520
553.78	0.9300	0.9355
556.82	1.0000	1.0000

TABLE 7

VAPOR LIQUID EQUILIBRIUM FOR n-HEXANE (1)
+ METHYLCYCLOHEXANE (2) AT 760 mm Hg

Temperature °C	Liquid Mole Fraction x_1	Vapor Mole Fraction y_1
100.66	0.0000	0.0000
99.06	0.0310	0.0715
97.20	0.0685	0.1530
94.12	0.1350	0.2825
91.37	0.2015	0.3880
88.83	0.2655	0.4740
86.69	0.3245	0.5465
84.39	0.3895	0.6150
82.68	0.4415	0.6660
82.57	0.4455	0.6695
80.27	0.5210	0.7355
78.04	0.5990	0.7920
75.88	0.6805	0.8430
73.71	0.7680	0.8940
72.17	0.8345	0.9285
70.71	0.9000	0.9575
69.37	0.9640	0.9860
68.63	1.0000	1.0000

TABLE 8

VAPOR LIQUID EQUILIBRIUM FOR n-HEXANE (1)
+ METHYLCYCLOHEXANE (2) AT 70°C

Pressure mm Hg	Liquid Mole Fraction x_1	Vapor Mole Fraction y_1
292.23	0.0000	0.0000
320.32	0.0555	0.1335
349.95	0.1135	0.2565
388.46	0.1900	0.3865
426.03	0.2650	0.4910
458.18	0.3295	0.5640
487.07	0.3865	0.6235
500.36	0.4170	0.6525
517.41	0.4465	0.6785
535.17	0.4860	0.7120
574.52	0.5640	0.7715
616.23	0.6475	0.8265
664.16	0.7425	0.8815
715.77	0.8455	0.9335
759.17	0.9325	0.9720
793.23	1.0000	1.0000

TABLE 9

VAPOR LIQUID EQUILIBRIUM FOR n-HEXANE (1) + TOLUENE (2) AT 760 mm Hg

Temperature °C	Liquid Mole Fraction x_1	Vapor Mole Fraction y_1
110.57	0.0000	0.0000
104.67	0.0570	0.2020
100.27	0.1090	0.3345
96.03	0.1680	0.4495
93.29	0.2135	0.5165
90.63	0.2630	0.5790
85.51	0.3775	0.6890
87.08	0.3385	0.6575
83.80	0.4220	0.7240
81.01	0.5030	0.7765
78.49	0.5865	0.8240
76.02	0.6780	0.8690
73.71	0.7720	0.9090
70.66	0.9065	0.9640
68.65	1.0000	1.0000

TABLE 10

VAPOR LIQUID EQUILIBRIUM FOR n-HEXANE (1) + TOLUENE (2) AT 70°C

Pressure mm Hg	Liquid Mole Fraction x_1	Vapor Mole Fraction y_1
204.12	0.0000	0.0000
248.38	0.0480	0.2170
294.51	0.1045	0.3790
335.39	0.1590	0.4805
374.75	0.2160	0.5625
402.09	0.2570	0.6095
430.36	0.3025	0.6515
460.14	0.3530	0.6940
460.97	0.3555	0.6970
499.76	0.4240	0.7430
542.67	0.5040	0.7895
588.99	0.5950	0.8345
638.33	0.6935	0.8795
687.84	0.7935	0.9200
736.30	0.8905	0.9580
792.62	1.0000	1.0000

In the above tables, temperatures are reported to two decimal places, as the recorded variations in temperatures of the mixtures as well as instrumental uncertainty was about ±0.03°C, that of pressure was ±0.02 mm Hg and that of mole fraction was ±0.001. The mole fractions are presented to the nearest 0.0005.

Discussion of Results

The data from this study were evaluated in two ways, by

comparison with existing literature and by performing thermodynamic consistency tests. Each of these evaluation methods is described below.

Comparisons With Literature Data

Six binary systems were measured, and various amounts of literature data were available at each of these conditions. Thus, the ability to judge the present data by comparison to the data of others varied from system to system. The analysis of one isotherm and one isobar will be discussed in detail in this section; the other data behave similarly in terms of agreement with reliable literature data and with consistency tests. Thus, the details of the analysis for those systems have been appendicized (Appendix D).

For the system methylcyclohexane + toluene at 760 mm Hg, seven data sets were available for comparison. Figures 4 and 5 show plots of the type typically used to compare vapor-liquid equilibrium data sets. However, such plots emphasize the similarities, rather than differences, in the data. Thus, a more sensitive method was employed for the data comparisons of this work. The data sets were compared on plots which show deviations of the data from a selected reference function; in this case, the Wilson model was used as the reference model.

The reference model approach for data comparisons proceeded as follows. First, the experimental results from the present work were used to determine parameters in the

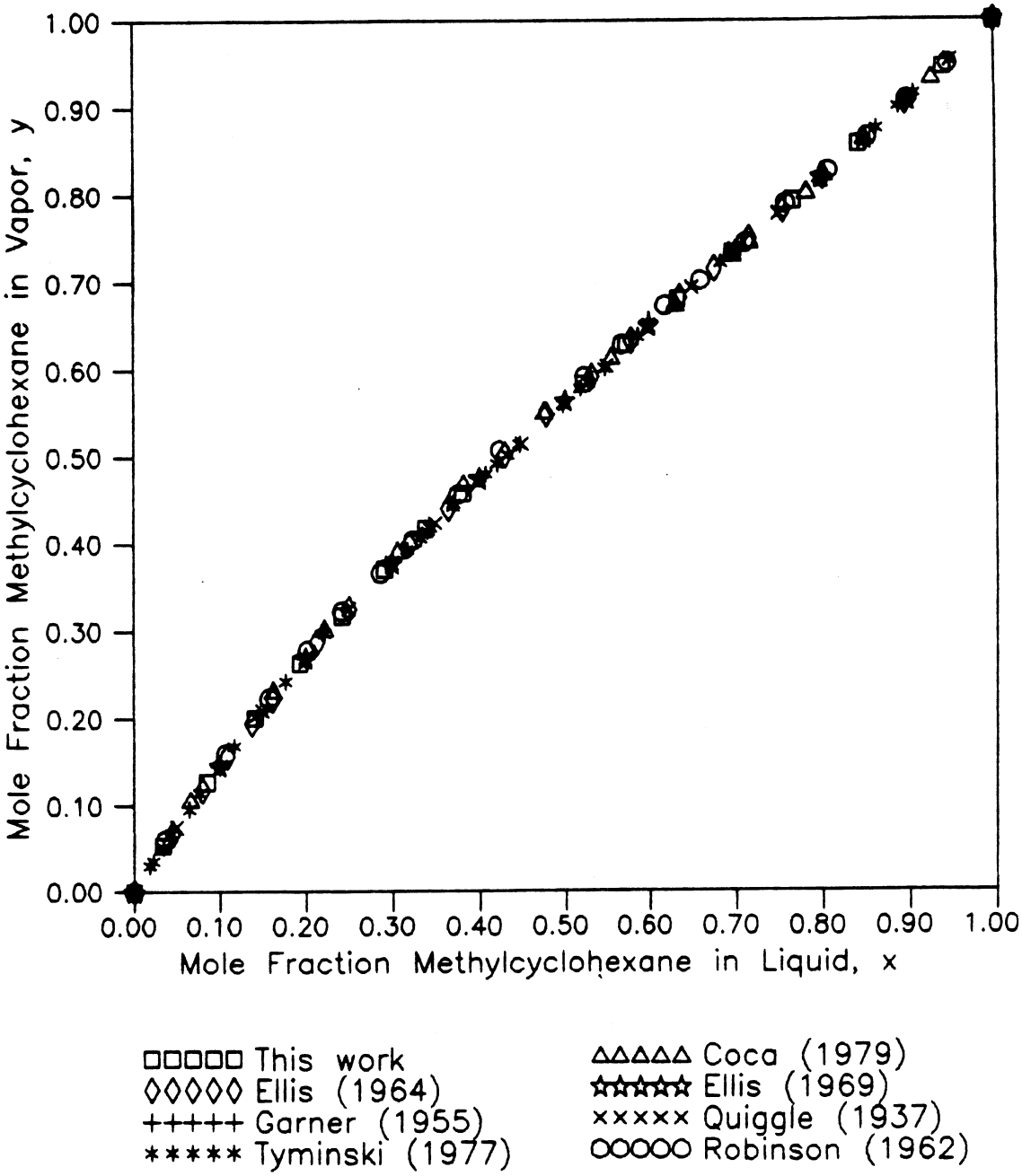

Figure 4. Experimental Equilibrium Phase Compositions for Methylcyclohexane + Toluene at 760 mm Hg

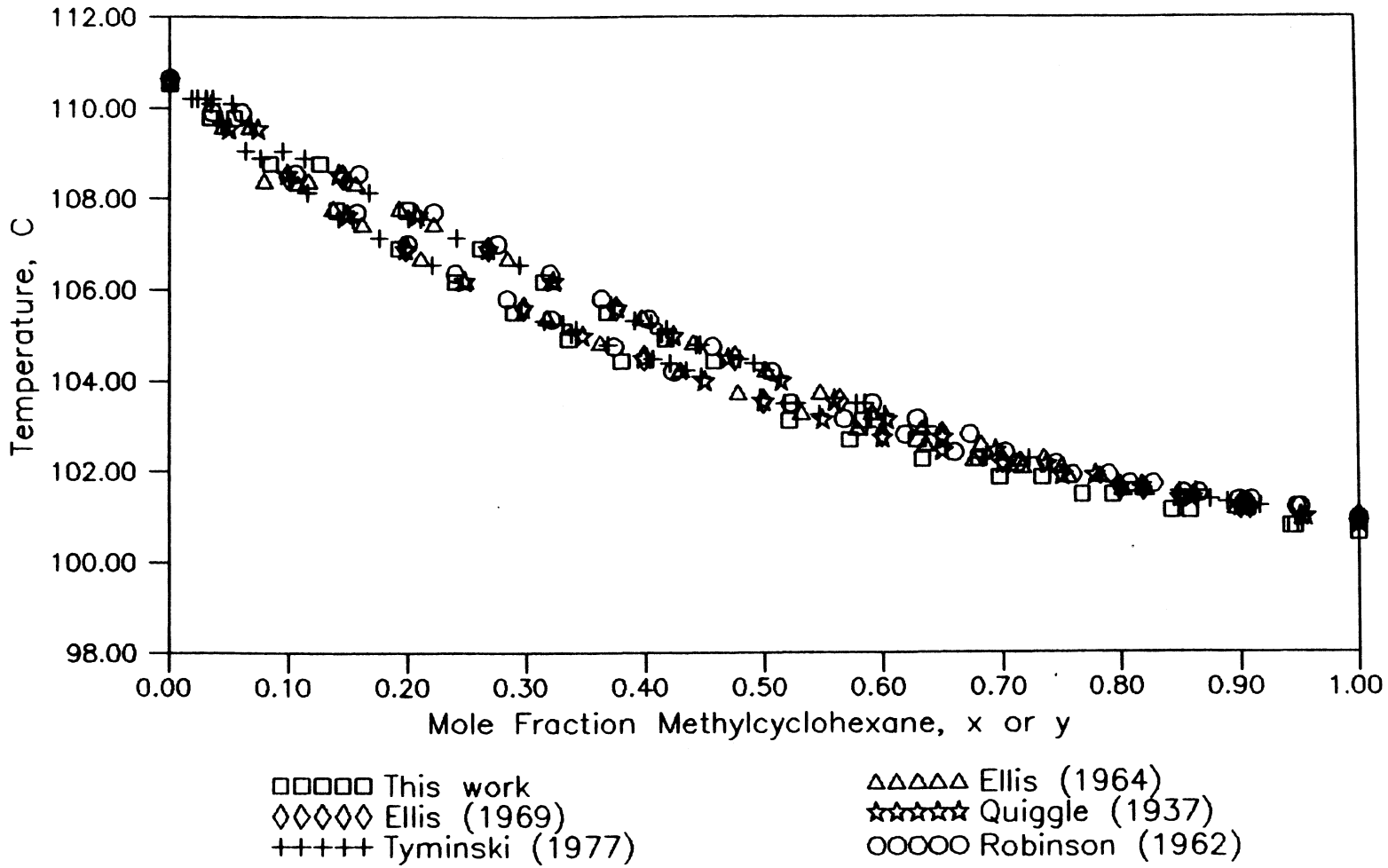

Figure 5. Experimental Phase Behavior (T−x,y) for Methylcyclohexane + Toluene at 760 mm Hg

Wilson equation (and the Van Laar equation), which were then used as the basis for comparison of results of this work with other investigators.

Data reduction was performed by using the virial equation terminated at the second coefficient for the vapor phase (as well by the ideal gas equation for comparison). The virial equation of state was chosen because, at low the pressures of this study, it can adequately represent the vapor phase behavior. The results of the model regressions and predictions using the regressed parameters, are given for the data of this work in Table 11.

TABLE 11

RESULTS OF MODEL REGRESSION AND PREDICTION

Liquid Model	Vapor Model	RMS Deviation	
		T °C	y
Methylcyclohexane + Toluene at 760 mm Hg			
Wilson	Ideal	0.01	0.0037
Wilson	Virial	0.01	0.0015
Vanlaar	Ideal	0.01	0.0015
Vanlaar	Virial	0.01	0.0015
n-Hexane + Methylcyclohexane at 760 mm Hg			
Wilson	Ideal	0.02	0.0050
Wilson	Virial	0.02	0.0020
Vanlaar	Ideal	0.02	0.0050
Vanlaar	Virial	0.02	0.0020

TABLE 11 (Continued)

Liquid Model	Vapor Model	RMS Deviation T °C	RMS Deviation y
n-Hexane + Toluene at 760 mm Hg			
Wilson	Ideal	0.01	0.0073
Wilson	Virial	0.01	0.0018
Vanlaar	Ideal	0.01	0.0073
Vanlaar	Virial	0.01	0.0018

Liquid Model	Vapor Model	RMS Deviation P mm Hg	RMS Deviation y
Methycyclohexane + Toluene at 90 °C			
Wilson	Ideal	0.08	0.0027
Wilson	Virial	0.08	0.0008
Vanlaar	Ideal	0.08	0.0027
Vanlaar	Virial	0.08	0.0008
n-Hexane + Methylcyclohexane at 70 °C			
Wilson	Ideal	0.50	0.0050
Wilson	Virial	0.51	0.0010
Vanlaar	Ideal	0.58	0.0051
Vanlaar	Virial	0.51	0.0010
n-Hexane + Toluene at 70 °C			
Wilson	Ideal	0.37	0.0036
Wilson	Virial	0.28	0.0029
Vanlaar	Ideal	0.35	0.0036
Vanlaar	Virial	0.28	0.0029

The binary parameters obtained by regression for the Wilson and Van Laar models in dimensionless form are shown in

Table 12. Predictions using the Wilson parameters from Table 12 and Virial Equation facilitate comparisons with the various investigators, as given in Table 13. These are predictions with Antoine constants adjusted to give zero error in temperature or pressure at the pure component end points. The parameters are from fits to data of this work.

TABLE 12

BINARY MODEL PARAMETERS FOR WILSON AND VAN LAAR MODELS

Liquid Model	Vapor Model	A(1,2)	A(2,1)
METHYLCYCLOHEXANE(1) + TOLUENE(2) AT 760 mm Hg			
Wilson	Ideal	0.9074	0.8672
Wilson	Virial	0.8876	0.8922
Van Laar	Ideal	0.2297	0.2348
Van Laar	Virial	0.2267	0.2262
n-Hexane + Methylcyclohexane at 760 mm Hg			
Wilson	Ideal	0.7615	1.2697
Wilson	Virial	1.1917	0.8010
Van Laar	Ideal	0.0246	0.0006
Van Laar	Virial	0.0234	0.3031
n-Hexane + Toluene at 760 mm Hg			
Wilson	Ideal	0.8535	0.8565
Wilson	Virial	0.8341	0.8465
Van Laar	Ideal	0.3013	0.3007
Van Laar	Virial	0.3340	0.3315
Methylcyclohexane + Toluene AT 90°C			
Wilson	Ideal	0.8220	0.9342
Wilson	Virial	0.8030	0.9590

Table 12 (continued)

Liquid Model	Vapor Model	A(1,2)	A(2,1)
Van Laar	Ideal	0.2614	0.2456
Van Laar	Virial	0.2599	0.2385
n-Hexane (1) + METHYLCYCLOHEXANE(1) AT 70°C			
Wilson	Ideal	0.5926	1.5045
Wilson	Virial	0.7946	1.1999
Van Laar	Ideal	0.0228	0.0032
Van Laar	Virial	0.0300	0.2316
n-Hexane + Toluene at 70°C			
Wilson	Ideal	0.6691	1.0187
Wilson	Virial	0.6842	0.9764
Van Laar	Ideal	0.3821	0.3114
Van Laar	Virial	0.4018	0.3384

where A(1,2) and A(2,1) are the model parameters in Equations 2-13 to 2-16.

TABLE 13

COMPARISONS AMONG VARIOUS INVESTIGATORS

Investigator	RMS Deviation	
	T °C	y
Methylcyclohexane + Toluene at 760 mm Hg		
Coca (1979)	0.29	0.0053
Ellis (1964)	0.13	0.0013
Ellis (1969)	0.05	0.0008
Garner (1955)	0.27	0.0016
Quiggle (1937)	0.10	0.0037
Tyminski (1977)	0.13	0.0036

Table 13 (continued)

Investigator	RMS Deviation	
	T °C	y
Robinson (1962)	0.11	0.0035
This Work	0.01	0.0015
n-Hexane + Methylcyclohexane at 760 mm Hg		
Myers (1957)	0.27	0.0060
Robinson (1962)	0.11	0.0124
This Work	0.02	0.0020
n-Hexane + Toluene at 760 mm HG		
Sieg (1950)	0.36	0.0030
Michishita (1971)	0.26	0.0076
Saito (1969)	0.40	0.0212
Robinson	0.12	0.0132
This Work	0.01	0.0018

Investigator	RMS Deviation	
	mm Hg	y
Methylcyclohexane + Toluene at 90°C		
Schneider (1961)	3.68	0.0024
This work	0.08	0.0008

Investigator	RMS Deviation	
	mm Hg	y
n-Hexane + Methylcyclohexane at 70°C		
This work	0.51	0.0010
n-Hexane + Toluene at 70°C		
Wichterle (1969)	19.18	0.0268
This work	0.28	0.0029

Plots of (Tcalc - Texp) or (Pcalc - Pexp) as functions of x_1 permit detailed analysis in terms of deviations of the data from the Wilson equation. The plots are based on Wilson parameters optimized to fit the present data. The purpose of these figures is solely to emphasize differences among the various studies. It is the difference between the deviations for any two sets which shows their mutual agreement (not their individual deviations from the reference model). Figure 6 shows the deviations of experimental temperatures of this work from those calculated by the Wilson equation, which reveal a good fit by the Wilson equation. Comparisons of the deviations of the temperatures of the various investigators from temperatures calculated using the Wilson model are shown in Figure 7. This figure shows that the boiling points of the pure substances differ among the various investigators; this effect (possibly due to differences in the purities of the pure materials used by various investigators) was removed from the comparisons (Figure 8) by slightly adjusting the Antoine constants for the pure substances so that each data set shows zero error in temperature at the pure component end points, thus allowing comparisons on a more uniform basis. Deviations of experimental vapor compositions from those calculated using the model appear in Figure 9, which reveals that the maximum deviation of the Wilson model from the data is 0.003 mole fraction. Comparison of deviations of the experimental vapor compositions among various investigators is shown in Figure 10, which indicates that data of this work

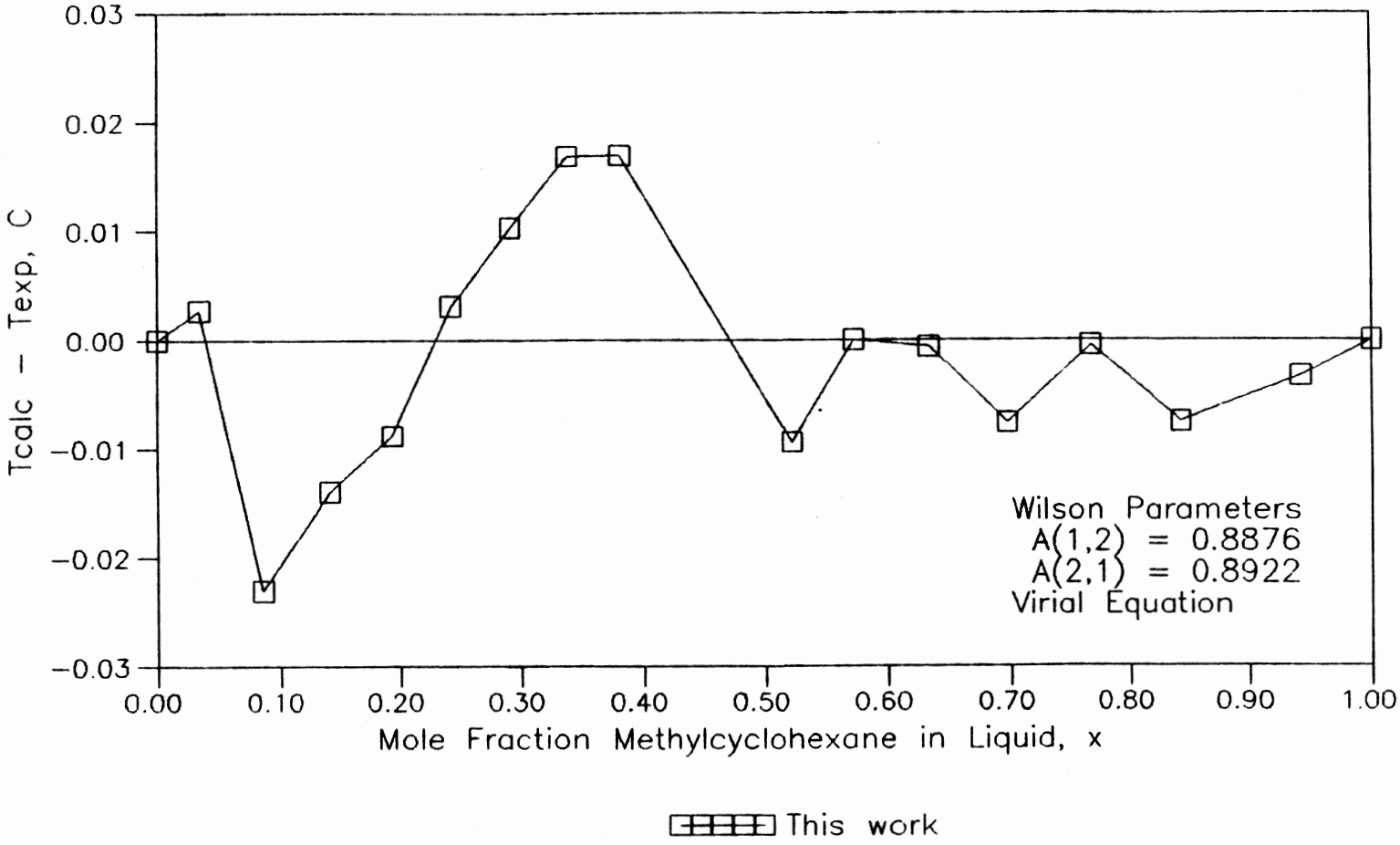

Figure 6. Deviations of Calculated Temperatures from Wilson Equation for Methylcyclohexane + Toluene at 760 mm Hg

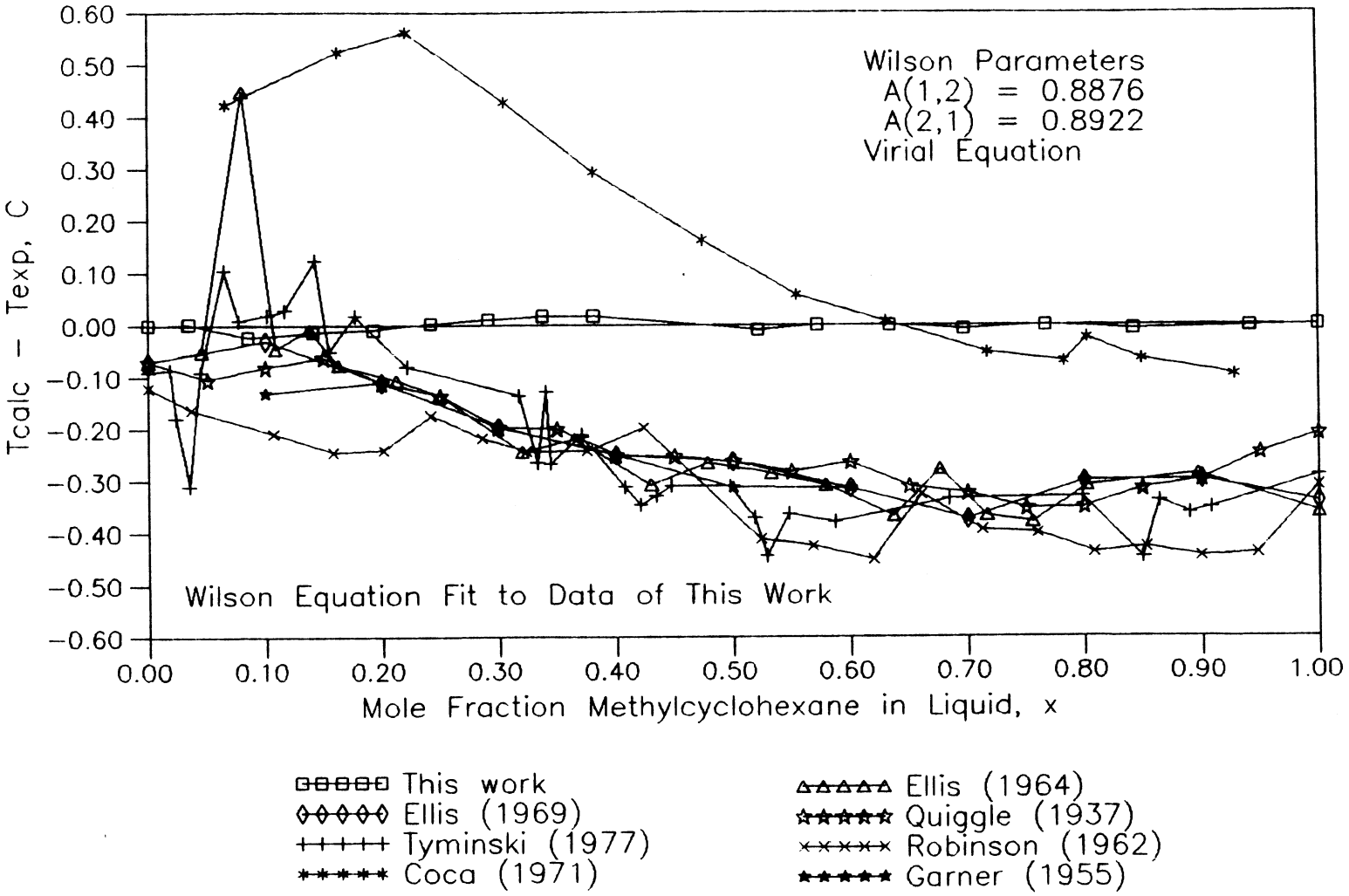

Figure 7. Comparision of Experimental Temperatures for Methylcyclohexane + Toluene at 760 mm Hg

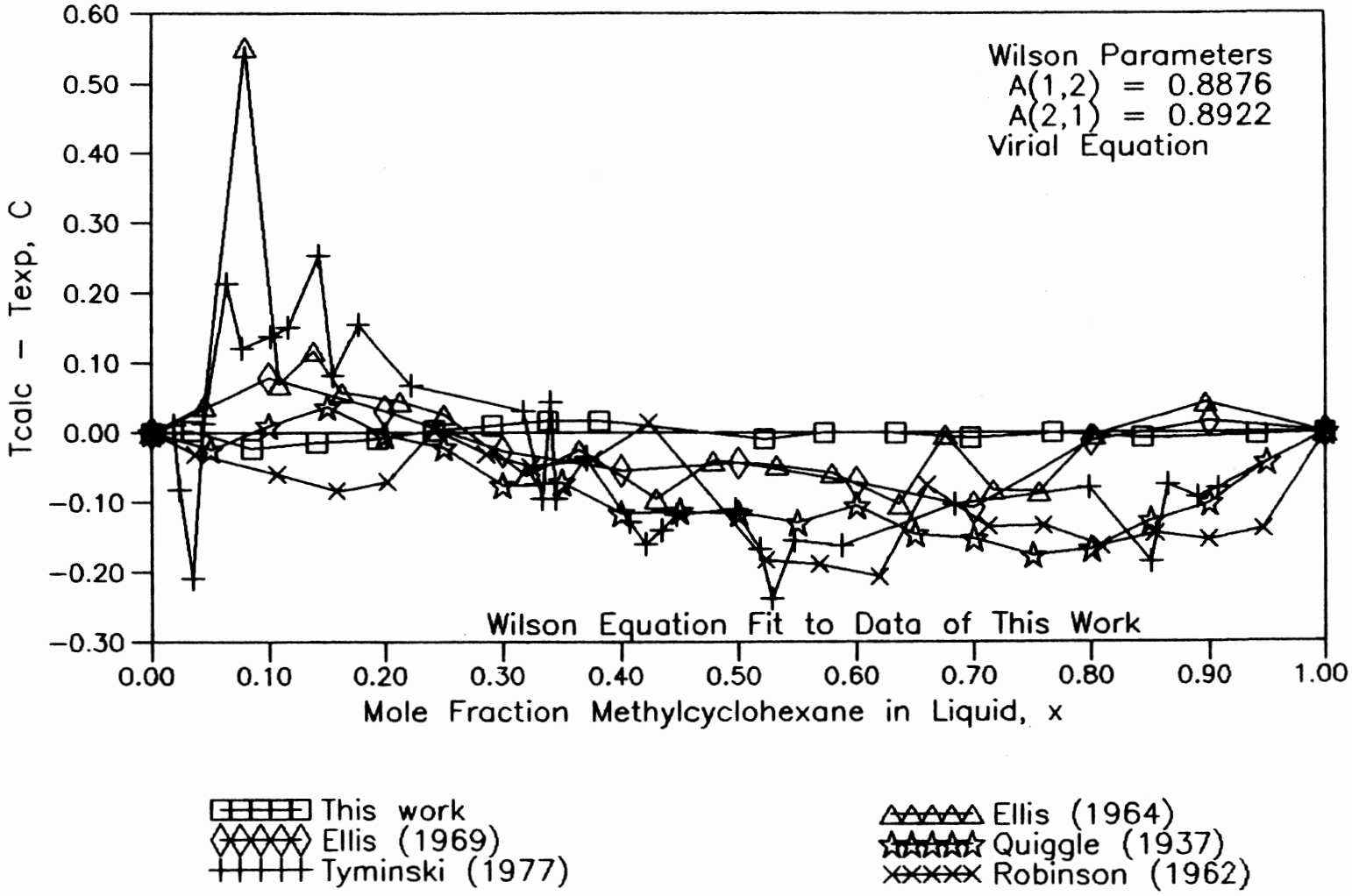

Figure 8. Detailed Comparison of Experimental Temperatures for Methylcyclohexane + Toluene at 760 mm Hg

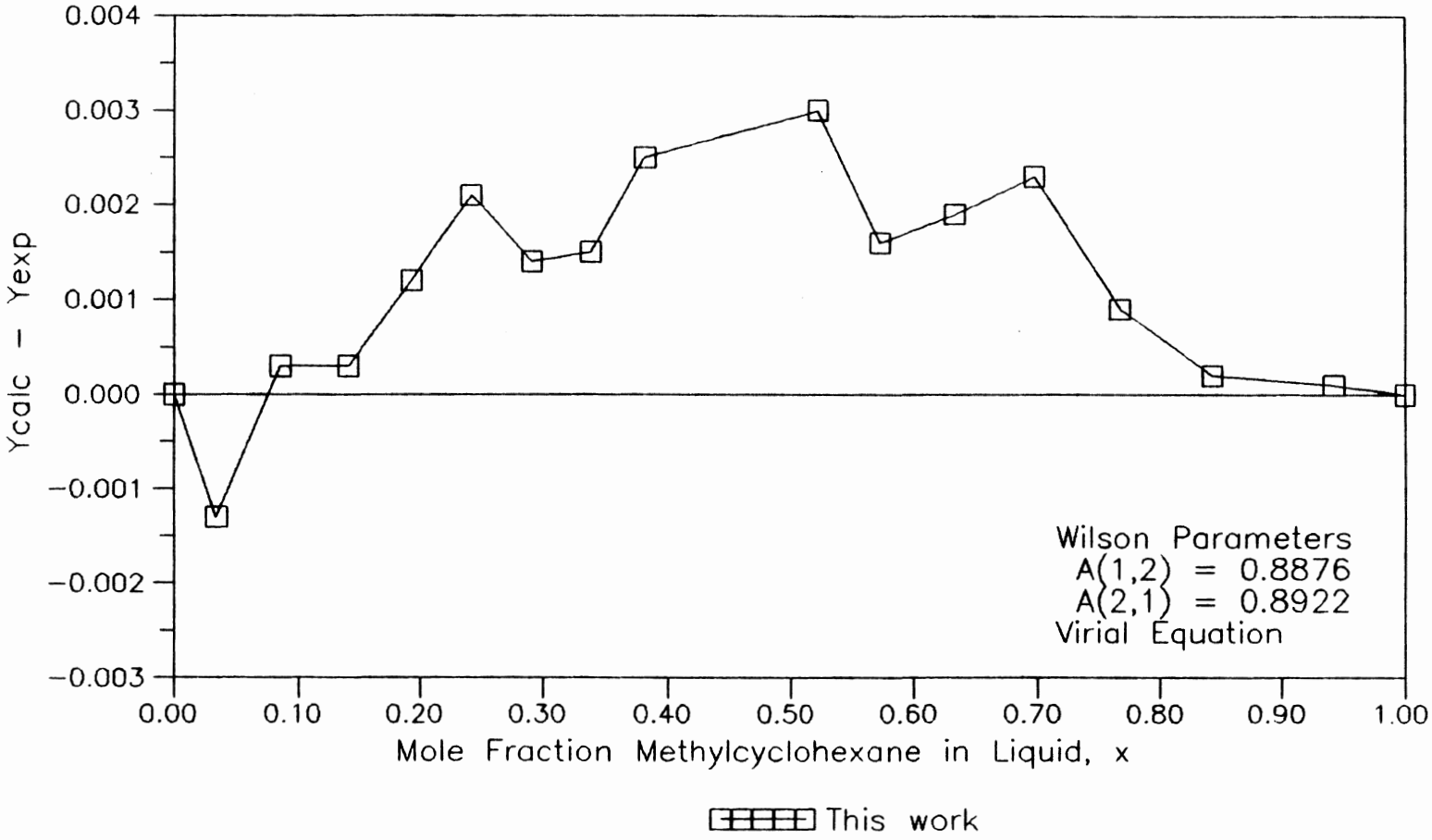

Figure 9. Deviations of Calculated Vapor Compositions from Wilson Equation for Methylcyclohexane + Toluene at 760 mm Hg

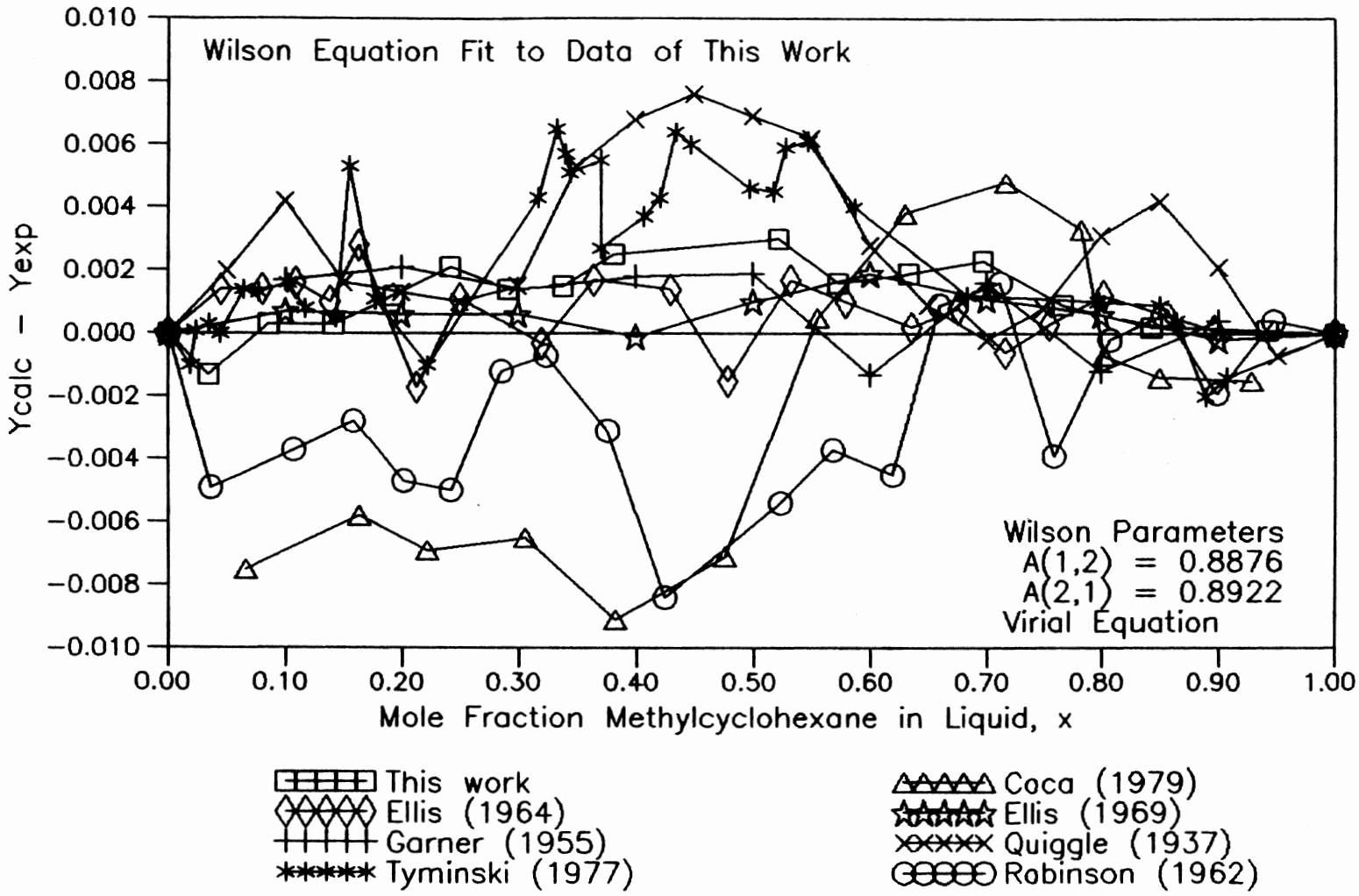

Figure 10. Comparison of Experimental Vapor Compositions for Methylcyclohexane + Toluene at 760 mm Hg

agree well with the works of Ellis (10, 11) and of Garner (15). The work of Thijssen (38) was not included as he reported only x-y data. The works of Coca (8), Quiggle(30), Robinson(32) and Tyminski(42) shows deviations which are much larger than the experimental uncertainty of this work. Figure 11 provides a more sensitive comparison of selected investigators, which shows that deviations from the model for most of the data points are positive. Deviations for the different works of Ellis are generally less than 0.001 and similar to the agreement among the various investigators, including the present work. These good agreements confirm the working of equilibrium still and the procedures employed.

For n-hexane + methylcyclohexane at 70°C the results of regression and predictions are given in Table 11. As no other work for this system at the conditions studied was found in the literature, it cannot be compared with any other work. The x-y and P-x,y plots are shown in Figures 12 and 13; as stated earlier such plots do not provide much information. However, the analysis shows that the differences in the experimental pressure and the pressure calculated from the Wilson model (Figure 14) are random, although the experimental scatter in the pressure measurements was highest for this system. Deviations of experimental vapor compositions from those (Figure 15) calculated using Wilson model show random scatter and are generally within the experimental uncertainty of this work. Data in the n-hexane-rich range of the mixture shows

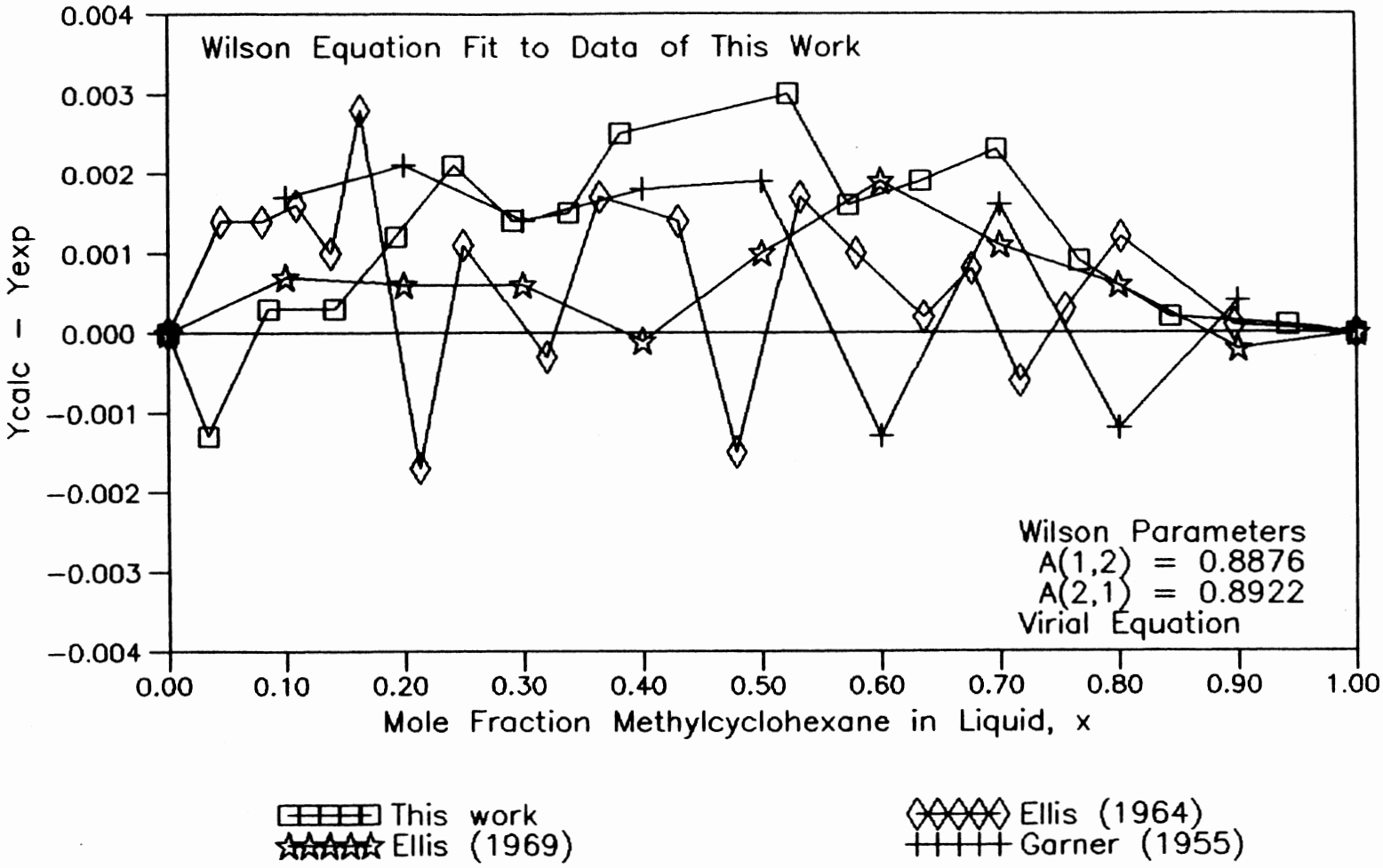

Figure 11. Detailed Comparison of Experimental Vapor Compositions for Methylcyclohexane + Toluene at 760 mm Hg

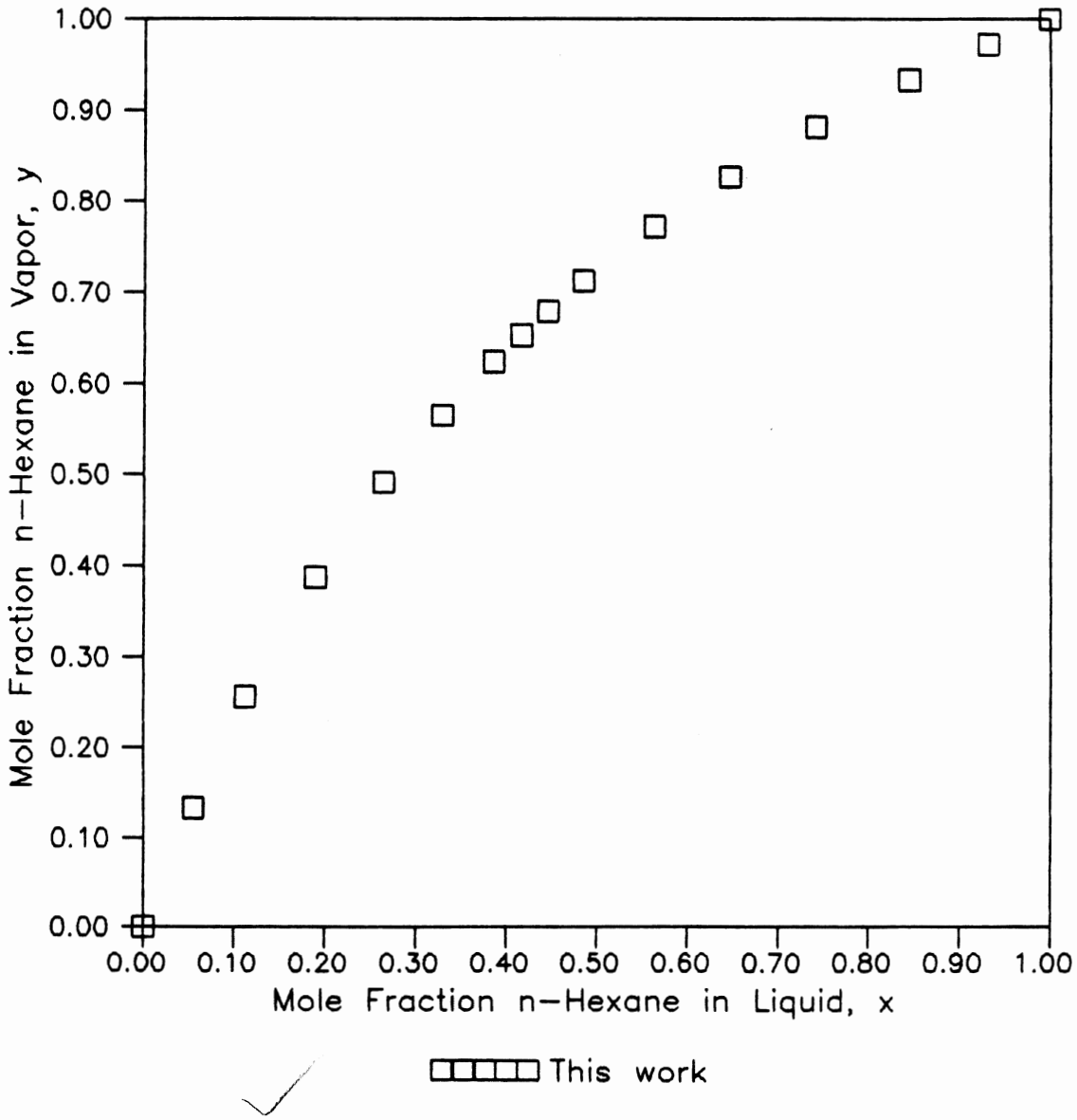

Figure 12. Experimental Equilibrium Phase Compositions for n-Hexane + Methylcyclohexane at 70 C

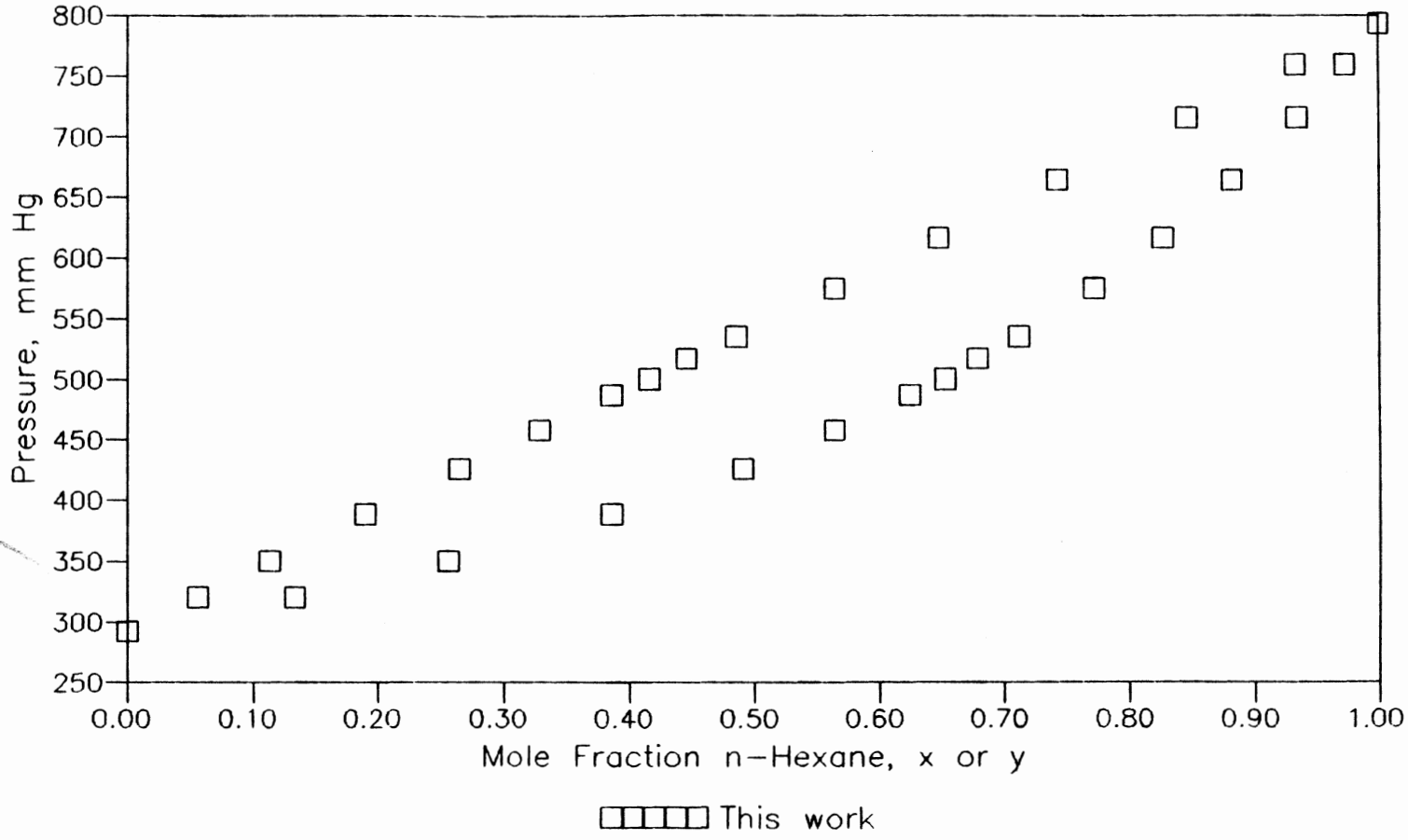

Figure 13. Experimental Phase Behavior (P-x,y) for n-Hexane + Methylcyclohexane at 70 C

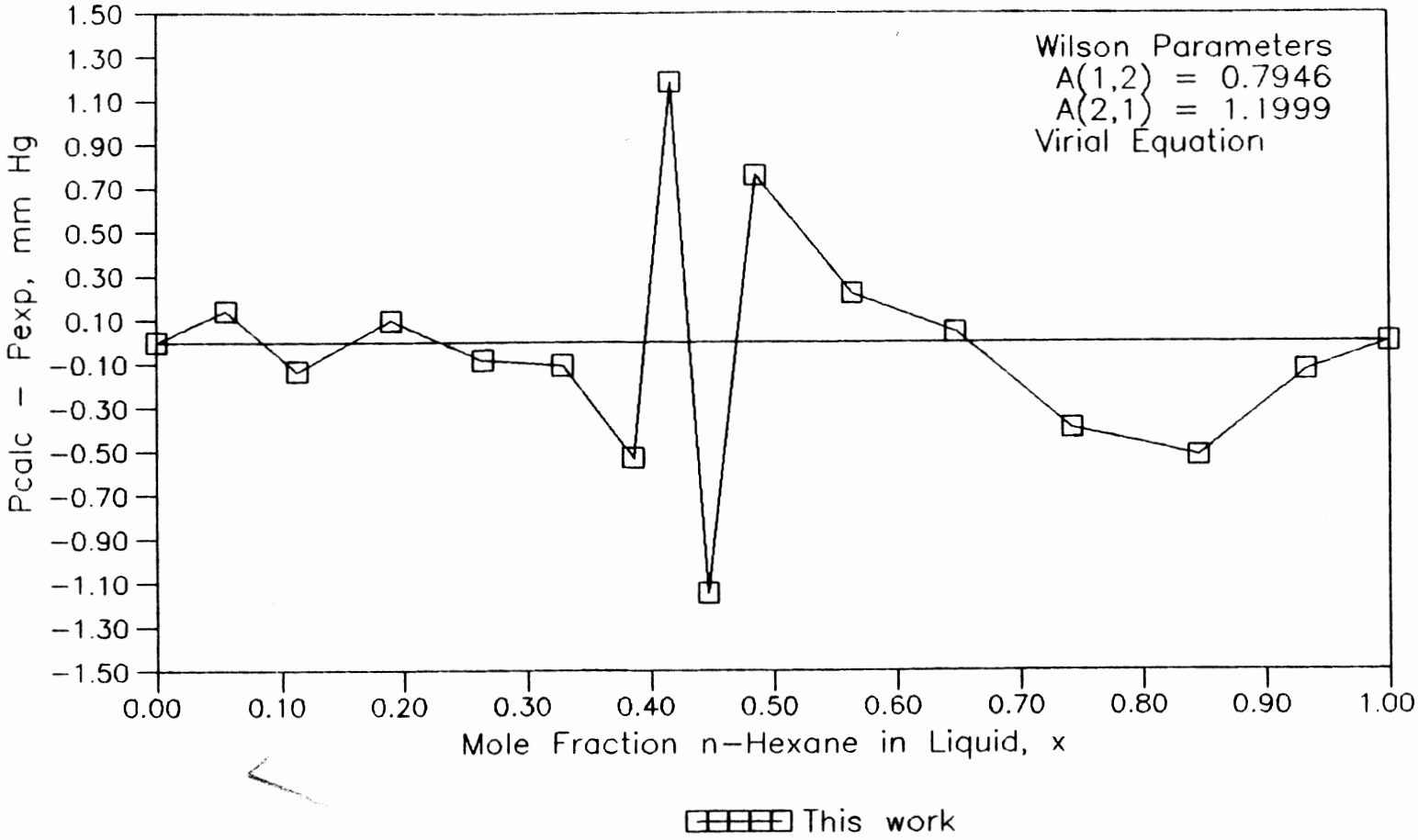

Figure 14. Deviations of Calculated Pressures from Wilson Equation for n-Hexane + Methylcyclohexane at 70 C

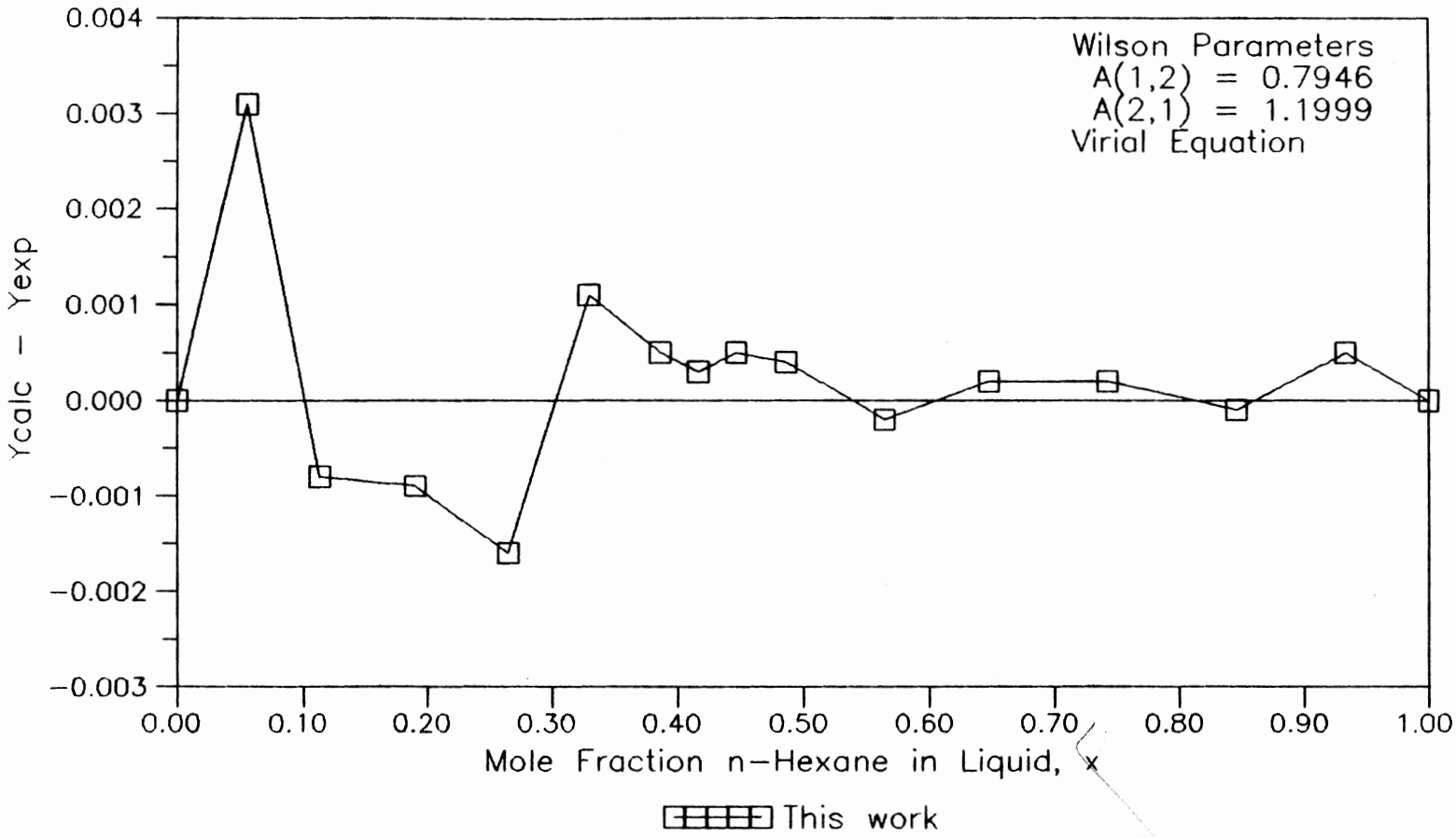

Figure 15. Deviations of Calculated Vapor Compositions From Wilson Equation for n−Hexane + Methylcyclohexane at 70 C

higher scatter than the methylcyclohexane-rich phase for the vapor composition.

The detailed analysis of other systems is given in Appendix D.

Thermodynamic Consistency Tests

The fits of the data of this work to the Wilson model serve as a basis for testing the data for thermodynamic consistency (as well as facilitating the comparisons of various data sets, as presented above). That is, if the data are fit by the Wilson model to within their experimental uncertainty, then the data are consistent since the Wilson equation satisfies the Gibbs-Duhem equation.

The $_1$, $_2$-x_1 plots for all systems studied are shown in this section. These plots (Figures 16 to 21) show the differences between the experimental $_1$ values (calculated using Equation 2-18, under the assumption that the models used in this equation are accurate for the systems studied) and those calculated from the Wilson equation. Error bars are shown on the experimental values of the activity coefficients, based on calculations of the propagation of experimental error, as explained in Appendix C. These error bars are based on estimated experimental uncertainties of 0.001 mole fraction, 0.02°C, and 0.05 mm Hg.

For the system methylcyclohexane + toluene at 760 mm Hg, Figure 16 shows that the calculated activity coefficients agree with the experimental values of this work within the

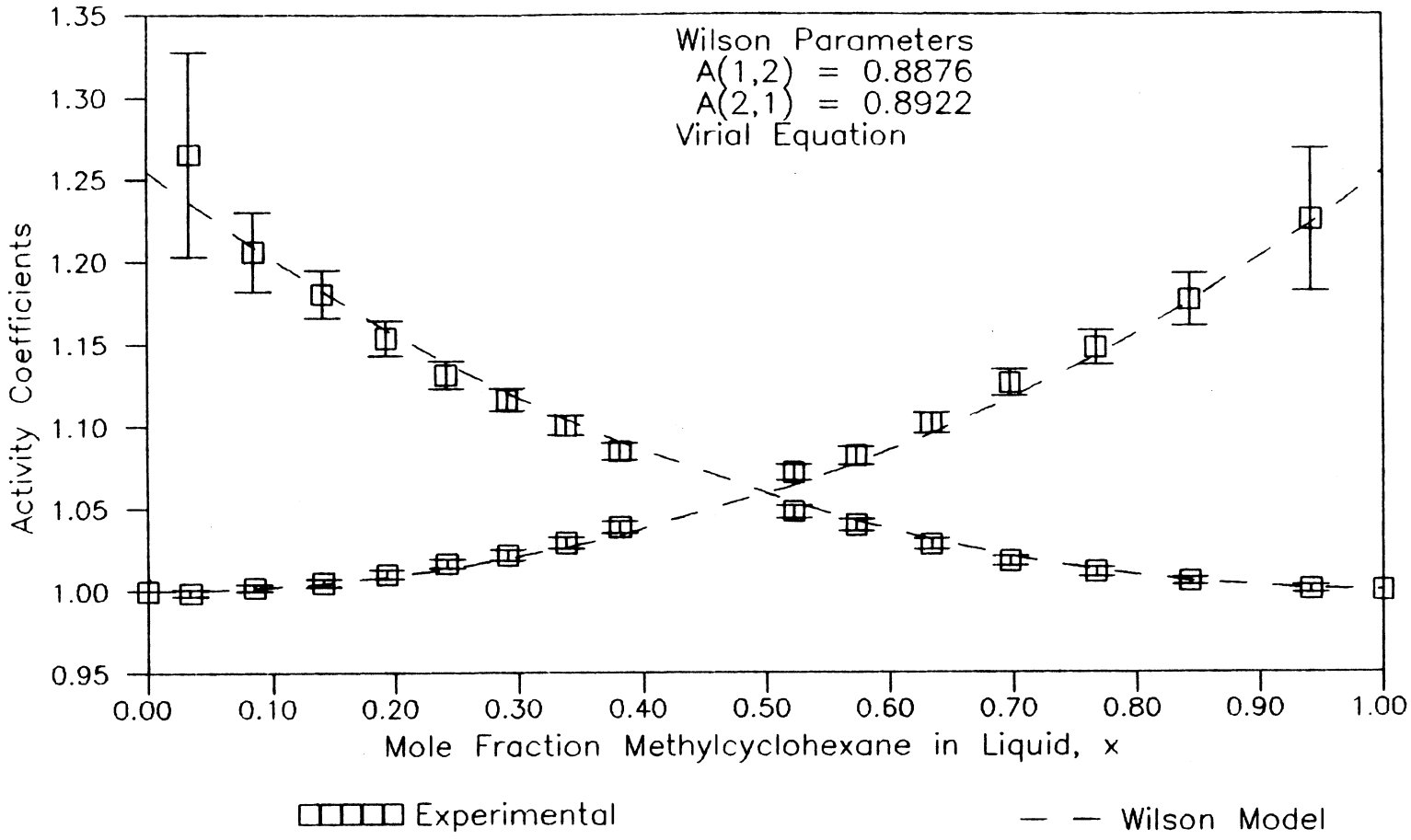

Figure 16. Activity Coefficients for Methylcyclohexane + Toluene at 760 mm Hg

experimental uncertainity in the data. Hence the data are thermodynamically consistent within the estimated experimental uncertainties. All calculated activity coefficients are between 1.00 and 1.25, showing moderate deviations from ideality for this system.

For the system n-hexane + methylcyclohexane at 70 °C, Figure 17 also shows that calculated activity coefficients are within the experimental values; hence, these data are also consistent. All calculated activity coefficient are between 1.00 and 1.036, showing very small deviations from ideality. This is the most nearly ideal of all the systems studied.

For system methycyclohexane + toluene at 90 °C, Figure 18 shows that the calculated activity coefficients are within the experimental uncertainty of this work; hence, the data are consistent for this system. All activity coefficients are between 1.00 and 1.30 showing moderate deviations from ideality.

For the system n-hexane + methylcyclohexane at 760 mm Hg (Figure 19) the calculated activity coefficient for some points in the methylcyclohexane-rich region of the mixture are not within the estimated experimental uncertainty. The above estimated uncertainties were very small; if the uncertainity in liquid and vapor composition measurements was increased to 0.0025 from 0.001, then the calculated activity coefficients for all the points would be within the experimental uncertainity. All calculated activity

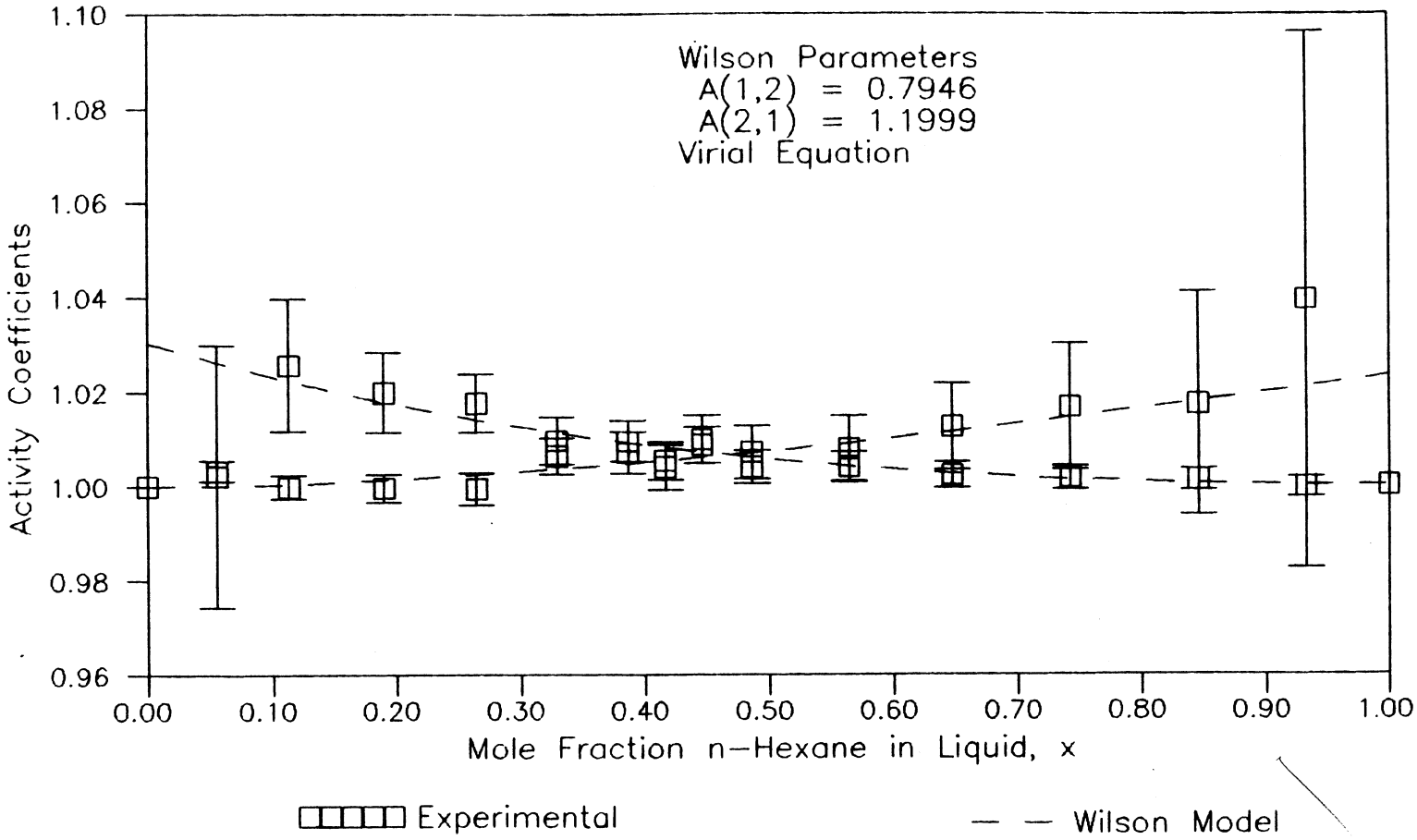

Figure 17. Activity Coefficients for n-Hexane + Methylcyclohexane at 70 C

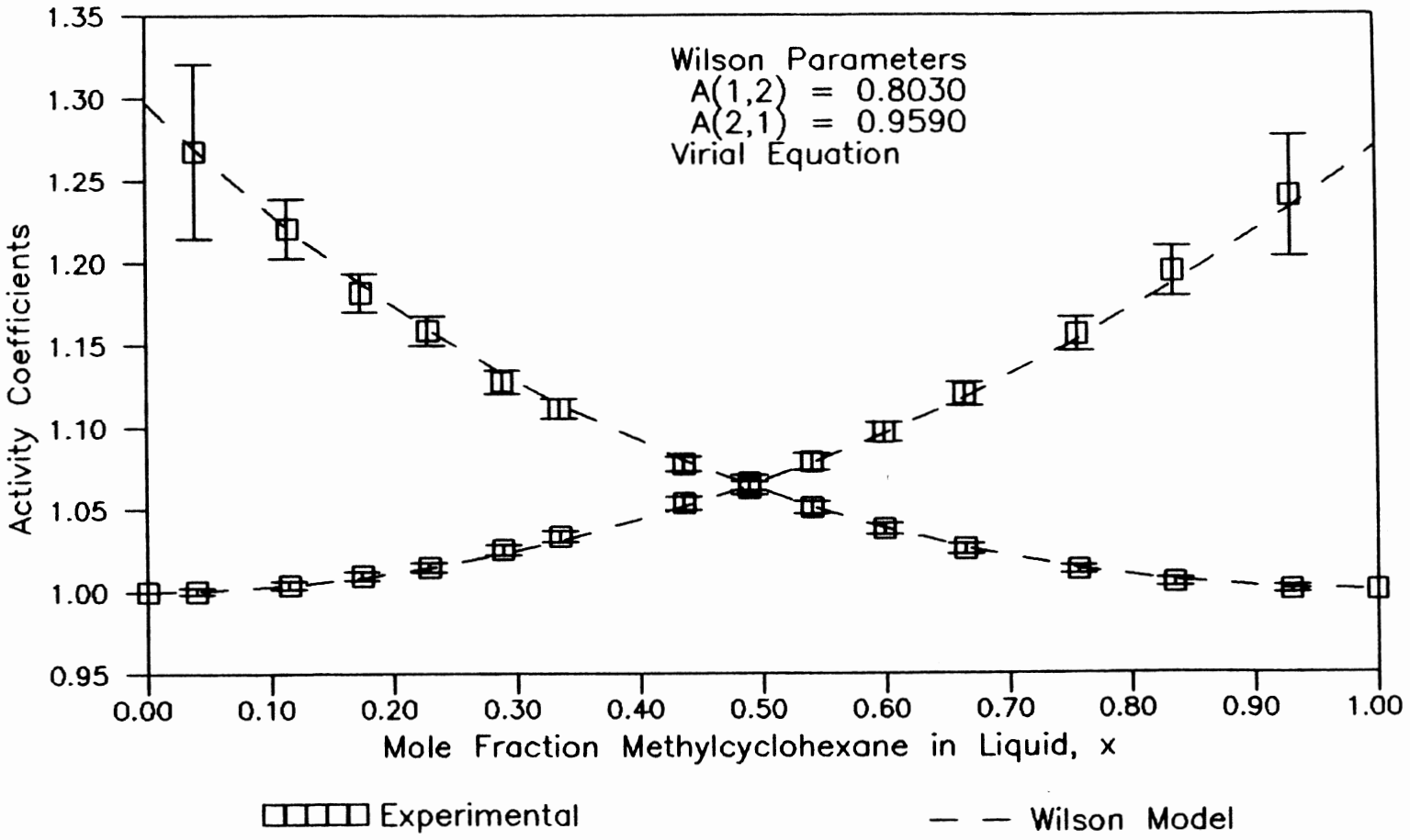

Figure 18. Activity Coefficients for Methylcyclohexane + Toluene at 90 C

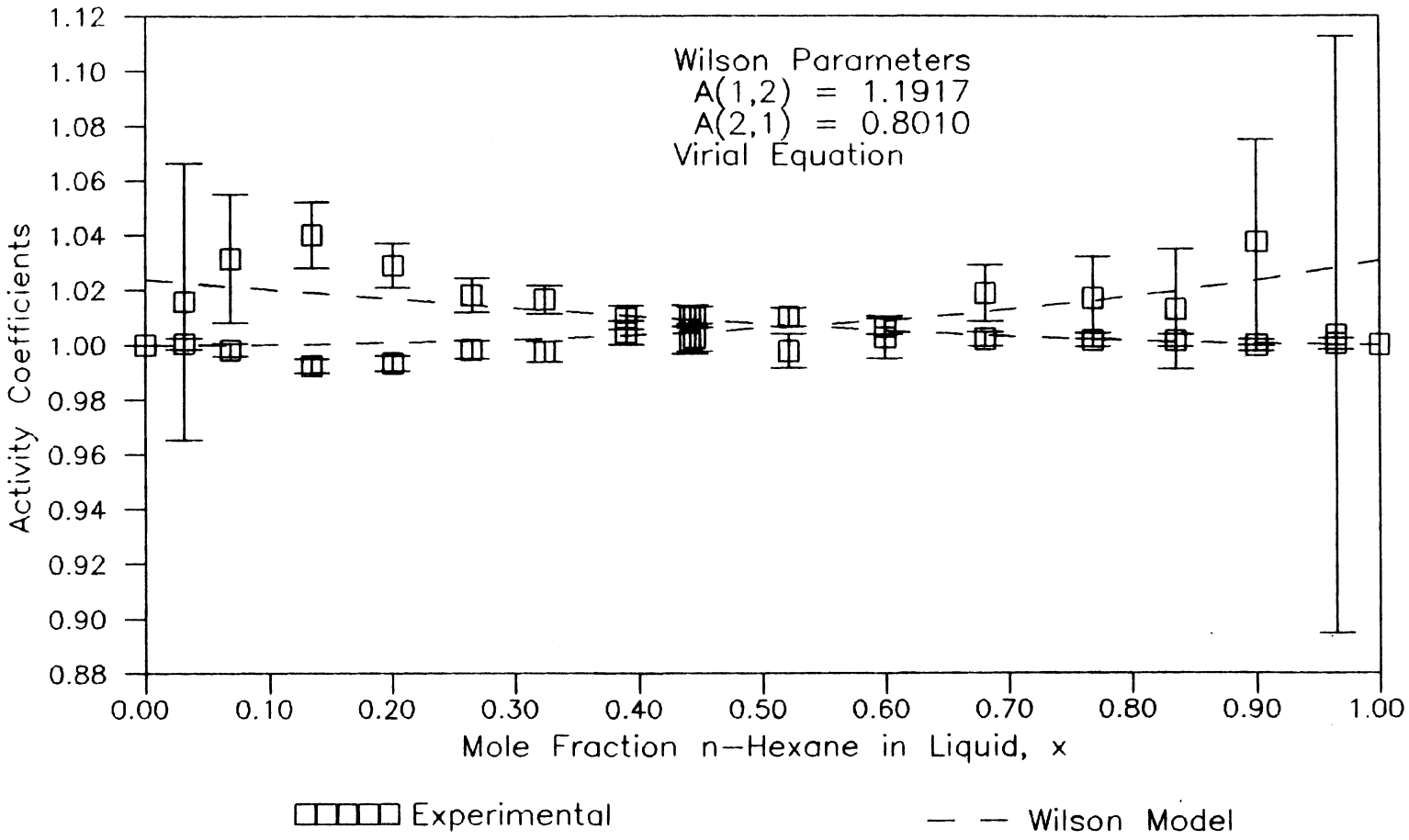

Figure 19. Activity Coefficients for n-Hexane + Methylcyclohexane at 760 mm Hg

coefficients are between 1.00 and 1.40 showing moderate deviations from ideality.

For system n-hexane + toluene at 760 mm Hg (Figure 20) the calculated activity coefficient are within the experimental values and hence the data are consistent for this system.

For the system n-hexane + toluene at 70 °C (Figure 21) the calculated activity coefficient are within the experimental uncertainty of this work, hence the data are consistent for this system.

The $\ln(\gamma_1/\gamma_2)$ plot is sensitive to scatter in the measured x and y values, but is relatively insensitive to scatter in the temperature and very insensitive to (almost independent of) scatter in the pressure values. The reason for this behavior is explained in the previous section.

For the system methylcyclohexane + toluene at 760 mm Hg the plot of activity coefficient ratio is shown in Figure 22, with error bars. As shown in this figure, a straight line can be drawn through mole fraction of 0.5 which touches all the error bars, while satisfying the equality of the positive and negatives areas, hence satisfying the area test for thermodynamic consistency. Similarly, straight lines can be drawn through the activity coefficient ratio plots (passing through x axis at x = 0.5) for the other systems, but they are not shown here.

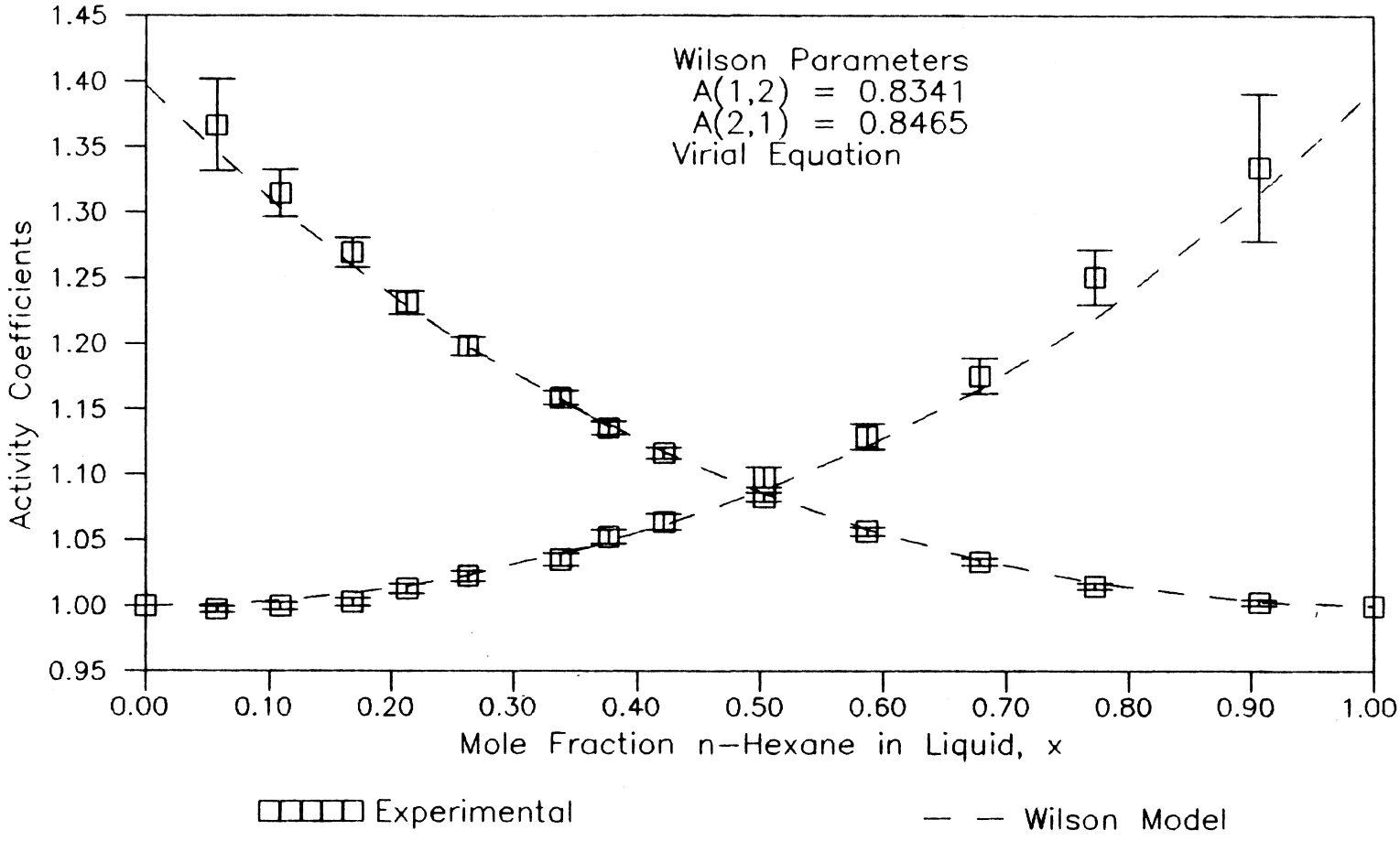

Figure 20. Activity Coefficients for n-Hexane + Toluene at 760 mm Hg

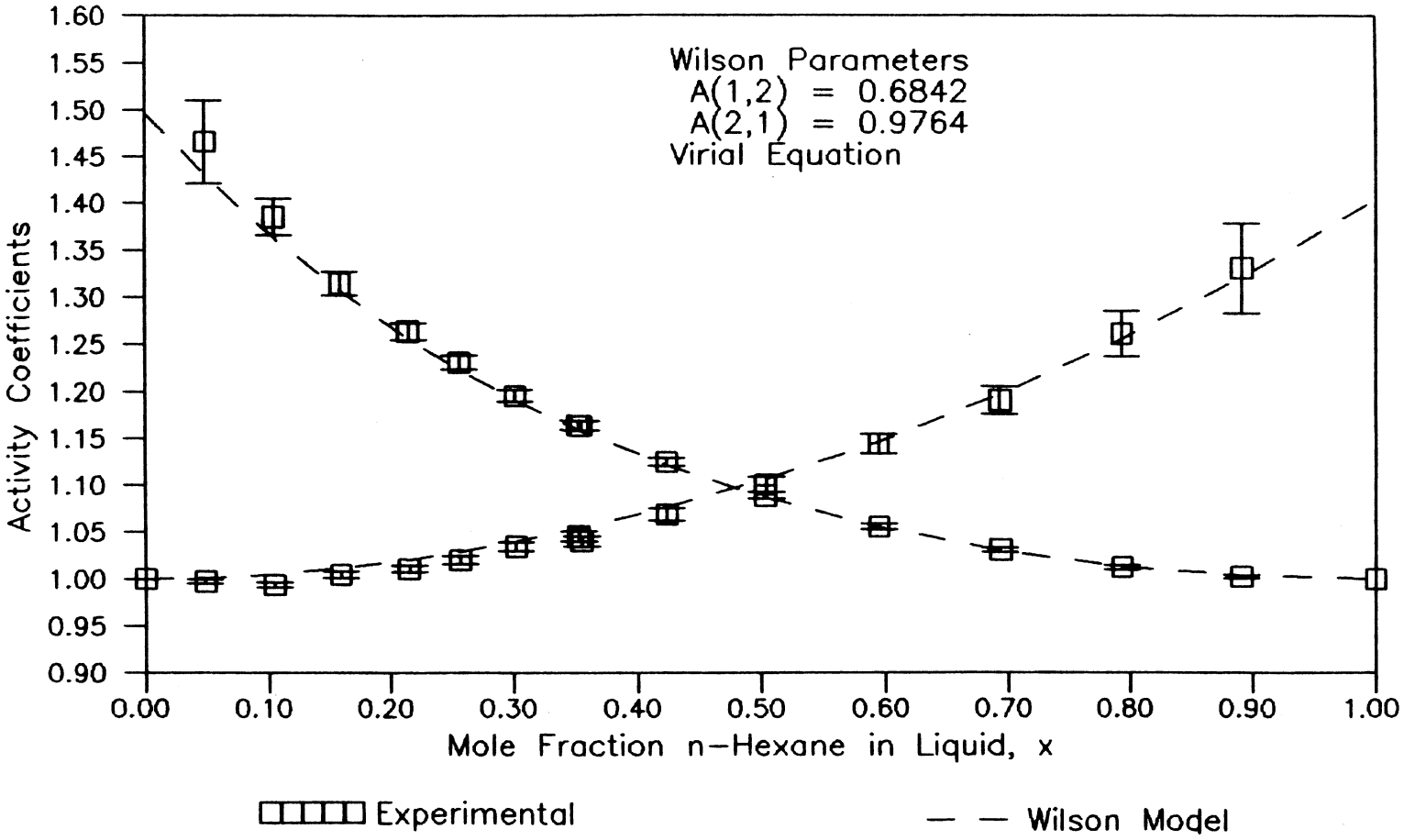

Figure 21. Activity Coefficients for n-Hexane + Toluene at 70 C

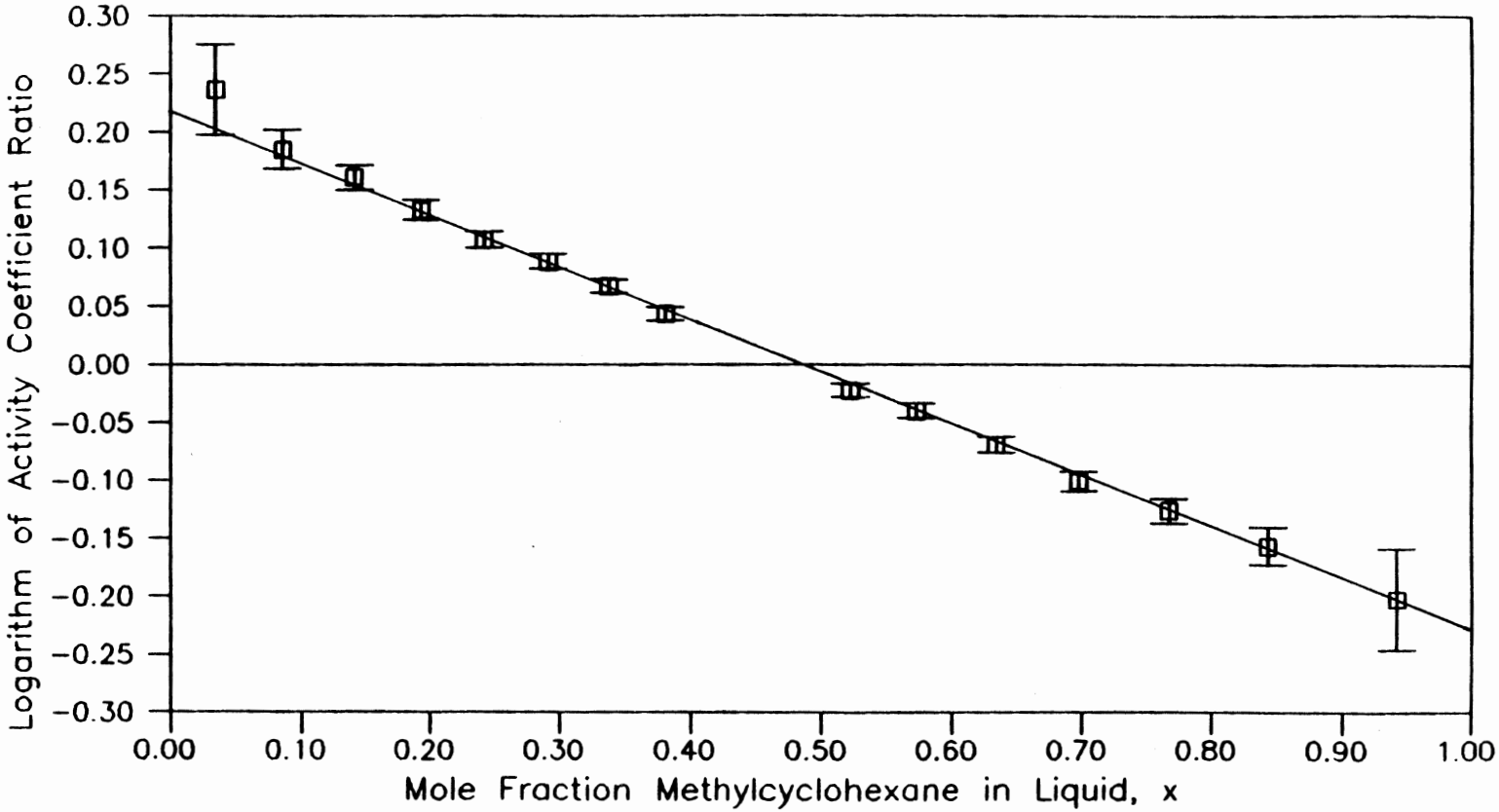

Figure 22. Experimental Acitivity Coefficient Ratio for Methylcyclohexane + Toluene at 760 mm Hg

CHAPTER VII

CONCLUSIONS AND RECOMMENDATIONS

The objective of the work reported in this thesis was to establish a low pressure vapor-liquid equilibrium facility. This involved design, construction and testing of new apparatus. The work included (a) review of the apparatuses used for studying low pressure vapor-liquid equilibrium, and (b) review of the subject of thermodynamic consistency of experimental data.

The major results from this study can be summarized as

1. An all glass still was designed and constructed which showed stable hydrodynamic and thermal behavior.
2. By measuring the vapor-liquid equilibrium data for the binaries formed among the constituents n-hexane, methylcyclohexane and toluene, stable operation of the still was confirmed for pressures range of 200-795 mm Hg and temperatures range of 70-110°C.
3. Comparisons with the works of other investigators confirm the accuracy of this work.
4. The analysis of the results shows that the data are thermodynamically consistent within their experimental uncertainty.
5. Pure component normal boiling point and vapor pressure

values obtained in this study do not agree with literature values.

From the information gained in this study, the following recommendations concerning future work may be made.

1. The vials used in determining the refractive index calibration curves should be sealed, to prevent vaporization while withdrawing samples.
2. The temperature probe should be replaced by a smaller one so that heat loss, if any, is reduced.
3. The vacuum jacket surrounding the equilibrium chamber should be silvered to reduce heat loss, if any, from the equilibrium chamber.
4. In future vapor-liquid equilibria studies, the auxiliary data (excess heats or volumes) required to employ rigorous thermodynamic consistency tests should be determined as an integral part of the study.
5. The cause for the differences in pure substance boiling points should be investigated and modifications in the apparatus and/or procedures made to correct this problem.
6. Measurements on more nonideal systems should be made to validate the applicability of the apparatus for such systems.

SELECTED BIBLIOGRAPHY

1. Abbot, M. M., Van Ness, H. C., "Classical Thermodynamics of Nonelectrolyte Solutions", Mc Graw-Hill Book Company, New York (1982).

2. Abbot, M. M., "Low Pressure Phase Equilibria: Measurement of VLE", Fluid Phase Equilibria, 29, 193-207 (1986).

3. Ambrose, D., "Vapor Pressures of Some Aromatic Hydrocarbons", J. Chem. Thermodynamics 19, 1007-1008 (1987).

4. Ambrose, D., "Vapor-Liquid Critical Properties", Report 107, National Physical Laboratory, Teddington, Middlesex TW11 OLW 107, February 1980.

5. Bedell, M., "The Effect of Fluid Properties on Ebuliometer Operation", Fluid Phase Equilibria, 46, 85-94 (1989).

6. Besley, L. M., Bottomley, G. A., "Vapor Pressure of Toluene From 273.15 to 298.15 K", J. Chem. Thermodynamics, 6, 577-580 (1974).

7. Boublik, T., Fried, V., Hala, E., "The Vapor Pressures of Pure Substances", Elsevier, New York, 1984.

8. Coca, J., Pis, J. J., "Effect of Morpholine on Vapor-Liquid Equilibrium of the System Methylcyclohexane-Toluene", J. Chem. Eng. Data., 24, 103-105 (1979).

9. Denbigh K., "Principles of Chemical Equilibrium", The University Press, Cambridge, 1955.

10. Ellis, S.R.M., Broughton, F. R., Soares, L.J.S., "Recommended Test Mixtures For Distillation Columns", Inst. Of Chem. Eng., London, (1969)

11. Ellis, S.R.M., Contractor, R. M., "Vapor-Liquid Equilibria at Reduced Pressure", Birmingham Univ. Chem. Engr. 15, 10-13 (1964).

12. DECHEMA, Chemistry Data Series, Dechema, Schon & Wetzel Gmbh, Frankfurt (1986).

13. Engineering Sciences Data, ESDU International Plc., London (1987).

14. Fenske, M. R., Myers, H. S., Quiggle, D., "Binary Mixture For Determining Efficiences of Fractionating Columns Operating At Reduced Pressures", Ind. Eng. Chem., 42, 649-653 (1950).

15. Garner, F. H., Hall, R. T. W., "Vapor-Liquid Equilibria of C_7-Hydrocarbon-Furfural Systems", J. Petrol. Inst., 41, 1-28 (1955).

16. Gibbs, R. E., Byer, S. M., Van Ness, H. C., "Vapor Liquid Equilibrium, Part 1. An Appraisal of Data Reduction Methods", AICHE J., 19(2) 238-244 (1973).

17. Hala, E., Pick, J., Fried, V., Vilim, O., "Vapor Liquid Equilibrium", Pergman Press, New York, 1967.

18. Harsted, B. S., Thomsen, E. S., "Excess Enthalpies From Microcalorimetry 3. Excess Enthalpies for Binary Liquid Mixtures of Aliphatic and Aromatic Hydrocarbons, Carbon Tetrachloride, Cholrobenzene, and Carbon Disulphide", J. Chem. Thermodynamics, 7, 369-376 (1975).

19. Kay, W. B., "Vapor Pressures and Saturated Liquid and Vapor Densities of Cyclopentane, Methylcyclopentane Ethylcyclopentane and Methylcyclohexane", Ind. Eng. Chem., 28, 1273-1277 (1936).

20. Lencka, M., "Measurements of the Vapor Pressures of Pyridine, 2-Methyl Pyridine, 2-4, Dimethylpyridine, 2,6-Dimethyl Pyridine, and 2,4,6-Trimethyl Pyridine from 0.1 kpa to Atmospheric Pressure Using a Modified Swietoslawski Ebuliometer", J. Chem. Thermodynamics, 22, 473-480, (1990).

21. Letcher, T. M., "Thermodynamics of Aliphatic Amine Mixtures 1. The Excess Volumes of Mixing for Primary, Secondary, and Tertiary Aliphatic Amines With Benzene and Substituted Benzene Compounds", J. Chem. Thermodynamics, 4, 159-173 (1972).

22. Letcher, T. M., "Thermodynamics of Mixtures Containing Aliphatic Amines 2. The Excess Volumes of Primary, or Secondary, or Tertiary Aliphatic Amines + Substituted Cyclohexanes", J. Chem. Thermodynamics, 4, 551-564 (1972).

23. Liebermann, E., Fried, V. F., "Estimation of The Excess Gibbs Free Energy and Enthalpy of Mixing of Binary Nonassociated Mixtures", Ind. Eng. Chem. Fundam., 11, 350-354 (1972).

24. Malanowski, S., "Experimental Methods for Vapor Liquid Equilibria; Part I. Circulation Methods", Fluid Phase Equilibria, 8, 197-219 (1982).

25. Michishita, T., Arai, Y., Saito, S., "Vapor-Liquid Equilibriums of Hydrocarbons at Atmospheric Pressure", Kagaku Kogaku, 35, 111-116 (1971).

26. Myers, H. S., "Vapor-Liquid Equilibrium Data for Binary Mixtures of Paraffins and Aromatics", Ind. Eng. Chem., 47, 2215-2219 (1955).

27. Myers, H. S., "V-L Equilibrium for Naphthenes and Paraffins", Petrol. Refiner., 36, 175-178 (1957).

28. Olson, J. D., "Measurement of Vapor-Liquid Equilibria by Ebuliometry", Fluid Phase Equilibria, 52, 209-218 (1989).

29. Prausnitz, J., Anderson, T., Grens, E., Eckert, C., Hsieh, R., O'Connell J., "Computer Calculations for Multicomponent Vapor-Liquid and Liquid-Liquid Equilibria", Prentice Hall, Inc., New Jersey (1980).

30. Quiggle, D., Fenske, M. R., "Vapor-Liquid Equilibria of Methylcyclohexane-Toluene Mixtures", J. Am. Chem. Soc. 59, 1829-1832 (1937).

31. Reid, R. C, Prausnitz, J. M., Sherwood, T. K, "The Properties of Gases and Liquids", Third Edition, McGraw-Hill Book Company, New york (1977).

32. Robinson, R. L., "A Theoretical And Experimental Investigation Of Vapor Liquid Equilibria in The Binary Systems Formed Among The Constituents Normal Hexane, Methylcyclohexane, And Toluene", M.S. Thesis, Oklahoma State University (1962).

33. Rogalski, M., Malanowski, S., "Ebuliometer Modified For The Accurate Determination Of Vapor Liquid Equilibrium", Fluid Phase Equilibria, 5, 97-112 (1980).

34. Rogalski, M., Rybakiewicz, K., Malanowski, S., "Rapid And Accurate Method For Determination Of Vapor Liquid Equilibrium", Berichte der Bunsen-Gesellschaft. Bd. 81.Nr.10., 1070-1073 (1977).

35. Saito, S., "Vapor-Liquid Equilibriums of Normal Paraffin-Aromatic Systems", Asahi Garasu Kogyo Gijutsu Shorekai Kenkyu Hokoku, 15, 397-407 (1969).

36. Schneider, G., "Verdampfungsgleichgewichte im System Methylcyclohexan-Toluol-Anilin", Z. Physik. Chem. (Frankfurt), 27, 171-184 (1961).

37. Sieg, L., "Flussigkeit-Dampf-Gleichgewichte in Binaren Systemem von Kohlenwasserstoffen Typs", Chem. Ing. Tech., 22, 322-326 (1950).

38. Thijssen H. A. C, "Thermodynamic Evaluation of Binary Vapor-Liquid Equilibria", Chem. Eng. Sci., 4, 75-80 (1955).

39. Timmermans J., "Physico-Chemical Constants of Pure Organic Compounds", Elsevier, New York, 1950.

40. Topping, J., "Errors of Observation and Their Treatment", Reinhold Publishing, New York, 1957.

41. Tsonopoulos, C., "An Empirical Correlation of Second Virial Coefficients", AICHE J. 20, 263-272 (1974).

42. Tyminski, B., Klepanska, A., "Rownowagi Ciecz-Para Dla Ukladu Metylocykloheksan-Toluen Podcisnieniami 200, 400 i 760 mm Hg", Inz. Chem. 7(1), 193-205 (1977).

43. Wichterle, I., Boublikova, L., "Semimicromethod for Determination of Partial Pressures of Solutions", Ind. Eng. Chem. Fundam., 8, 585-588, (1969).

44. Wichterle, I., Hala, E., "Vapor-Liquid Equilibrium Data Bibliography", Supplement 1-4, Elsevier, 1976, 1979, 1982, 1985.

45. Wisniak, J., Tamir A., "Physical Sciences Data 1. Mixing and Excess Thermodynamic Properties. A Literature Source Book", Elsevier Scientific Publishing Company, New York, 1978.

46. Yaws, C. L., Chen, D., Yang, H. C., Tan, L., Nico, D., "Critical Properties of Chemicals", Hydrocarbon Processing, July, 61 (1989).

47. Young, H. D., "Statistical Treatment of Experimental Data", McGraw-Hill, New York, 1962.

APPENDIX A

PRESSURE TEST SET CALIBRATION

The Texas Instrument pressure controller (model 156) used in this work was calibrated using a newly calibrated Texas Instrument Pressure Test Set (model 145), and the results are tabulated below. These results were fitted to a cubic equation, and the root-mean-square error resulting from this fit is 0.013 mm Hg. Table 14 gives the observations and Figure 23 shows the calibration results for the presure measurement, which shows that the maximum deviation from the cubic fit was 0.03 mm Hg, which is about the instrumental uncertainity of 0.02 mm Hg. The notation used in the tables and figure which follow is:

OBS = Observation number

R = Reading on pressure test set used in this work, model 156

Pobs. = Pressure on model 145, newly calibrated Texas Instrument pressure set, mm Hg.

Pcalc. = Pressure calculated from a cubic equation fitted to R as a function of Pobs.

DEV = Pcalc. - Pobs.

TABLE 14

CALIBRATION RESULTS FOR PRESSURE MEASUREMENTS

R	Pobs.	Pcalc.	Dev
226228	760	760.001	0.001
223240	750	749.997	-0.003
217277	730	730.026	0.025
214291	720	720.025	0.025
211298	710	710.003	0.003
208302	700	699.967	-0.032
205322	690	689.987	-0.013
202338	680	679.992	-0.007
199351	670	669.990	-0.010
196369	660	660.002	0.002
193383	650	649.999	-0.001
190403	640	640.019	0.018
187415	630	630.009	0.008
184427	620	620.002	0.002
181442	610	610.004	0.003
178454	600	599.993	-0.006
175467	590	589.988	-0.012
172480	580	579.984	-0.015
169491	570	569.972	-0.027
166511	560	559.989	-0.011
163524	550	549.985	-0.015
160548	540	540.015	0.015
157564	530	530.020	0.019
154574	520	520.006	0.006
151587	510	509.999	0.000
148597	500	499.986	-0.014
145615	490	489.996	-0.004
142631	480	480.001	0.001
139645	470	470.000	0.000
136660	460	460.002	0.002
133670	450	449.989	-0.010
130692	440	440.013	0.013
127707	430	430.018	0.017
124720	420	420.012	0.012
121733	410	410.010	0.010
118743	400	399.995	-0.005
115764	390	390.020	0.020
112777	380	380.017	0.017
109790	370	370.015	0.014
106803	360	360.012	0.012
103815	350	350.005	0.004
100827	340	340.001	0.001
97842	330	330.005	0.005
94856	320	320.007	0.007
91864	310	309.991	-0.008

TABLE 14 (Continued)

R	Pobs.	Pcalc.	Dev
88877	300	299.991	-0.009
85889	290	289.986	-0.014
82904	280	279.993	-0.007
79915	270	269.987	-0.013
76929	260	259.991	-0.008
73937	250	249.978	-0.022
70952	240	239.985	-0.014
67965	230	229.989	-0.010
64977	220	219.987	-0.012
61991	210	209.994	-0.006
59006	200	200.007	0.006
56015	190	189.999	-0.005
53028	180	180.003	0.003
50042	170	170.012	0.012
47051	160	160.006	0.006
44061	150	150.003	0.003
41076	140	140.016	0.015

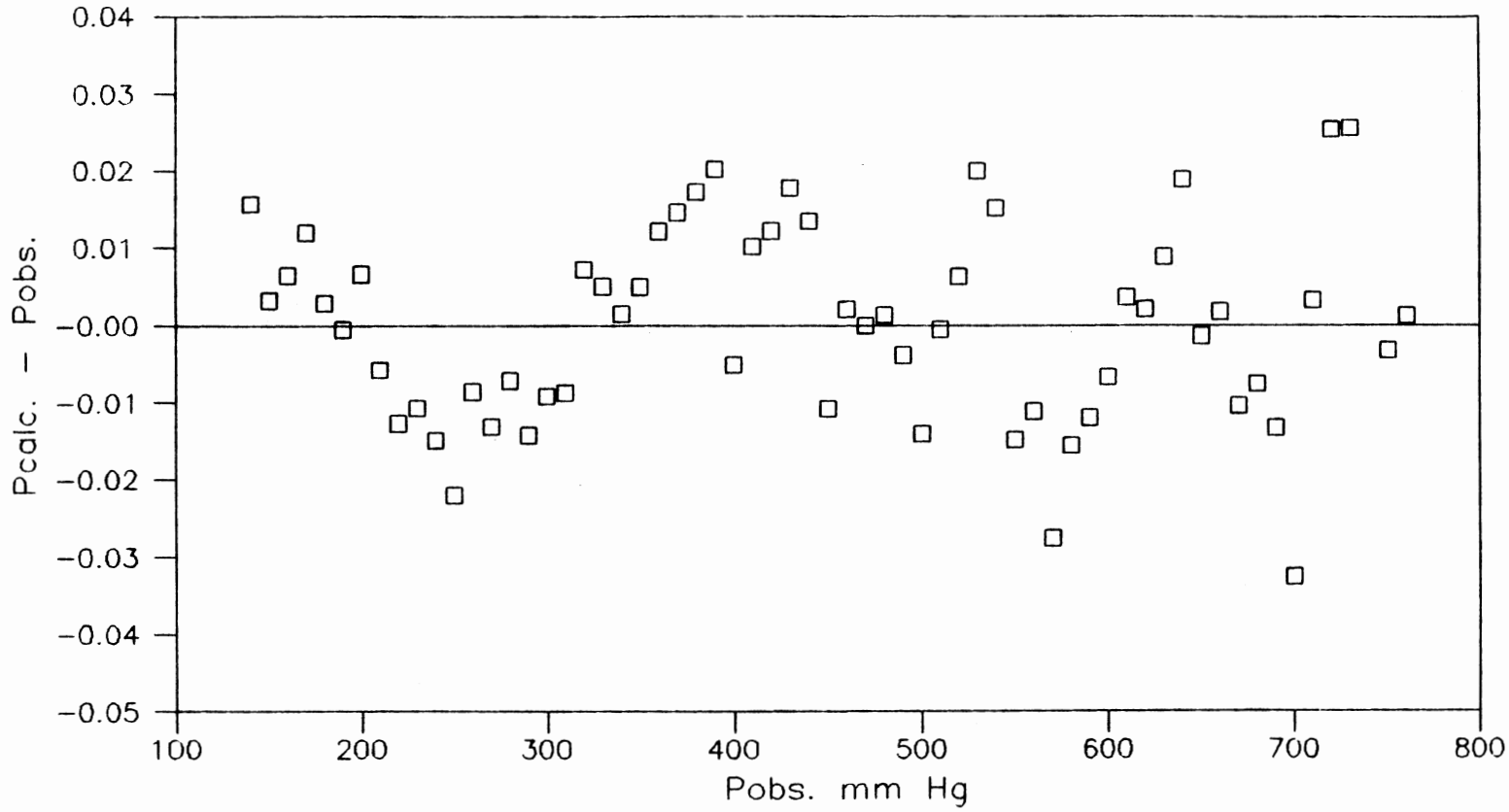

Figure 23. Calibration Results for Pressure Measurements.

The root-mean-square error resulting from this fit is 0.013 mm Hg. The fitted equation is:

$$P = 2.66983525 + 0.003341989*R + 4.53326\ E(-11)*(R)^2 - 8.9688\ E(-17)*(R)^3$$

This equation was used to calculate pressures from the readings on the pressure regulator.

APPENDIX B

REFRACTIVE INDEX-COMPOSITION CALIBRATIONS

The relationship between composition and refractive index for each binary system studied in this work is given below. Calibration of composition to refractive index shows that the root-mean-square error in composition for different species was about 0.001 (0.00096, for methylcyclohexane + toluene mixture, 0.0011 for n-hexane + methylcyclohexane mixture and 0.0013 for n-hexane + toluene mixture). Table 15-17 gives the observations, and plots (Figures 24-26) used to determine the best curve fit are also shown for each system studied. The notation used in the tables and figures which follow is:

R = refractometer scale reading

x_1 = experimental mole fraction of component one

x_c = mole fraction of component one calculated from the fitted equation

DEV = $x_c - x_1$

TABLE 15

REFRACTIVE INDEX CALIBRATION FOR METHYLCYCLOHEXANE (1) + TOLUENE (2)

R	X1	XC	Dev
28.79	0.0000	-0.0007	-0.0007
27.76	0.0541	0.0548	0.0008
26.88	0.1027	0.1036	0.0008
26.08	0.1498	0.1491	-0.0007
25.26	0.1972	0.1972	0.0000
23.63	0.2978	0.2979	0.0001
22.07	0.4025	0.4022	-0.0003
20.77	0.4975	0.4962	-0.0012
19.59	0.5876	0.5881	0.0004
18.28	0.6962	0.6980	0.0018
17.25	0.7918	0.7911	-0.0006
16.22	0.8913	0.8905	-0.0008
15.71	0.9417	0.9422	0.0005
15.16	1.0000	0.9998	-0.0001

TABLE 16

REFRACTIVE INDEX CALIBRATION FOR
n-HEXANE (1) + TOLUENE (2)

R	X1	XC	Dev
28.820	0.0000	-0.0006	-0.0006
27.270	0.0526	0.0529	0.0004
25.875	0.1017	0.1027	0.0009
24.610	0.1493	0.1492	-0.0001
23.315	0.1981	0.1982	0.0016
20.750	0.3027	0.3005	-0.0022
18.335	0.4016	0.4038	0.0022
16.330	0.4967	0.4955	-0.0012
14.270	0.5960	0.5958	-0.0002
12.275	0.6987	0.6996	0.0009
10.500	0.7968	0.7978	0.0009
8.880	0.8941	0.8925	-0.0015
8.060	0.9428	0.9424	-0.0004
7.130	1.0000	1.0007	0.0007

TABLE 17

REFRACTIVE INDEX CALIBRATION FOR METHYLCYCLOHEXANE (1) + n-HEXANE (2)

R	X1	XC	Dev
7.130	0.0000	-0.0001	-0.0001
7.540	0.0526	0.0524	-0.0002
7.955	0.1044	0.1047	0.0004
8.340	0.1527	0.1543	0.0016
8.700	0.2015	0.1999	-0.0015
9.530	0.3057	0.3045	-0.0012
10.295	0.4000	0.4003	0.0002
11.110	0.5012	0.5017	0.0005
11.720	0.5769	0.5773	0.0004
12.700	0.6972	0.6982	0.0009
13.500	0.7979	0.7964	-0.0015
14.340	0.8988	0.8993	0.0004
14.695	0.9436	0.9427	-0.0009
15.170	1.0000	1.0007	0.0007

The fitted equations are

For methylcyclohexane + toluene:

xc = 3.655328644 - 0.26013874*4R + 0.006696383*R**2

-0.000071955*R**3

For n-hexane + toluene:

xc = 1.512398 - 0.080444*R + 0.001300*R**3 - 0.000011465*R**3

For methylcyclohexane + n-hexane:

xc = -0.960835 + 0.14227*R - 0.001235*R**2 + 0.000025069*R**3

These equations were used for calculating the experimental equilibrium vapor-liquid compositions from the corresponding

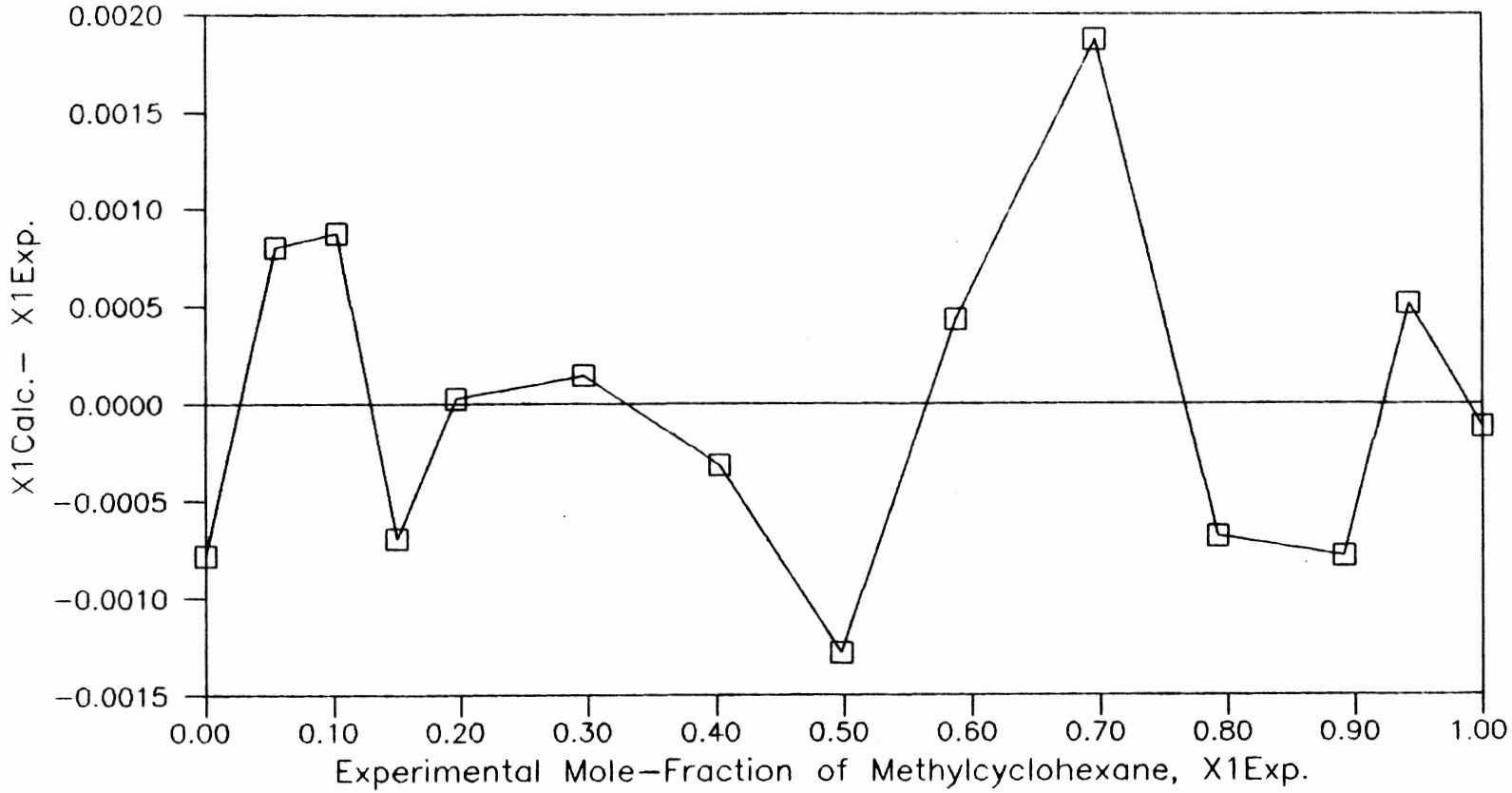

Figure 24. Results of Composition–Refractive Index Calibrations for Methylcyclohexane + Toluene

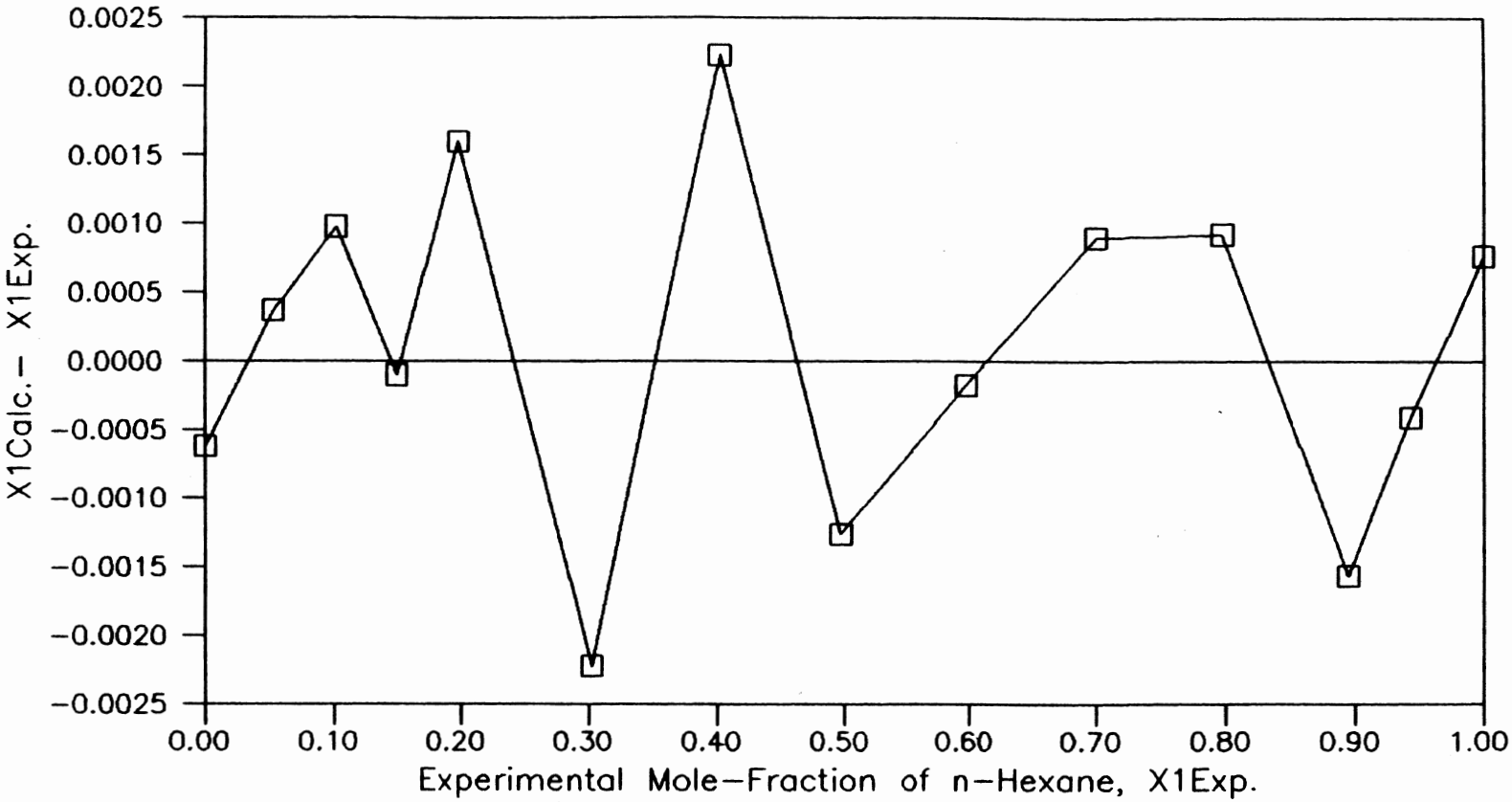

Figure 25. Results of Composition−Refractive Index Calibrations for n−Hexane + Toluene

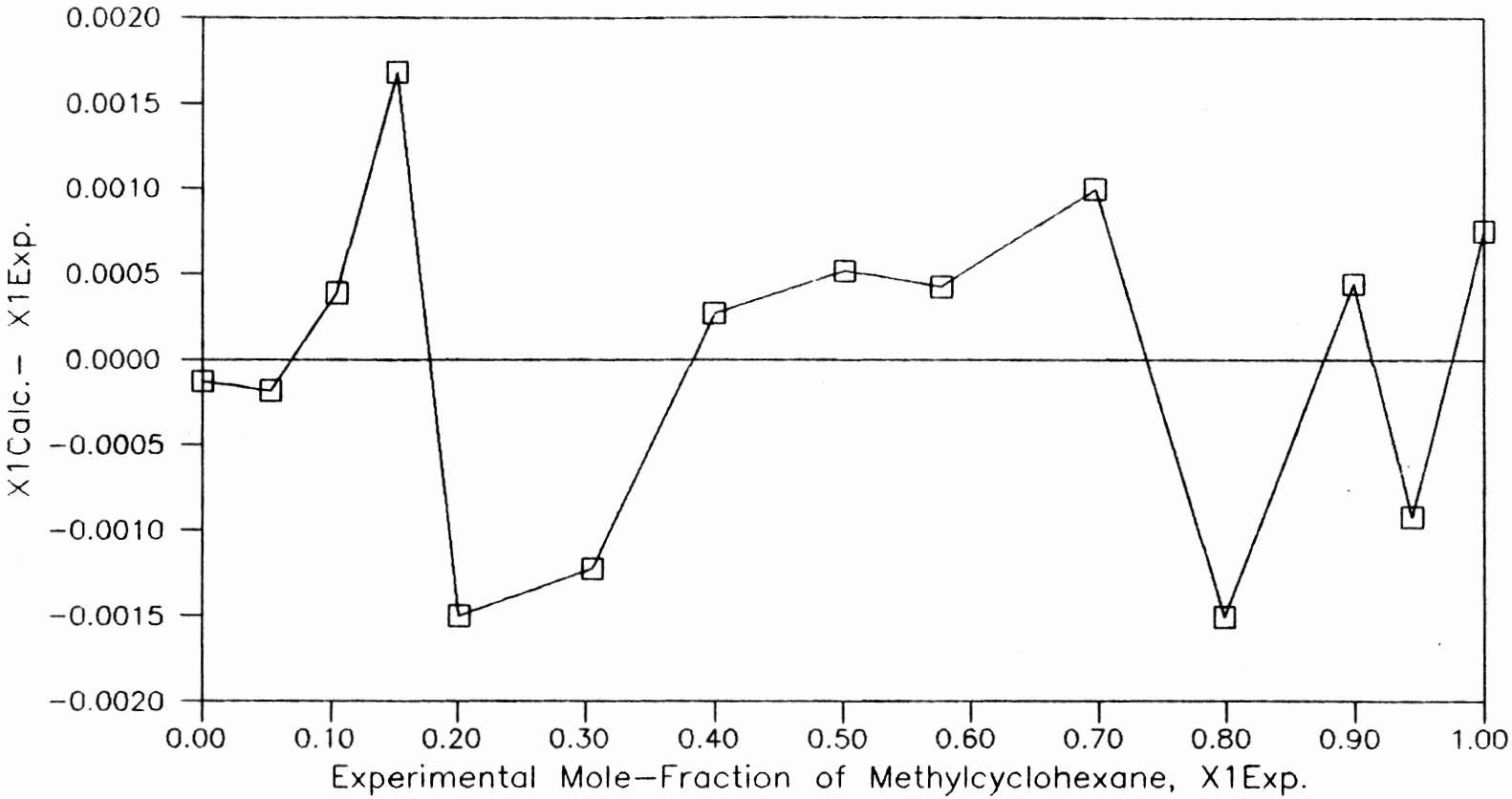

Figure 26. Results of Composition−Refractive Index Calibrations for Methylcyclohexane + n−Hexane

refractometer readings.

APPENDIX C

ERROR PROPAGATION

Experimental results or observations are invariably given in terms of numbers. Experimental observations always have inaccuracies. In using numbers which result from experimental observations, it is necessary to know the extent of these inaccuracies. If one is comparing a number based on a theoretical prediction with one based on experiment, it is necessary to know something about the accuracies of both of these in order to judge the extent of their agreement.

Errors are usually distinguished as systematic and random errors. Systematic errors are errors associated with the particular instruments or technique of measurement being used. These errors can be reduced or eliminated through experience, as was done in this work by repeated measurements.

Random errors are produced by a large number of unpredictable and unknown variations in the experimental conditions. Random errors can be dealt with statistically, as was done in this work.

If one uses various experimental observations to calculate a result, and if the observations have errors associated with them, then the result will also be in error

by an amount which depends on the errors of individual observation. The effect which errors in measurements have on the error of the result of a calculation which incorporates these measurements can be explained as follows.

For our case is calculated from several observed quantities P, x, y, P^{sat}, expressed as γ'

$$\gamma = f (P, x, y, P^{sat}) \qquad (C-1)$$

As explained by Topping (40), it can be shown that in terms of fractional standard deviations we obtain,

$$(\sigma_\gamma / \gamma)^2 = (\sigma_y / y)^2 + (\sigma_x / x)^2 + (\sigma_p / p)^2 + (\sigma_{P^{sat}} / P^{sat})^2 \qquad (C-2)$$

Since P^{sat} is related to the measured temperature, we have

$$(\sigma_{P^{sat}} / P^{sat})^2 = [(dP/dT) \sigma_T / P^{sat}]^2 \qquad (C-3)$$

The above equations were used to find the error in calculating values. An example follows.

For methylcyclohexane + toluene at 760 mm Hg at x = 0.1415, y = 0.2010 and = 1.18 the above equations were used as follows:

$$\left(\frac{dT}{dP} \right)_{mch} = 0.04^\circ C/mm\ Hg \quad \text{and} \quad \left(\frac{dT}{dP} \right)_{toluene} = 0.044^\circ C/mm\ Hg$$

The above values were obtained from reference 13. Therefore for the mixture, the following was used:

$$\left(\frac{dT}{dP}\right)_{mch+tol} = 0.045\ ^{\circ}C/mm\ Hg$$

Also, the estimated uncertainties for temperature, pressure and compositions were 0.02°C, 0.05 mm Hg and 0.001 mole fraction respectively.

Hence from Equations C-2 and C-3,

σ_γ = 0.010 for the above point.

APPENDIX D

DISCUSSION OF DATA ANALYSIS

System Methylcyclohexane(1) + Toluene(2) at 90 °C

Figures 27 and 28 shows the data of this work and the work of Scheinder. Deviations of experimental pressure from the pressure calculated from Wilson equation (Figure 29) show random scatter for this work. The data of Scheinder (36) were not compared for deviations in pressures since he did not present the pure component vapor pressures. Deviations of experimental vapor composition (Figure 30) from vapor composition calculated using Wilson parameters are all positive and small for this work. Comparison of deviations (Figure 31) of experimental vapor compositions from vapor compositions calculated using Wilson parameters between this work and work of Scheinder shows that the scatter in the data of Scheinder are higher than this work.

System n-Hexane(1) + Methylcyclohexane(2) at 760 mm Hg

The detailed analysis of this system is shown in Figures 32-37.

The x-y and T-x,y, plots (Figure 32 and 33) show the qualitative similarity of the data by several investigators. The deviations of experimental temperatures from temperatures

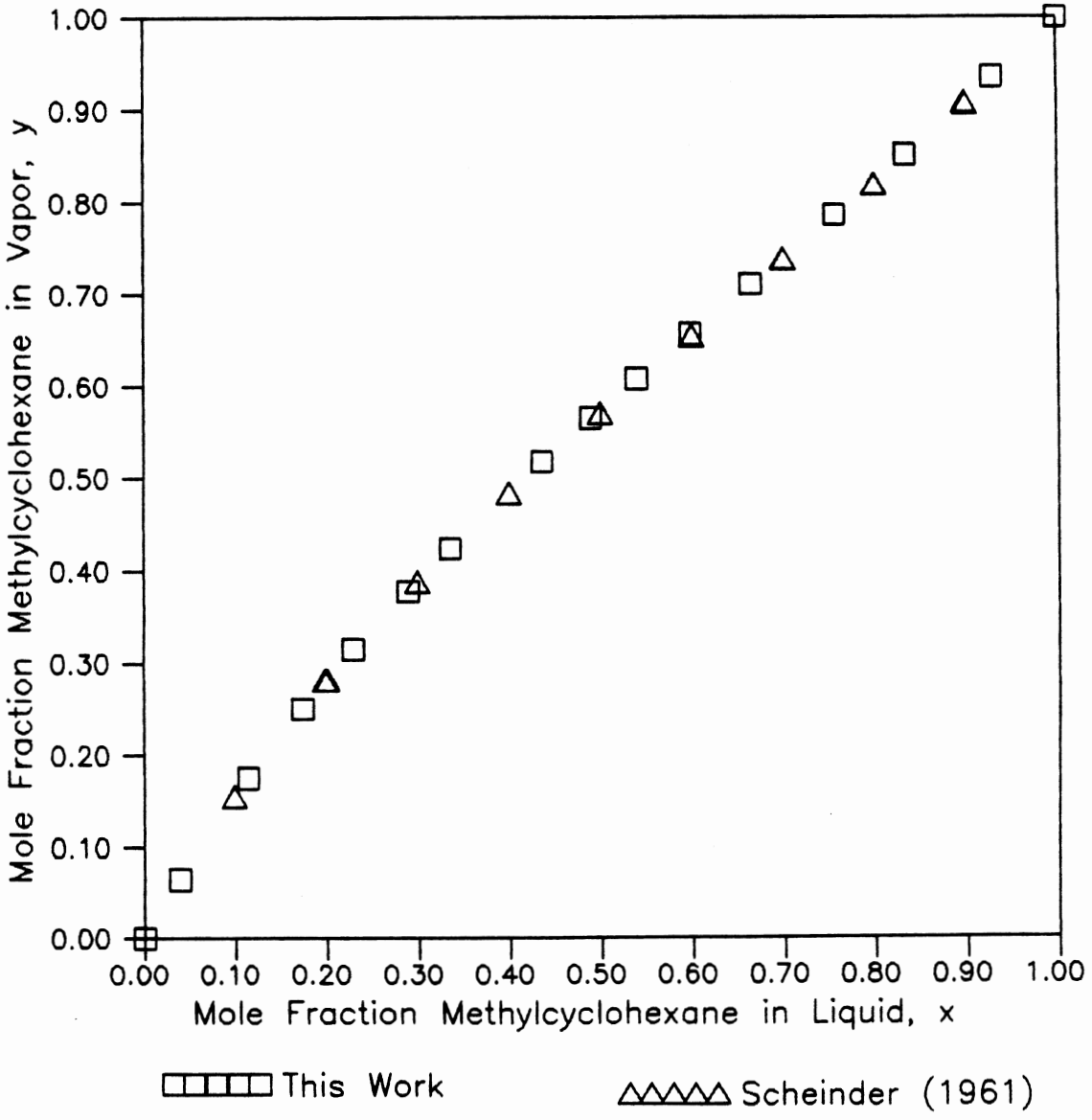

Figure 27. Experimental Equilibrium Phase Compositions for Methylcyclohexane + Toluene at 90 C

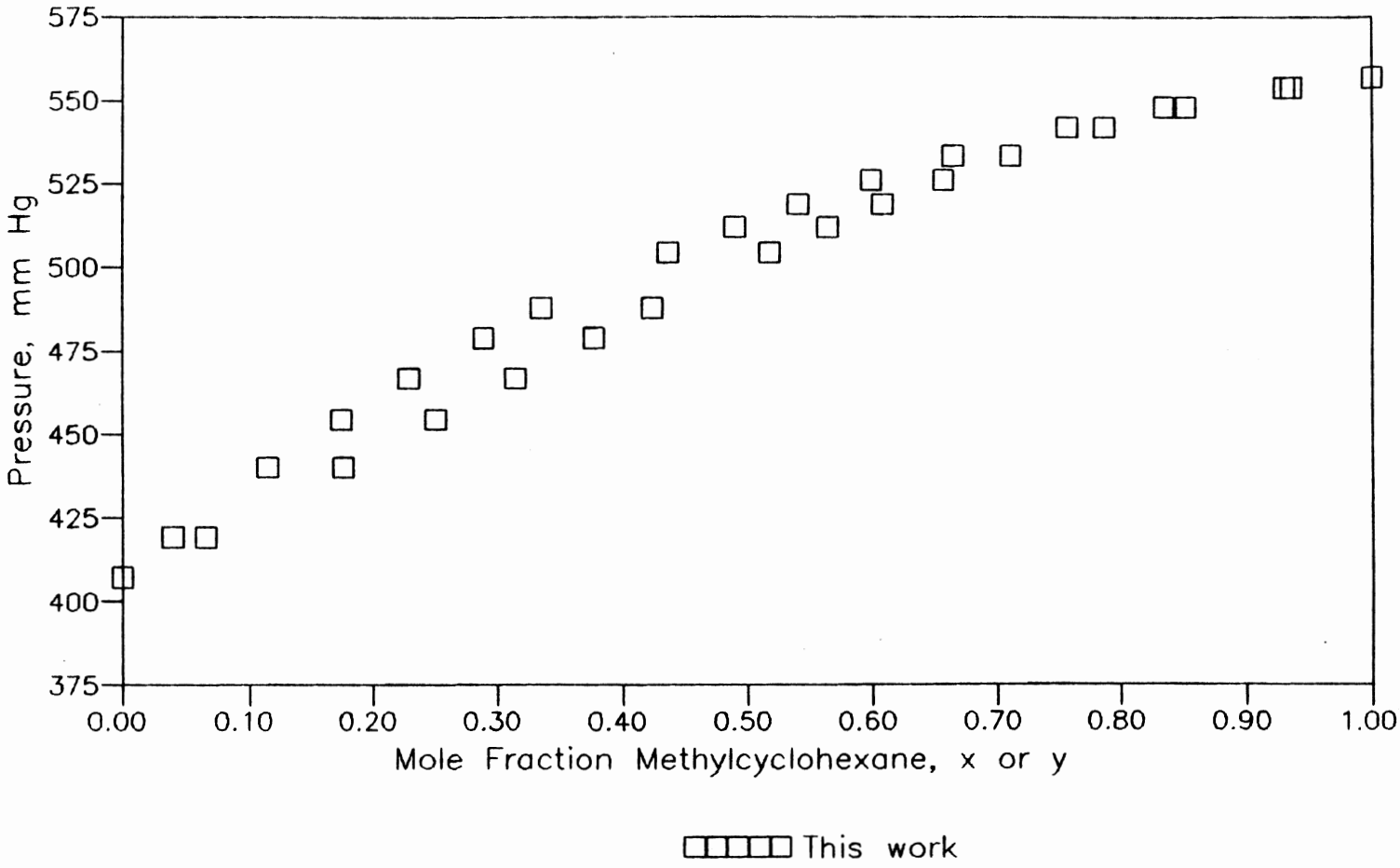

Figure 28. Experimental Phase Behavior (P−x,y) for Methylcyclohexane + Toluene at 90 C

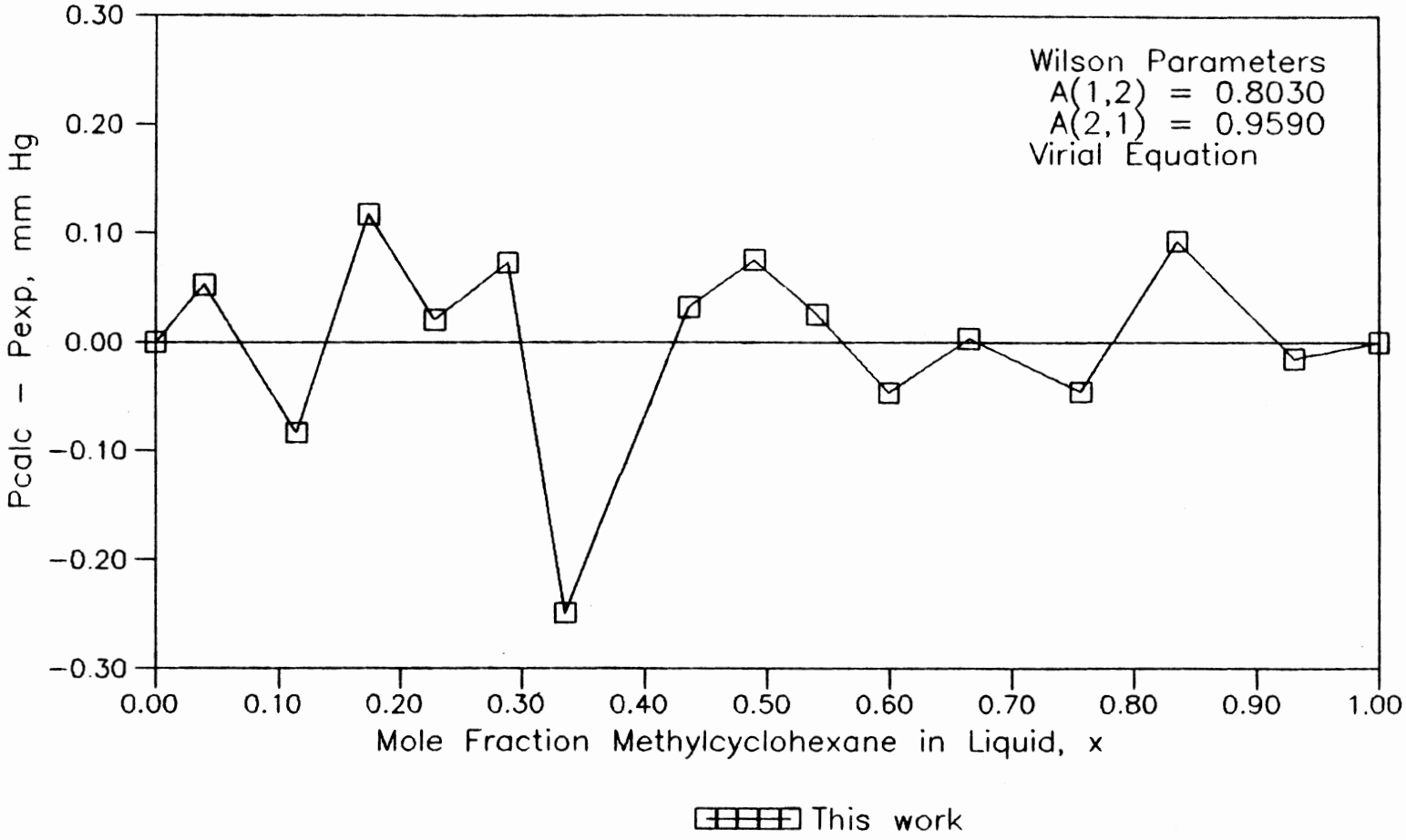

Figure 29. Deviations of Calculated Pressures from Wilson Equation for Methylcyclohexane + Toluene at 90 C

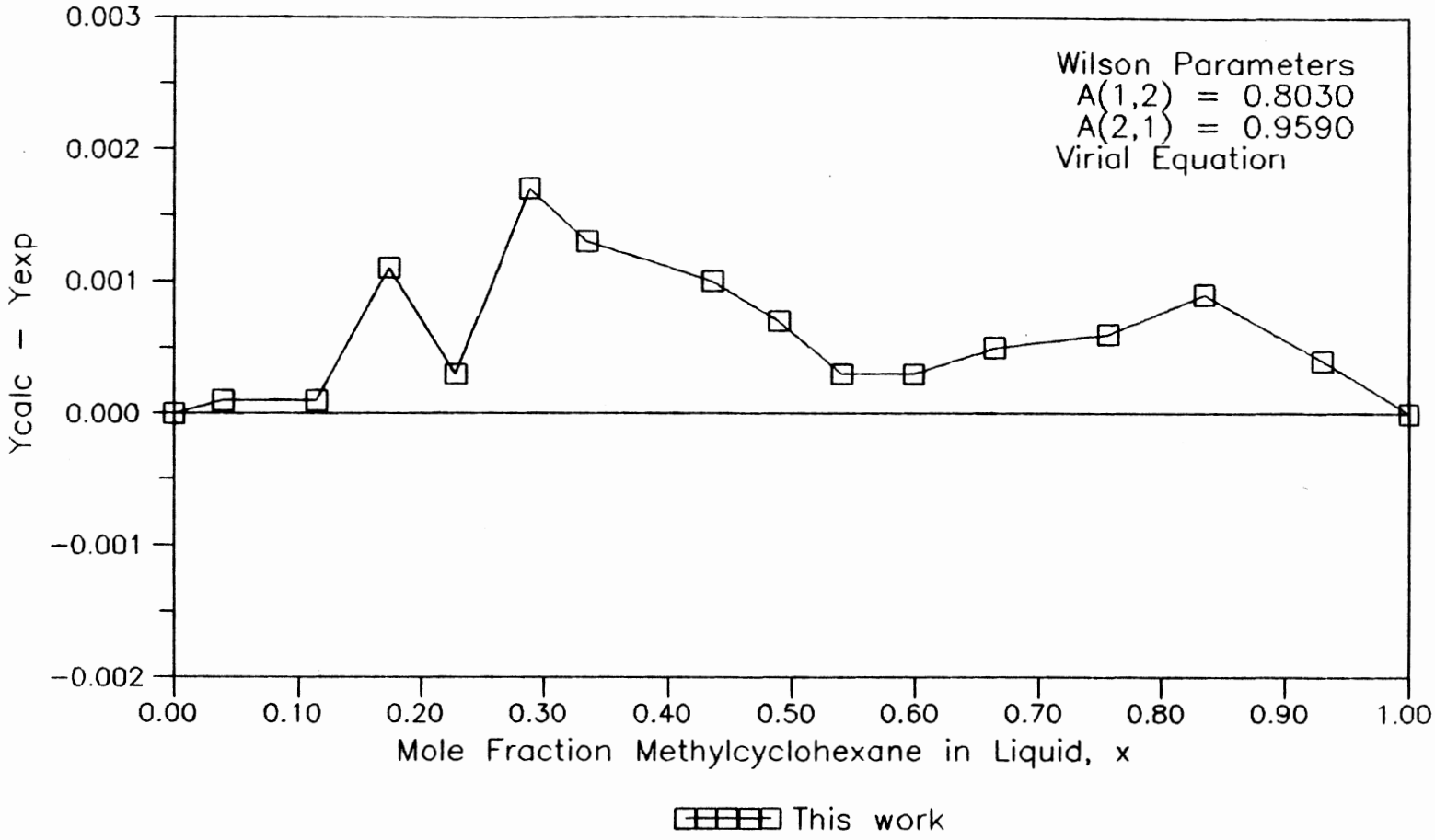

Figure 30. Deviations of Calculated Vapor Compositions from Wilson Equation for Methylcyclohexane + Toluene at 90 C

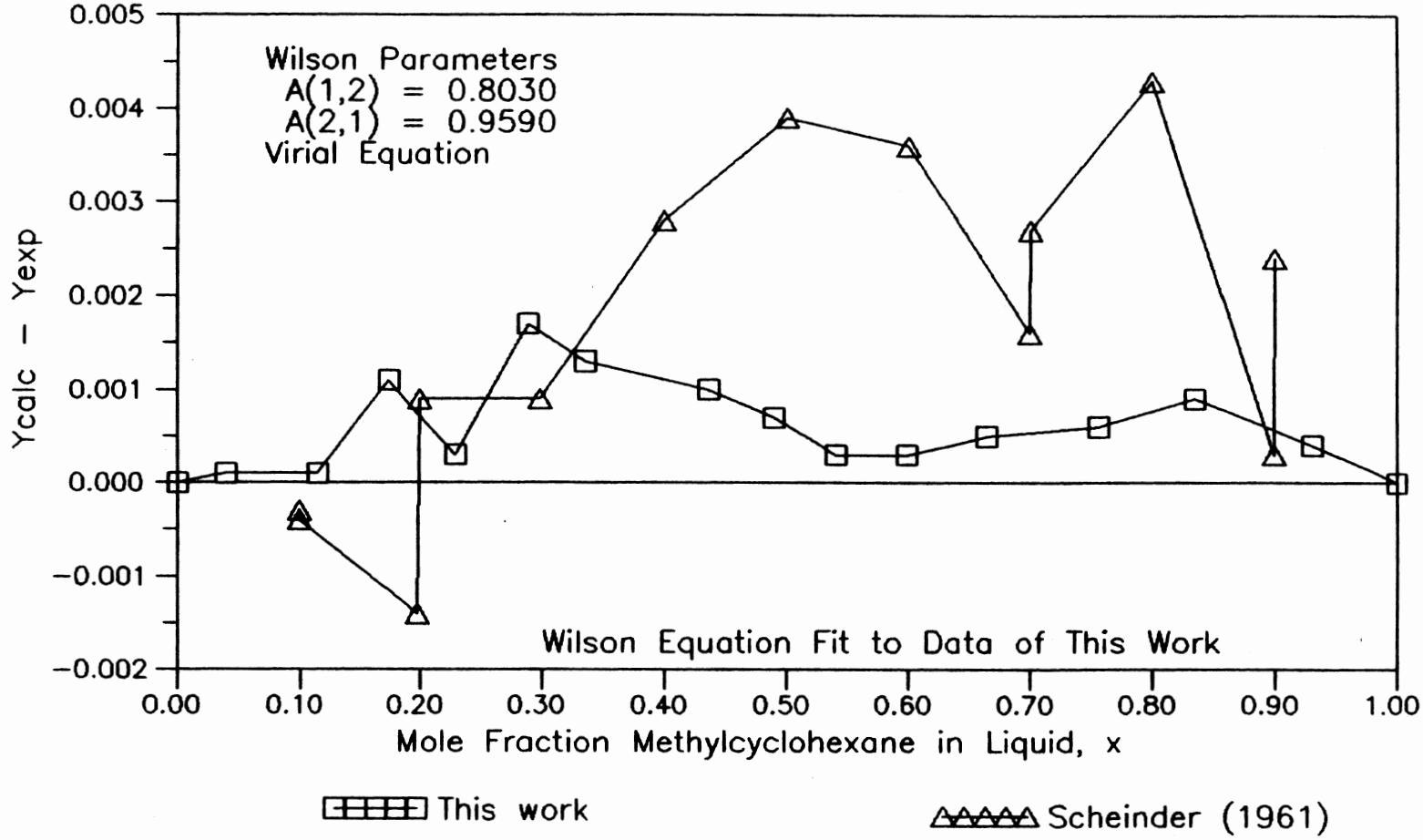

Figure 31. Comparison of Experimental Vapor Compositions for Methylcyclohexane + Toluene at 90 C

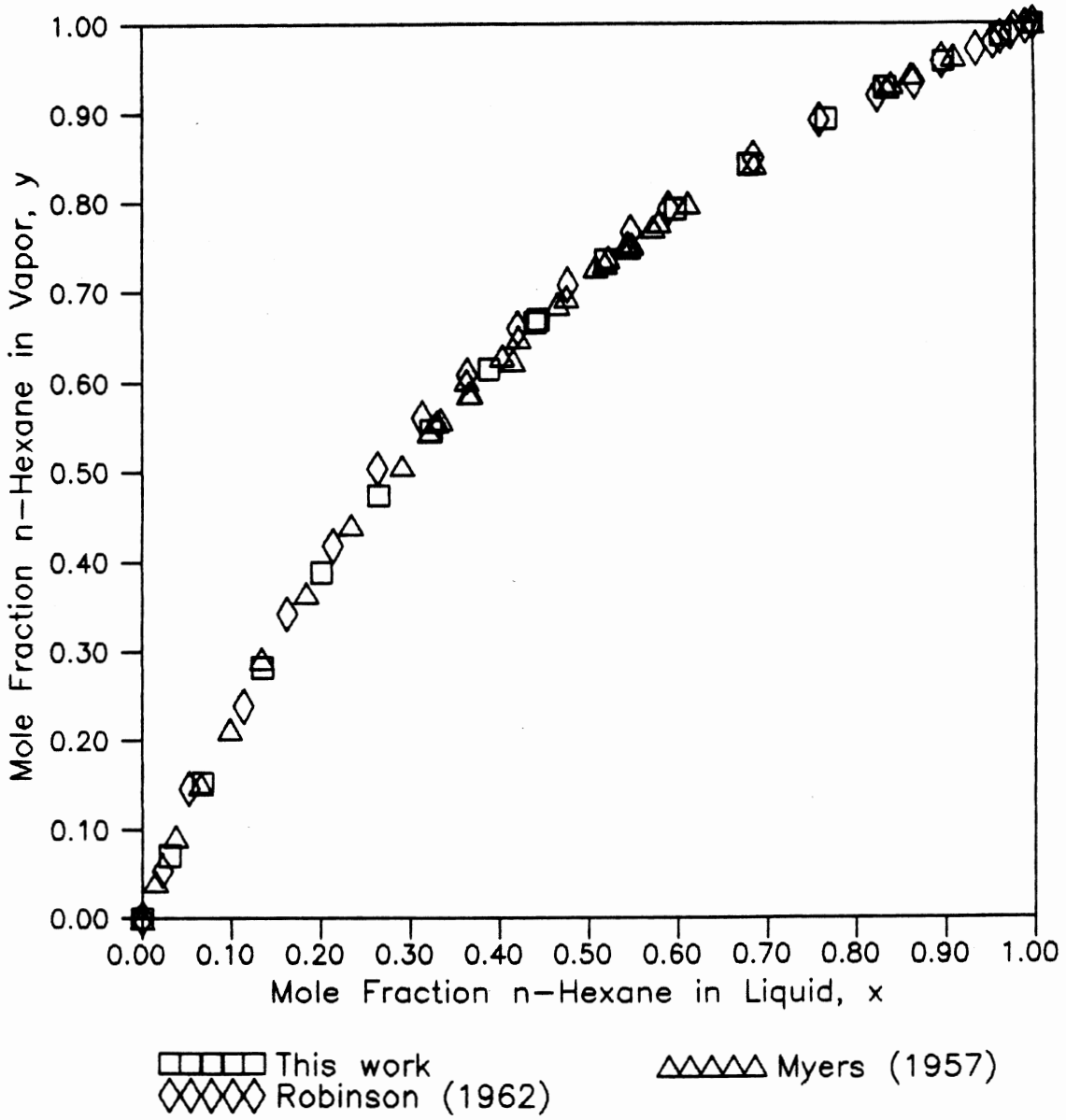

Figure 32. Experimental Equilibrium Phase Compositions for n−Hexane + Methylcyclohexane at 760 mm Hg

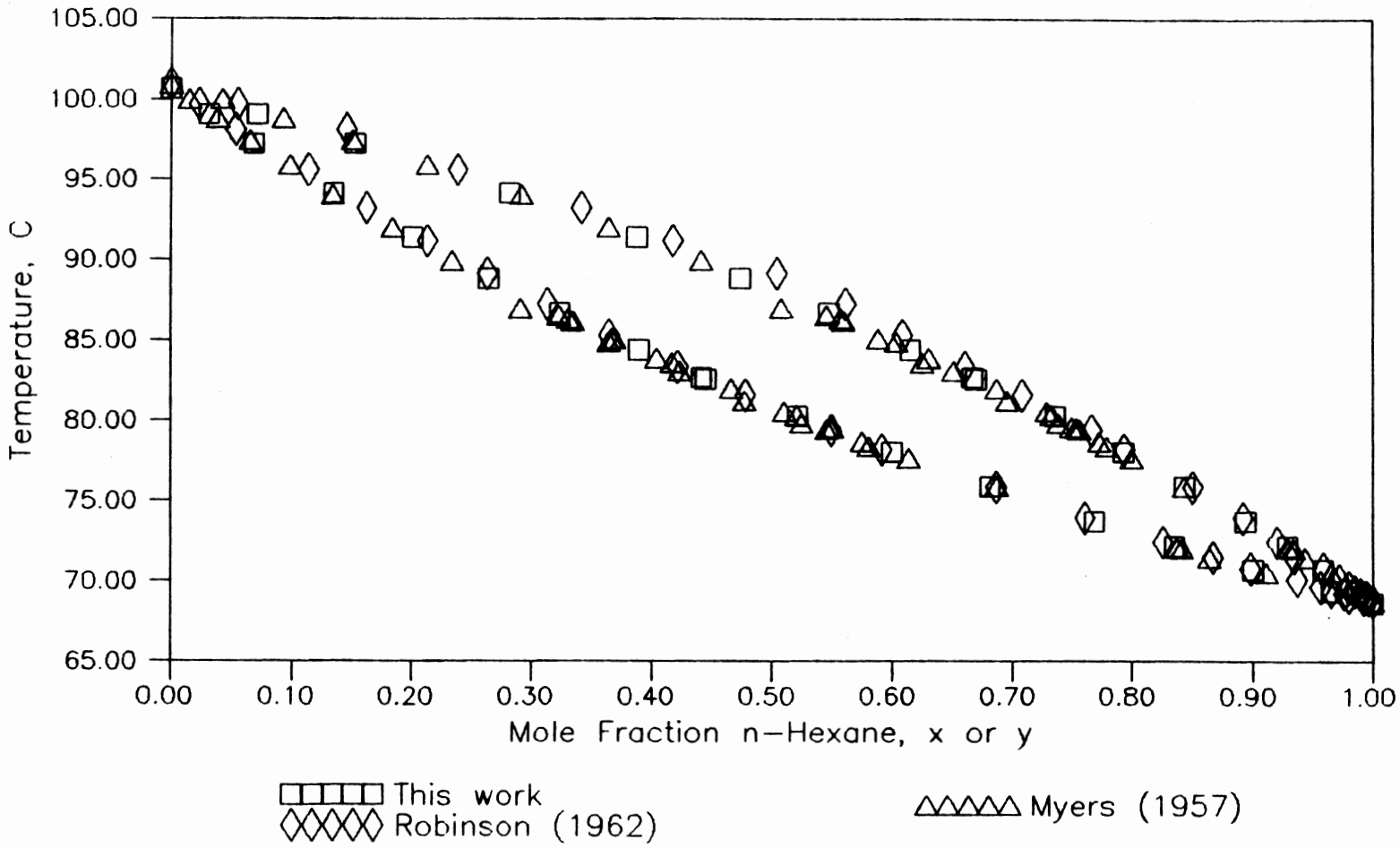

Figure 33. Experimental Phase Behavior (T-x,y) for n-Hexane + Methylcyclohexane at 760 mm Hg

calculated by using Wilson parameters (Figure 34) show random scatter for the data of this work. Comparison of deviations of experimental temperatures from temperatures calculated using Wilson parameters is also shown in Figure 35. The works of Myers (27) and Robinson (32) show higher scatter than this work. Deviations of experimental vapor composition from vapor compositions calculated using Wilson parameters (Figure 36) shows random scatter for the data of this work. Comparison of deviations of experimental vapor compositions from vapor compositions calculated using Wilson parameters among different investigators (Figure 37) shows that the data of this work are of very high precision compared to the works of Myers and Robinson. The data of Myers are in good agreement with this work, when account is taken for the considerable scatter in Myers' data.

System n-Hexane(1) + Toluene(2) at 760 mm Hg

The comparison of data on n-Hexane + Toluene is shown in the x-y, and T-x,y plots of Figures 38 and 39, which show the qualitative similarity of the data of several investigators. The deviations of experimental temperatures from temperatures calculated by using Wilson parameters (Figure 40) shows random scatter for the data of this work. Comparison of deviations of experimental temperatures from temperatures calculated using Wilson parameters (Figure 41) shows that the difference in temperature deviations between the data of this work and work of Sieg (37) is as large as 0.5 °C, which is

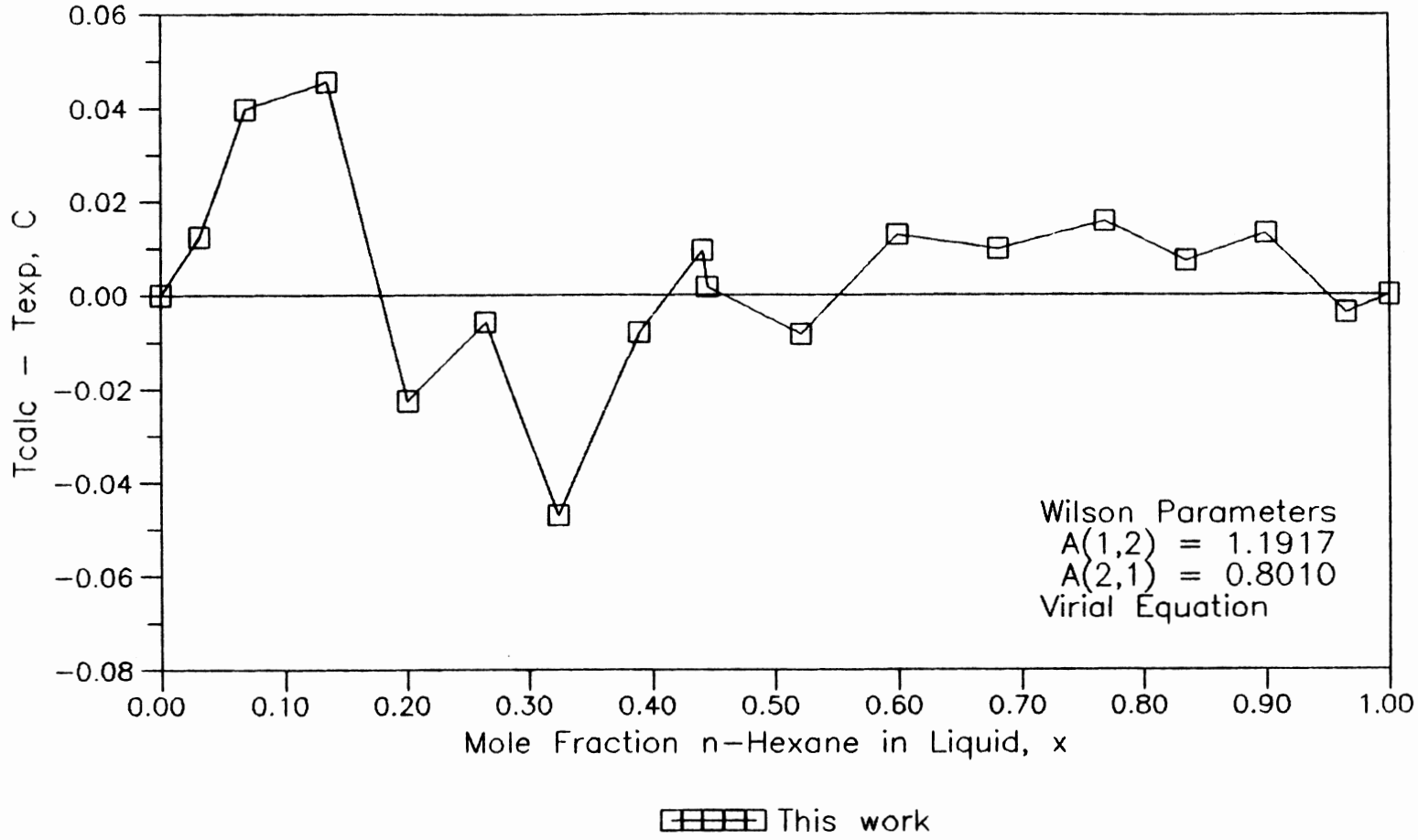

Figure 34. Deviations of Calculated Temperatures from Wilson Equation for n−Hexane + Methylcyclohexane at 760 mm Hg

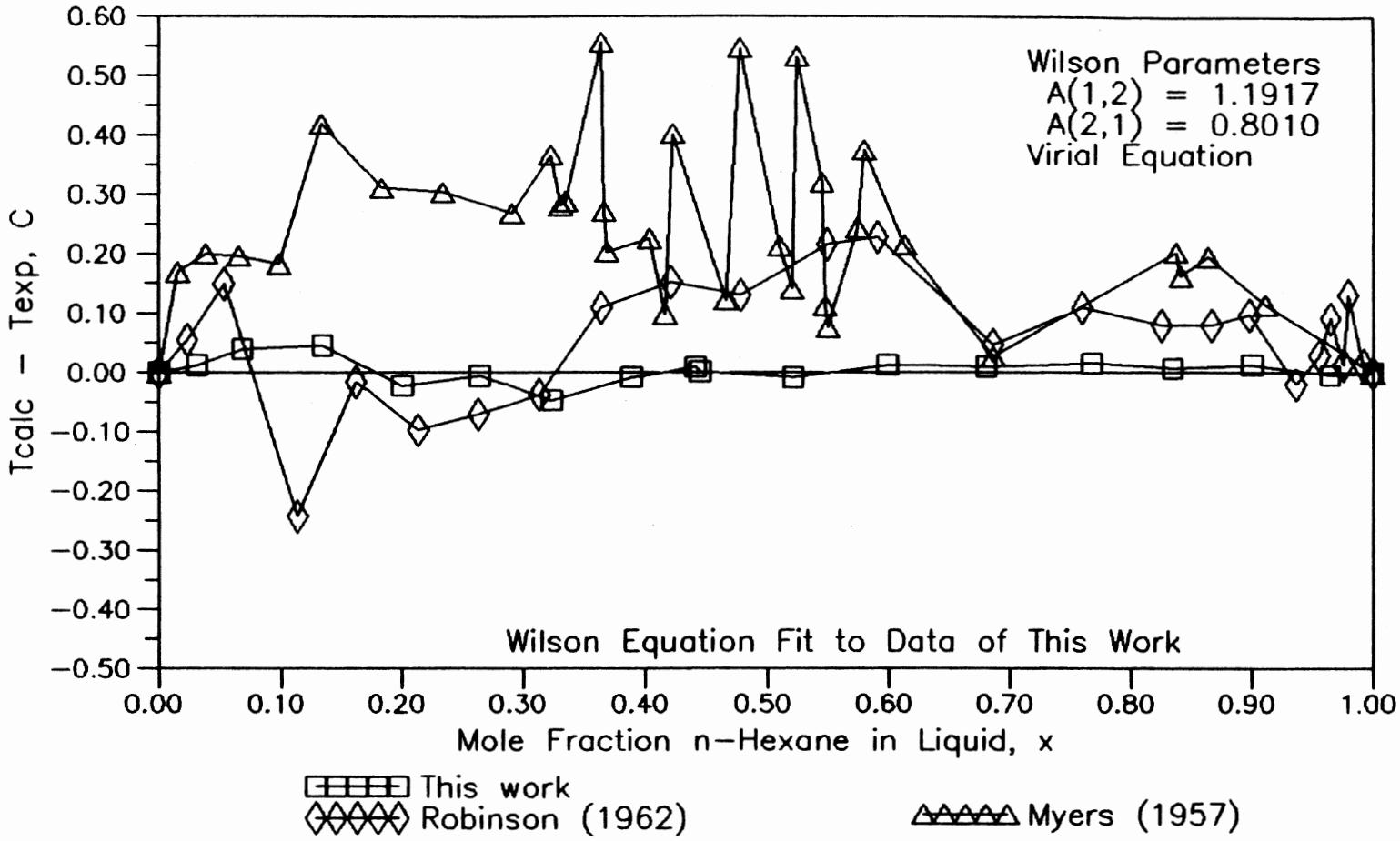

Figure 35. Comparison of Experimental Temperatures for n-Hexane Methylcyclohexane at 760 mm Hg

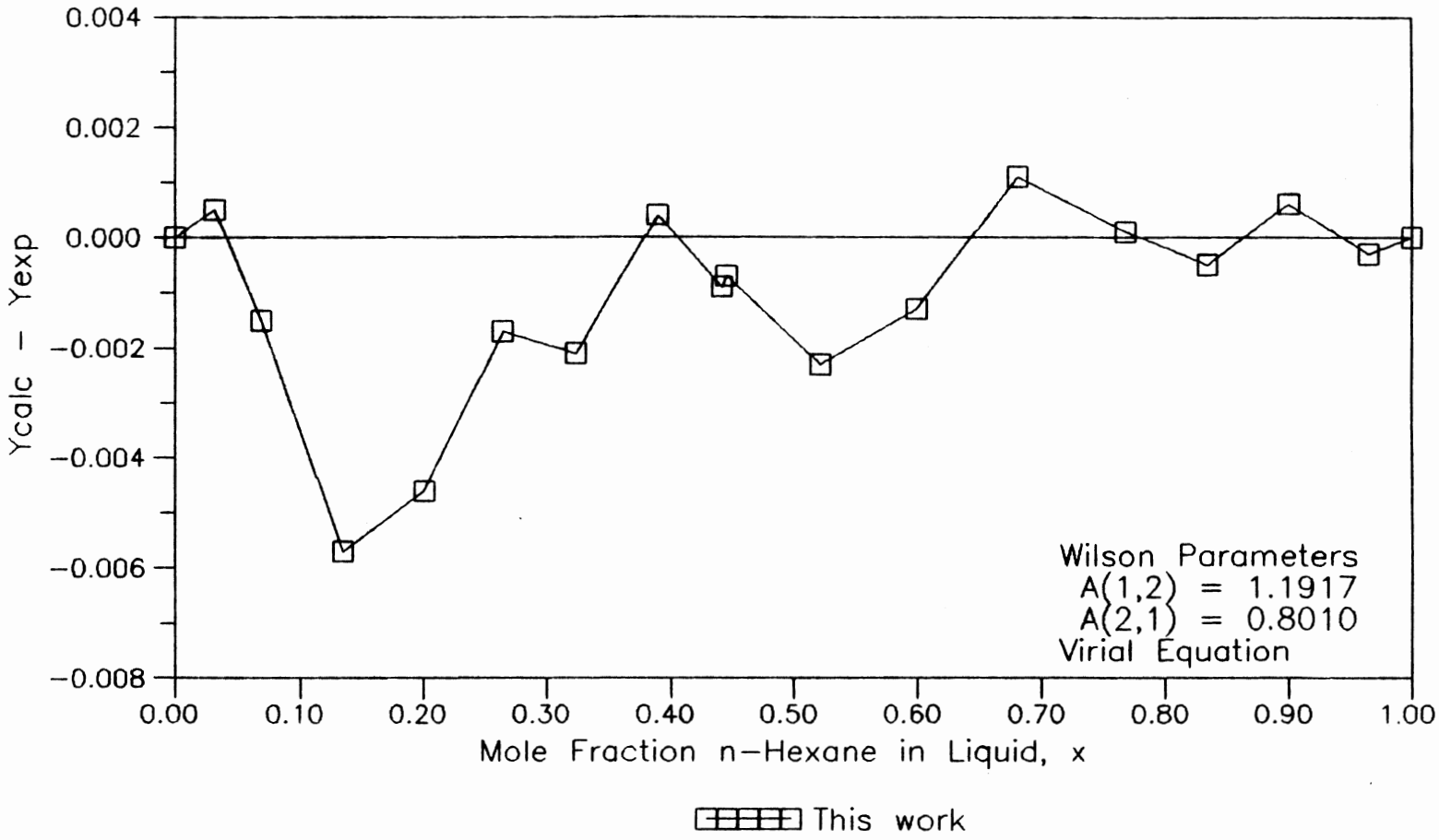

Figure 36. Deviations of Calculated Vapor Compositions from Wilson Equation for n−Hexane + Methylcyclohexane at 760 mm Hg

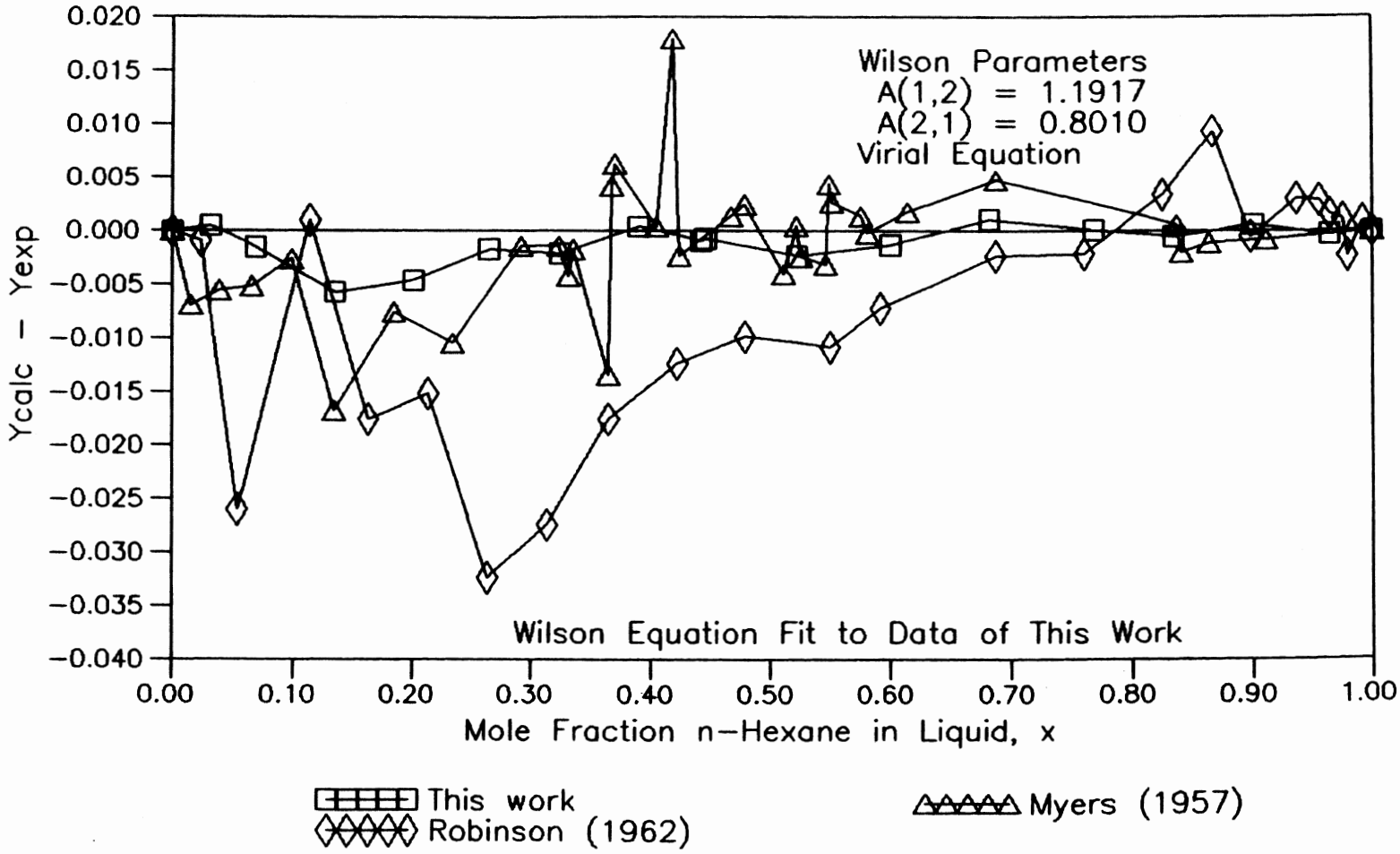

Figure 37. Comparison of Experimental Vapor Compositions for n-Hexane + Methylcyclohexane at 760 mm Hg

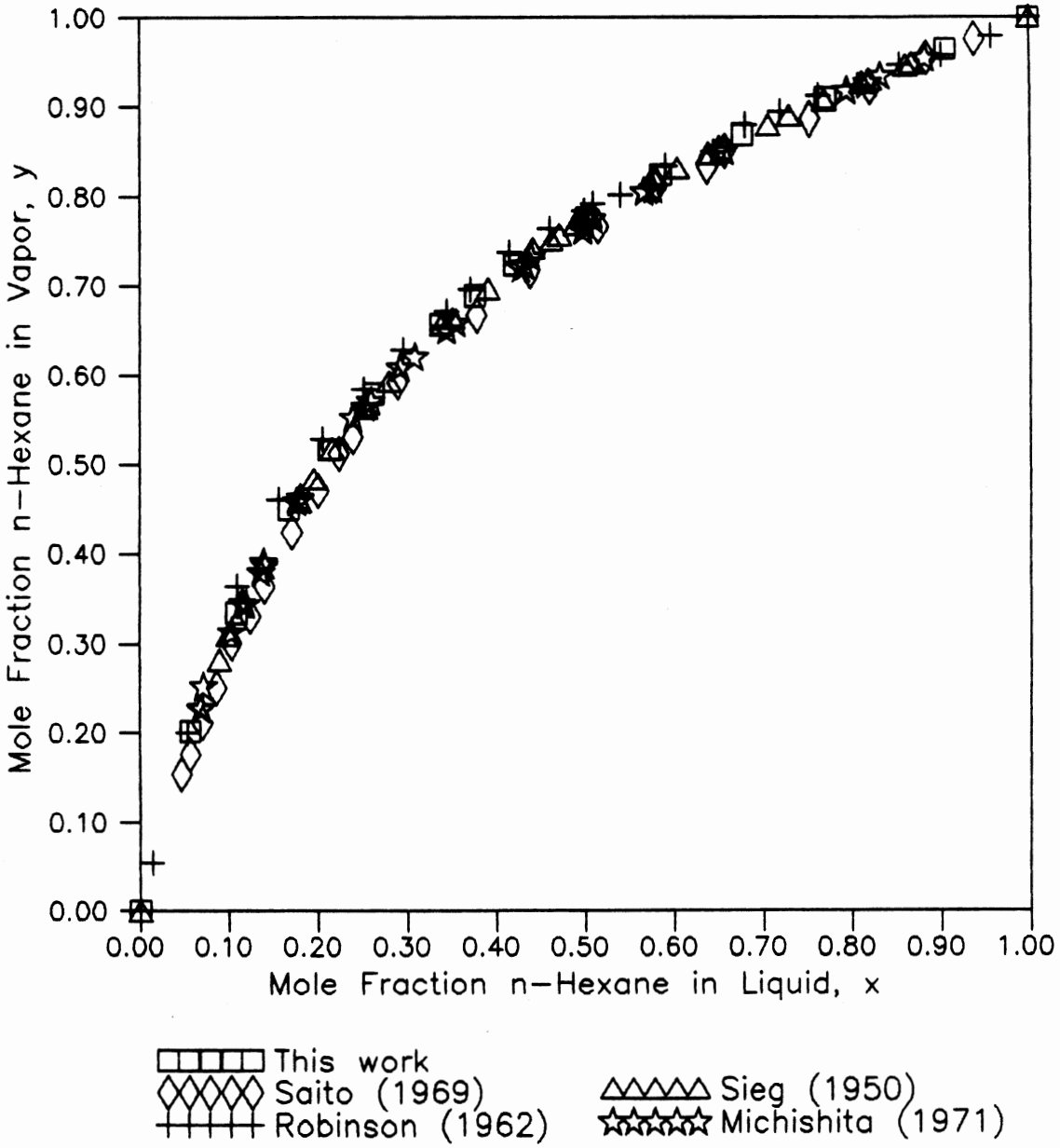

Figure 38. Experimental Equilibrium Phase Compositions for n-Hexane + Toluene at 760 mm Hg

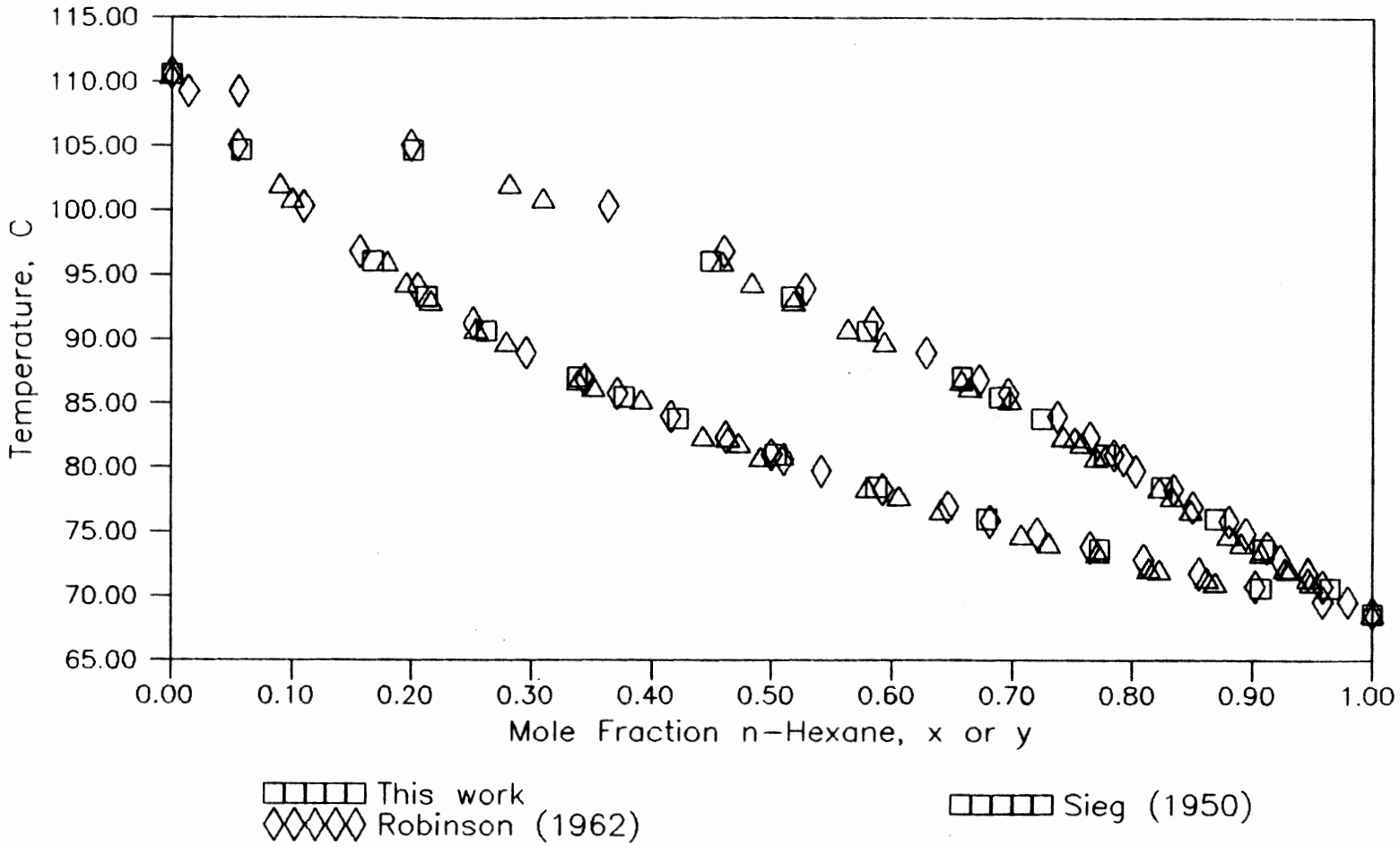

Figure 39. Experimental Phase Behavior (T-x,y) for n-Hexane + Toluene at 760 mm Hg

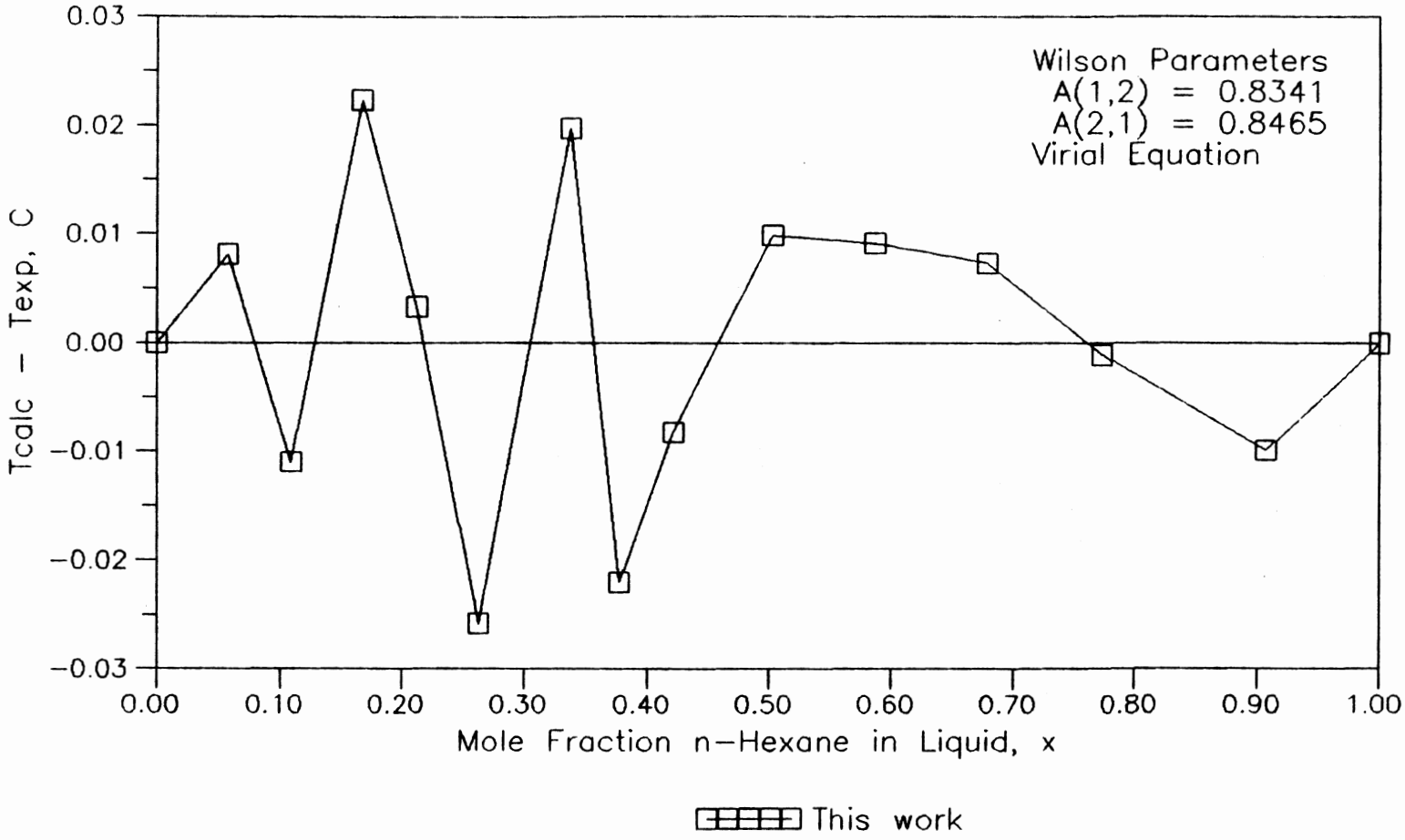

Figure 40. Deviations of Calculated Pressures from Wilson Equation for n−Hexane + Toluene at 760 mm Hg

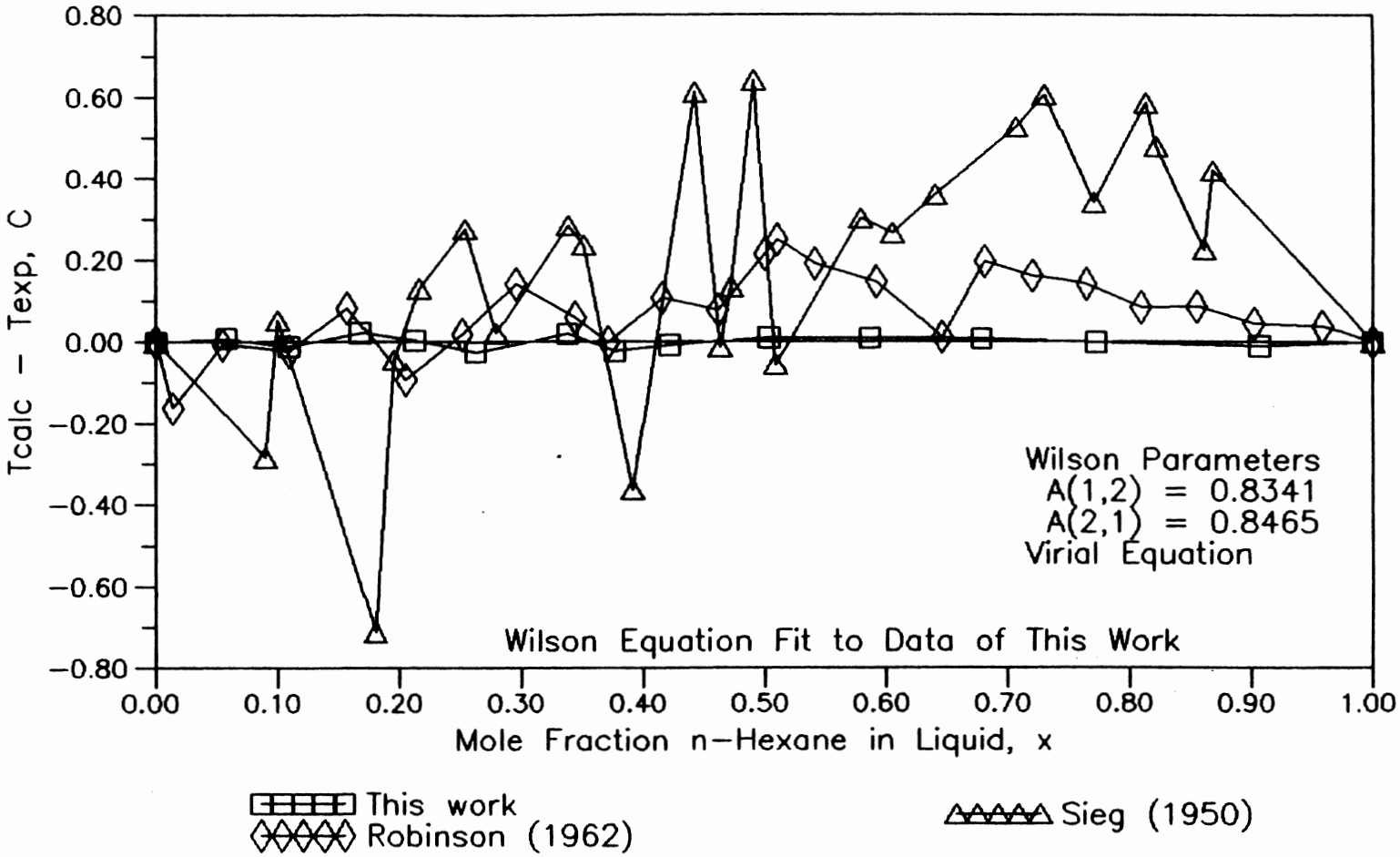

Figure 41. Comparison of Experimental Temperatures for n−Hexane + Toluene at 760 mm Hg

about 25 times the estimated experimental uncertainity of this work. Deviations of experimental vapor compositions (Figure 42) from vapor compositions calculated using Wilson parameters shows small negative scatter for n-hexane-rich region and positive scatter for toluene-rich region. Comparison of deviation of experimental vapor compositions from vapor compositions calculated using Wilson parameters between different investigators (Figure 43) shows that the data of this work agree with the work of Sieg (37). The works of Saito (35), Michishita (25) and Robinson (32) show deviations much higher than the experimental uncertainty of this work.

System n-Hexane(1) + Toluene(2) at 70 °C

The x-y and P-x,y plots (Figure 44 and 45) show comparisons between this work and the work of Wichterle. Deviations of experimental pressures (Figure 46) with the pressure calculated from Wilson parameters show random scatter for the data of this work. Comparison of deviations of the experimental pressure with the pressures calculated using the Wilson parameters (Figure 47) shows that the work of Wichterle (4) has very high deviations compared to the experimental uncertainty of this work. Deviations of experimental vapor compositions from vapor compositions calculated using Wilson parameters (Figure 48) show negative deviations except for few points and these deviations are the largest observed among all the systems studied. Comparison

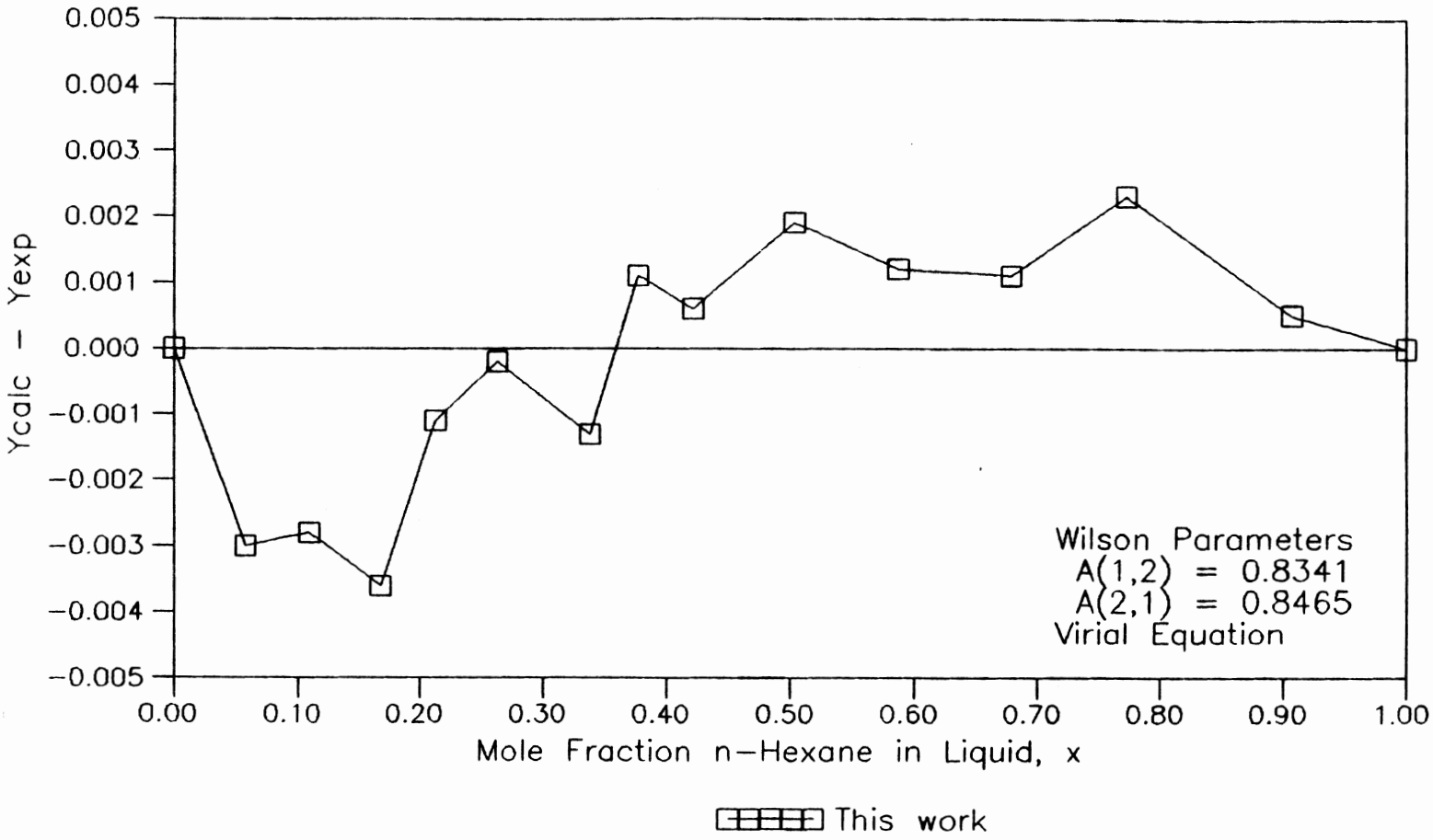

Figure 42. Deviations of Calculated Vapor Compositions from Wilson Equation for n−Hexane + Toluene at 760 mm Hg

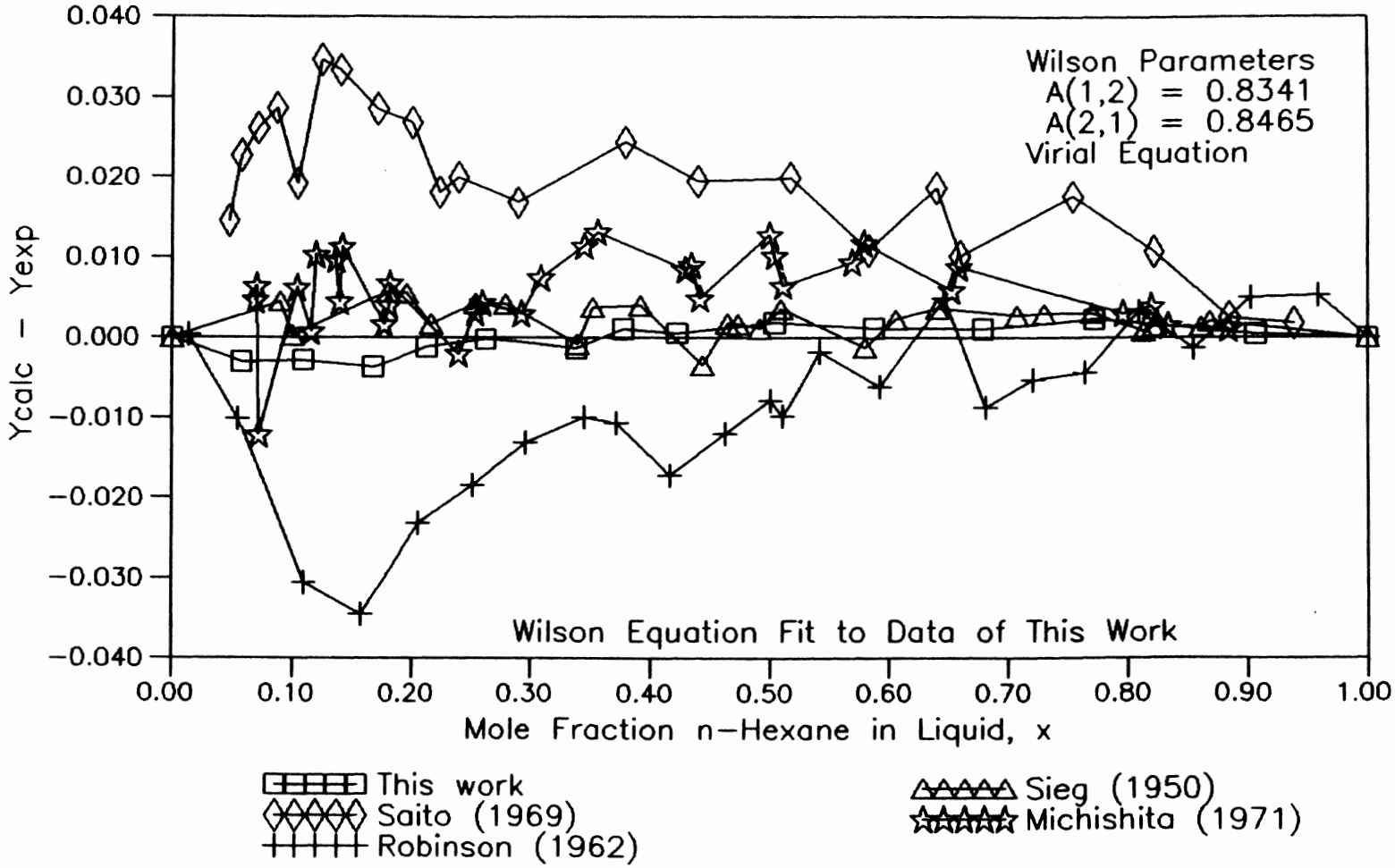

Figure 43. Comparison of Experimental Vapor Compositions for n−Hexane + Toluene at 760 mm Hg

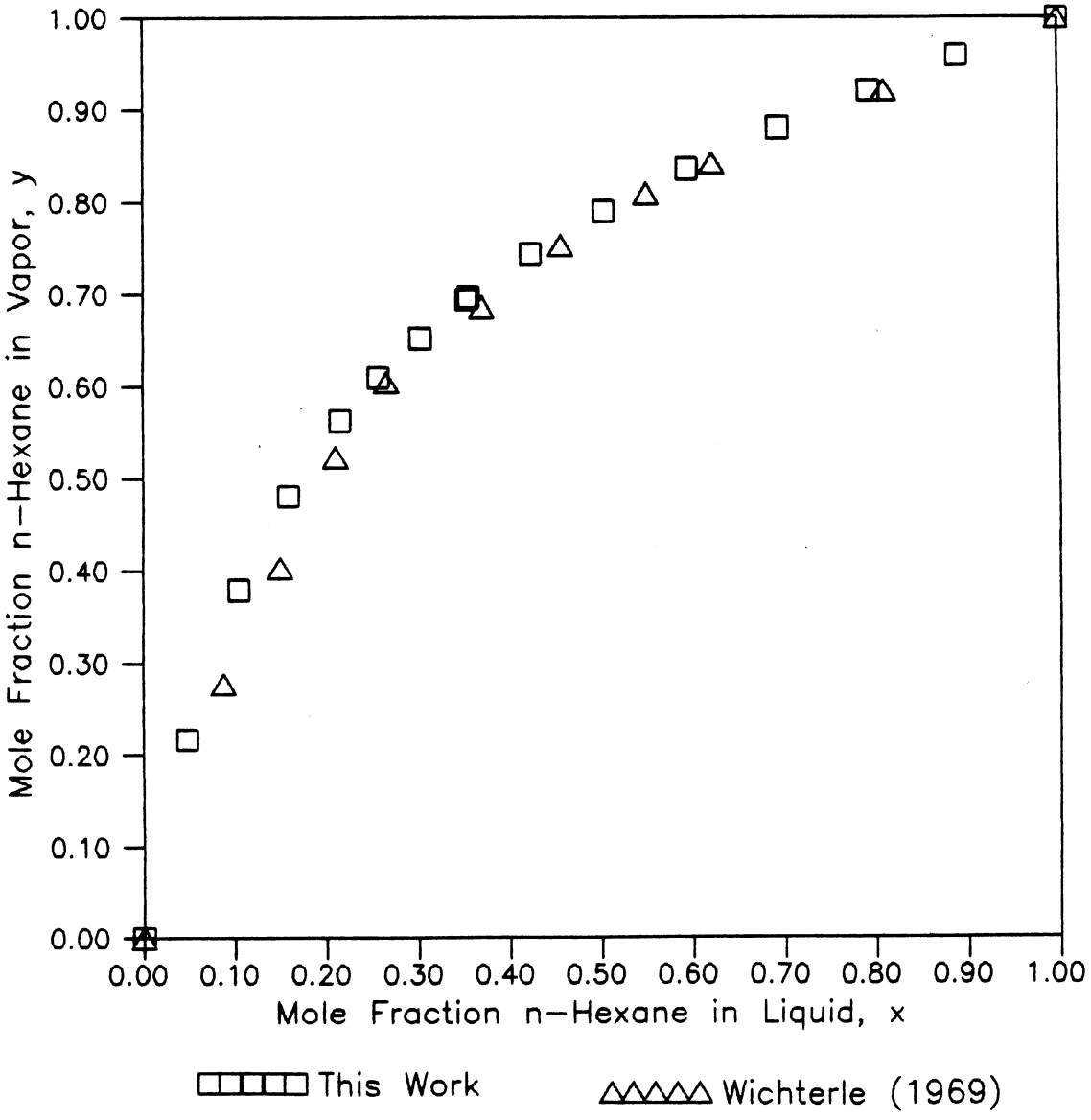

Figure 44. Experimental Equilibrium Phase Compositions for n-Hexane + Toluene at 70 C

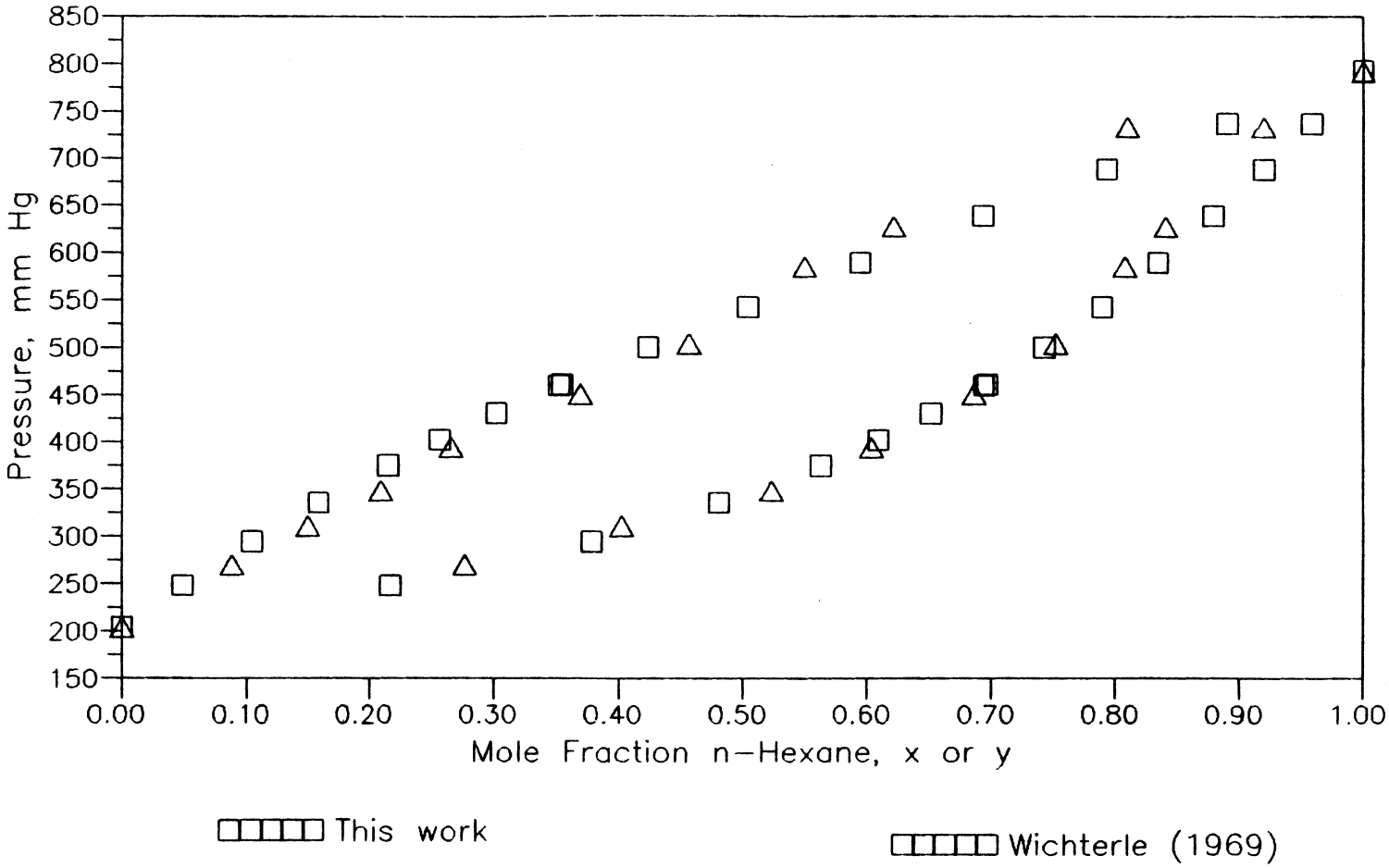

Figure 45. Experimental Phase Behavior (P-x,y) for n-Hexane + Toluene at 70 C

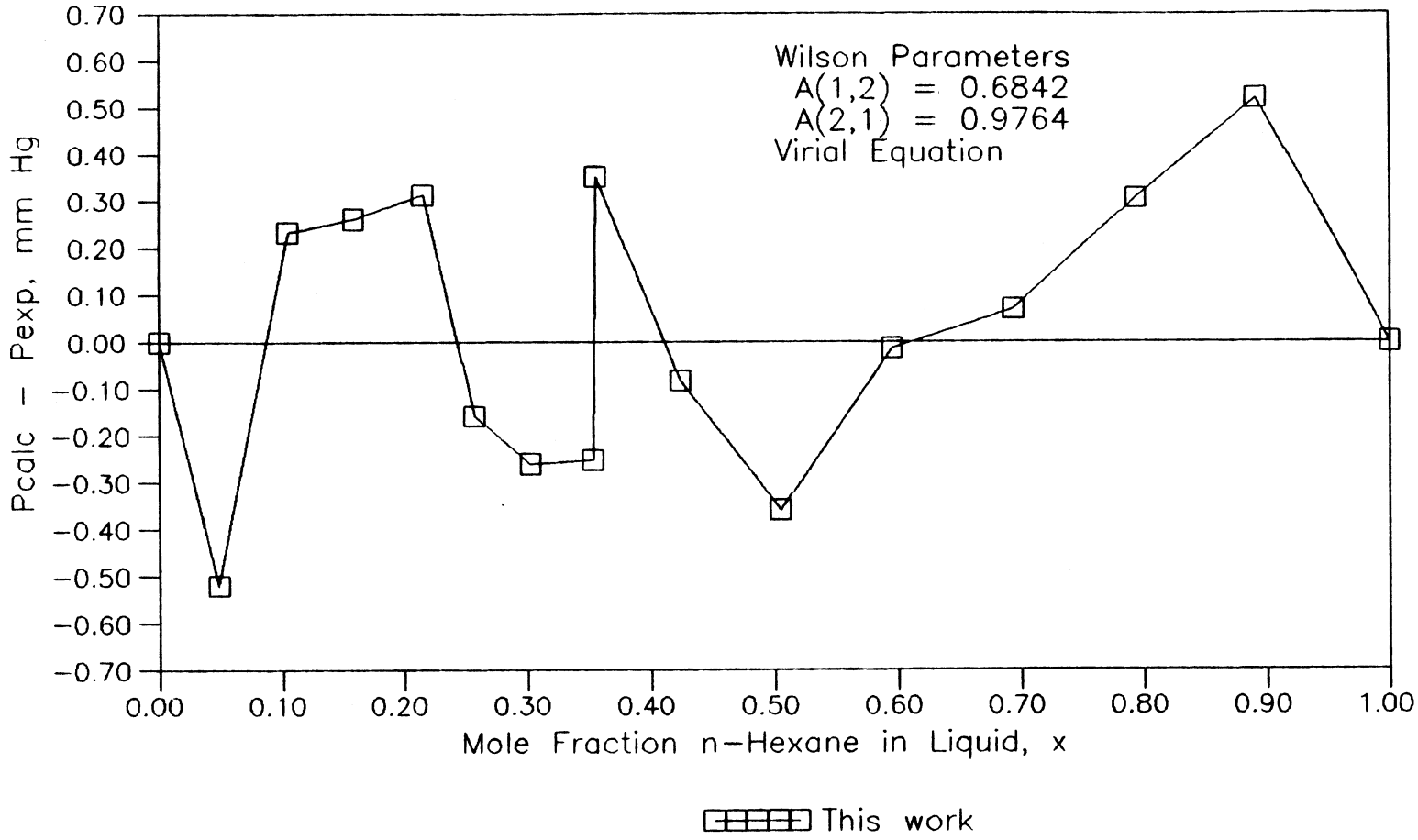

Figure 46. Deviations of Calculated Pressures from Wilson Equation for n-Hexane + Toluene at 70 C

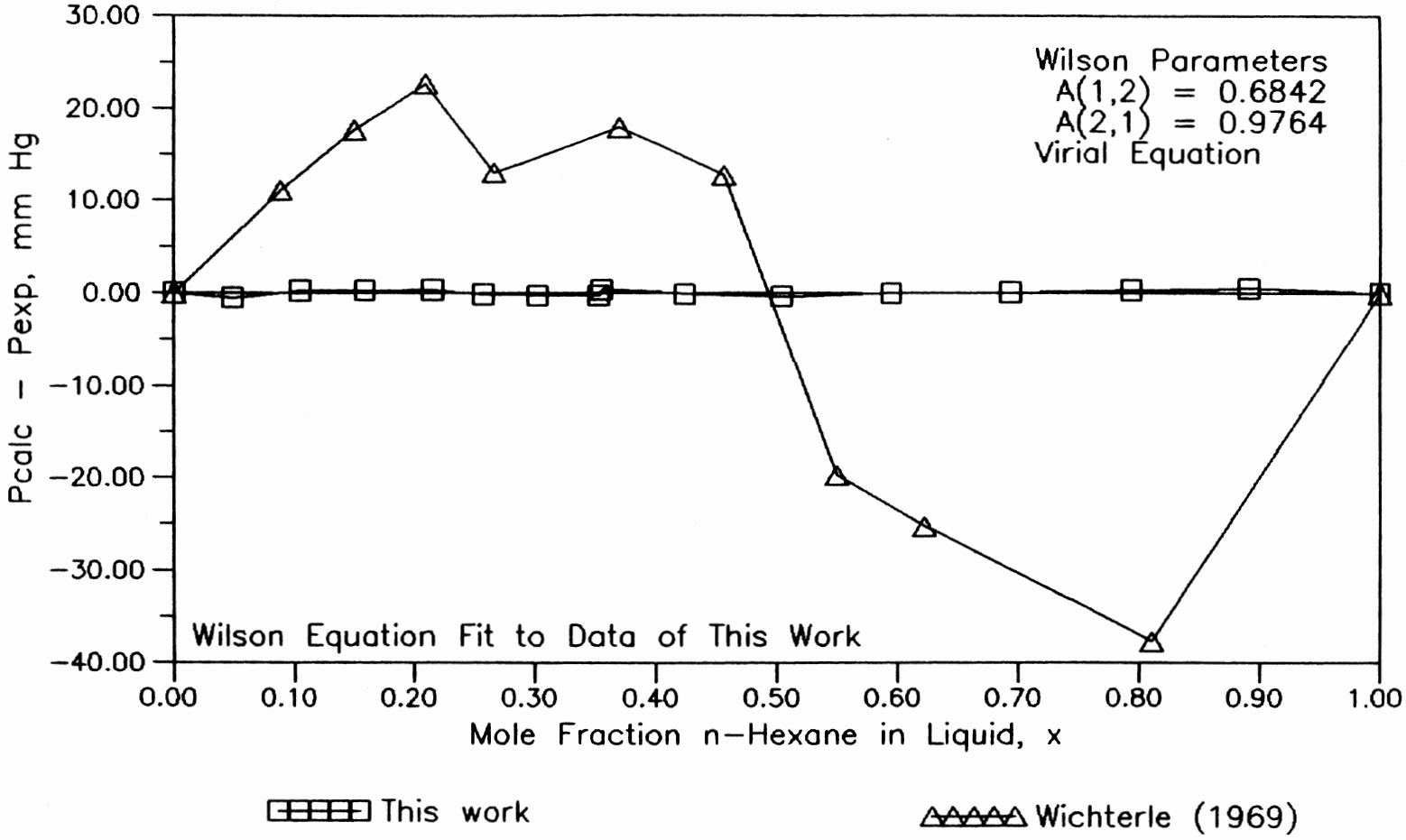

Figure 47. Comparison of Experimental Pressures for n−Hexane + Toluene at 70 C

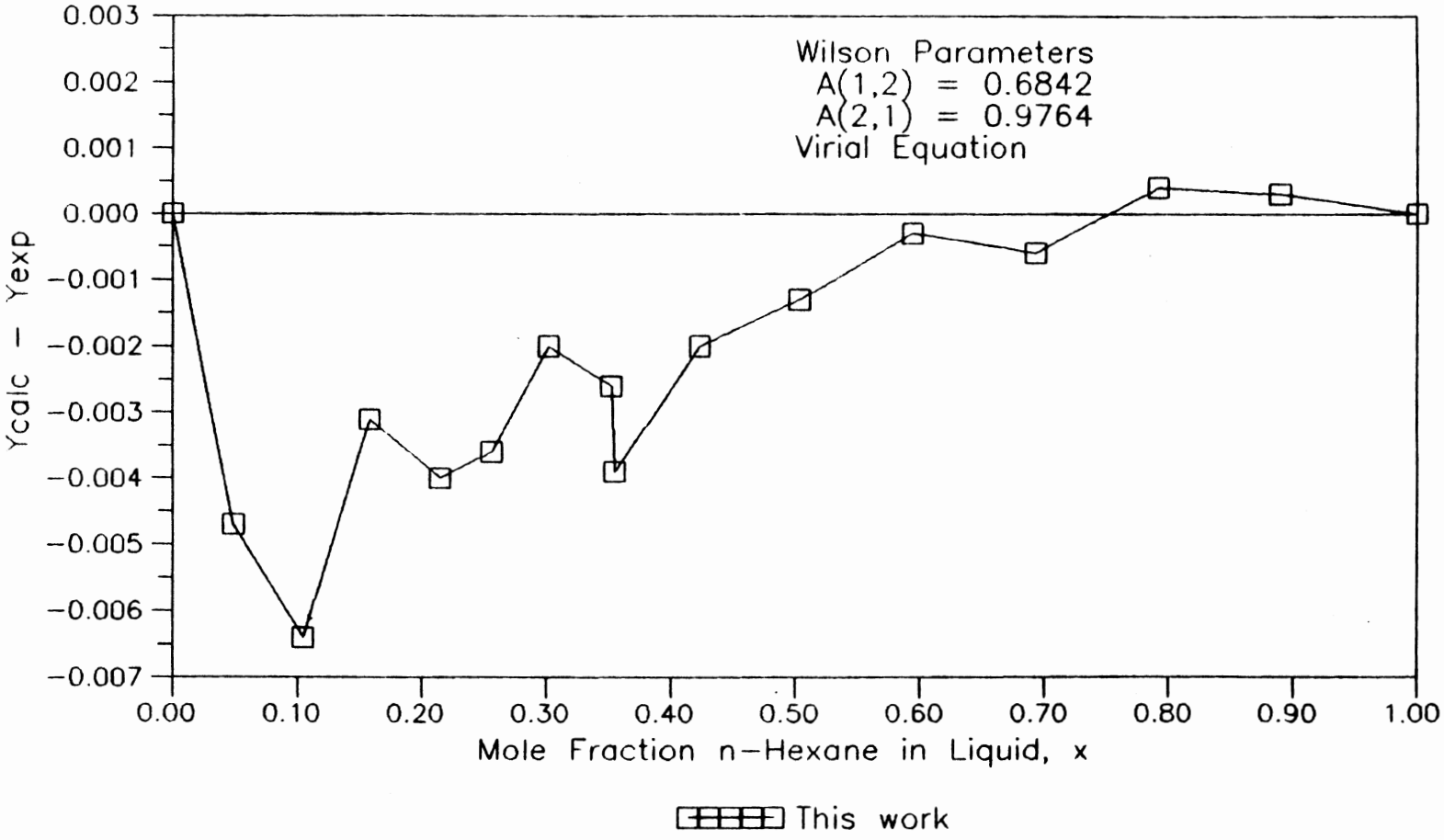

Figure 48. Deviations of Calculated Vapor Compositions from Wilson Equation for n-Hexane + Toluene at 70 C

of deviations of experimental vapor compositions from vapor compositions calculated using Wilson parameters between this work and work of Wichterle (Figure 49) shows that the deviations of the work of Wichterle are higher than the experimental uncertainty of this work.

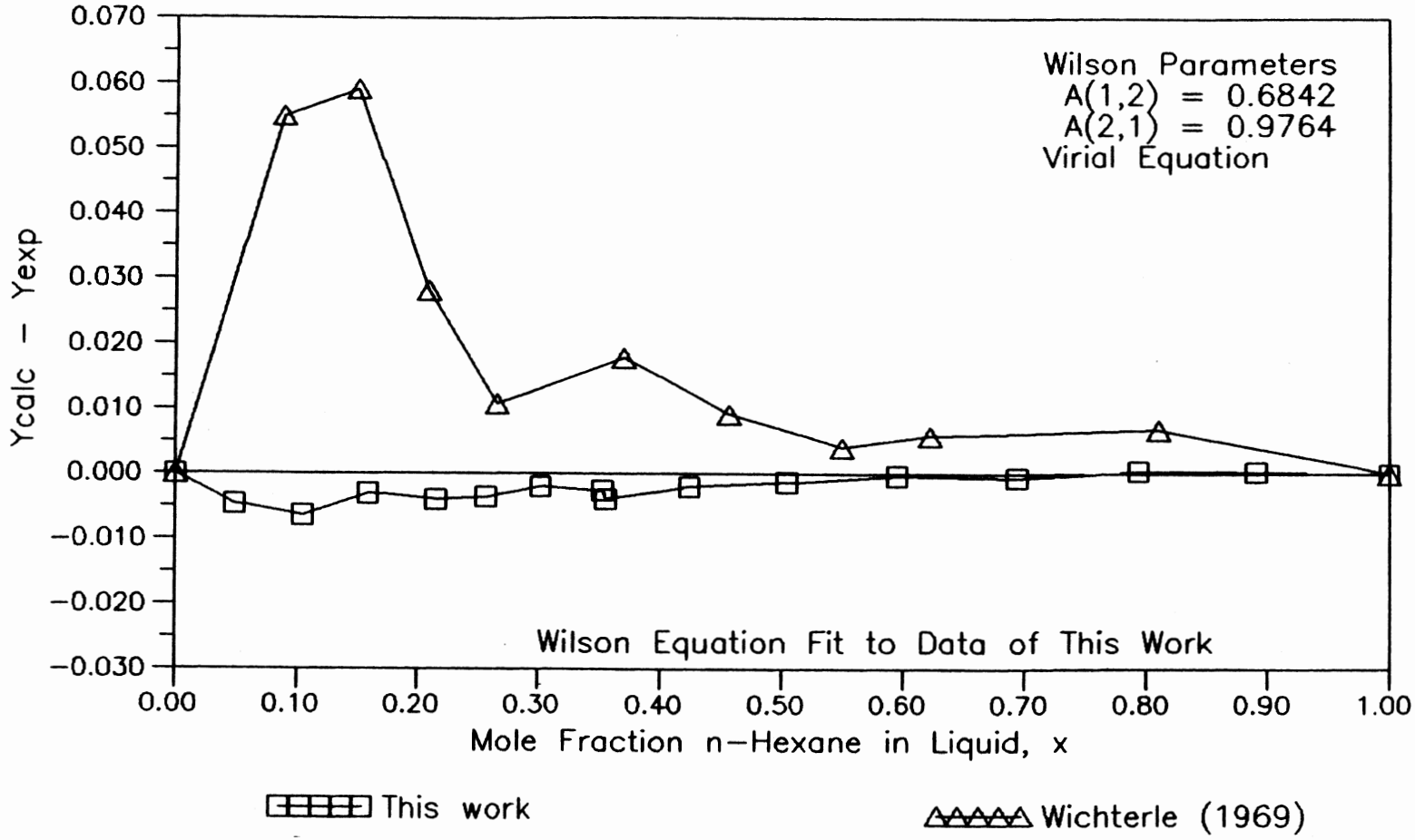

Figure 49. Comparison of Experimental Vapor Compositions for n-Hexane + Toluene at 70 C

APPENDIX E

DERIVATION OF GIBBS-DUHEM EQUATION

Properties of homogeneous fluids existing at equilibrium are functions of temperature, pressure and composition. Mathematically, the functional dependance of property M may be expressed by:

$$M = M\ (T,\ P,\ n_1,\ n_2, \ldots.) \qquad (E\text{-}1)$$

where n_1, n_2, ...etc. represent the mole numbers of species 1, 2, ...etc. for the entire system. Further, n, the total number of moles is $n = \Sigma n_i$ and $x_i = n_i/n$ and we can express the product nM as a function of the independent variables:

$$nM = M\ (T,\ P,\ n_1,\ n_2, \ldots\ldots) \qquad (E\text{-}2)$$

The quantity nM is proportional to n, and is therefore extensive. The symbol M may stand for any intensive thermodynamic property of a solution (excluding temperature, pressure and composition, the conditions which fix M). For example M can represent any of the molar properties V, U, H, etc.

The total differential of nM is written as

$$d(nM) = \left[\frac{\partial(nM)}{\partial T}\right]_{P,n} dT + \left[\frac{\partial(nM)}{\partial P}\right]_{T,n} dP + \Sigma\left[\frac{\partial(nM)}{\partial n_i}\right]_{T,P,n_j} dn_i \qquad \text{(E-3)}$$

As the subscript n signifies constancy of all mole numbers, and hence of composition. Equation 3 may also be written:

$$d(nM) = \left[\frac{\partial M}{\partial T}\right]_{P,x} dT + \left[\frac{\partial M}{\partial P}\right]_{T,x} dP + \Sigma\left[\frac{\partial(nM)}{\partial n_i}\right]_{T,P,n_j} dn_i \qquad \text{(E-4)}$$

Here, subscript x denotes constant composition.

But by definition partial molar properties are

$$\bar{M}_i = \left[\frac{\partial(nM)}{\partial n_i}\right]_{T,P,n_j} \qquad \text{(E-5)}$$

Substitution into Equation 4 gives an expression for the total differential d(nM) of any function.

$$d(nM) = n\left[\frac{\partial M}{\partial T}\right]_{P,x} dT + n\left[\frac{\partial M}{\partial P}\right]_{T,x} dP + \Sigma\bar{M}_i\, dn_i \qquad \text{(E-6)}$$

Further in an equilibrium state

$$nM = \Sigma n_i \bar{M}_i \qquad \text{(E-7)}$$

The differential of nM resulting from alteration of T,P or the n_i given by the total differential of (nM):

$$d(nM) = \Sigma\bar{M}_i\, dn_i + \Sigma n_i\, d\bar{M}_i \qquad \text{(E-8)}$$

Comparison of Equations 6 and 8 shows that they can both be true only if

$$n\left[\frac{\partial M}{\partial T}\right]_{P,x} dT + n\left[\frac{\partial M}{\partial P}\right]_{T,x} dP + \Sigma x_i d\bar{M}_i = 0 \qquad \text{(E-9)}$$

Equation 9 is the most general form of the Gibbs-Duhem equation, valid for any molar thermodynamic property M.

By definition, the Gibbs function is,

$$G = H - TS \qquad \text{(E-10)}$$

The Gibbs function can be nondimensionalized by dividing it by RT.

By definition,

$$G = \Sigma x_i \mu_i \qquad \text{(E-11)}$$

Hence,

$$\frac{G}{RT} = \frac{\Sigma x_i \mu_i}{RT} \qquad \text{(E-12)}$$

But,

$$\frac{G}{RT} = \frac{H}{RT} - \frac{S}{R} \qquad \text{(E-13)}$$

Differentiation gives

$$\left[\frac{\partial (G/RT)}{\partial T}\right]_{P,x} = \frac{1}{RT}\left(\frac{\partial H}{\partial T}\right)_{P,x} - \frac{H}{RT^2} - \frac{1}{R}\left(\frac{\partial S}{\partial T}\right)_{P,x} \qquad \text{(E-14)}$$

Further, by definition of constant pressure molar heat capacity

$$\left(\frac{\partial H}{\partial T}\right)_{P,x} = C_p \qquad \text{(E-15)}$$

also, from Maxwell relation and definition of heat capacity at constant pressure

$$\left(\frac{\partial S}{\partial T}\right)_{P,x} = \frac{C_p}{T} \qquad \text{(E-16)}$$

This reduces Equation 14 to

$$\left[\frac{\partial (G/RT)}{\partial T}\right]_{P,x} = -\frac{H}{RT^2} \qquad \text{(E-17)}$$

The pressure derivative of G/RT is found similarly.

$$\left[\frac{\partial (G/RT)}{\partial P}\right]_{T,x} = \frac{1}{RT}\left(\frac{\partial H}{\partial P}\right)_{T,x} - \frac{H}{RT^2} - \frac{1}{R}\left(\frac{\partial S}{\partial P}\right)_{T,x} \qquad \text{(E-18)}$$

From Maxwell equations, Equation 19 reduces to

$$\left[\frac{\partial (G/RT)}{\partial P}\right]_{T,x} = \frac{V}{RT} \qquad \text{(E-19)}$$

Equation 9, with M ≡ G/RT becomes

$$-\frac{H}{RT^2}\,dT + \frac{V}{RT}\,dP - \Sigma x_i\, d\left(\frac{\mu_i}{RT}\right) = 0 \qquad \text{(E-20)}$$

This is the form applicable for general T, P, x changes and is expressed in terms of γ and measurable quantities.

APPENDIX F

TABLE OF CONSTANTS USED

In the following table, all the constants used to obtain and reduce the data are listed. The constants which have units are given; the others are unitless.
The units and symbols are specified in parentheses after the symbol.

Antoine Constants (31)

Compound	A1	A2(°C)	A3(°C)
n-Hexane	15.8366	2697.55	-48.78
Methylcyclohexane	15.71914	2926.04	-51.75
Toluene	16.01643	3096.52	-53.67

(31) Reid, R.C, Prausnitz, J.M, Sherwood, T.K, "The properties of Gases and Liquids", Third Edition. McGraw-Hill Book Company, New york (1977).

These constants are consistent with the following equation:

$$\ln P^{sat} = A1 - A2/(T + A3)$$

where P^{sat} is in mm Hg and T in °C

Critical Properties (13)

Compound	T_c (K)	P_c (bar)	Z_c	w
n-Hexane	507.9	30.3	0.264	0.264
Methylcyclohexane	572.2	34.75	0.264	0.264
Toluene	591.8	41.06	0.265	0.265

(13) Engineering Sciences Data, ESDU International Plc. (1987).

APPENDIX G

EXCESS PROPERTIES FOR THE SYSTEMS STUDIED

The following approximation was used for calculating the excess heats and volumes of mixing for this study.

For isothermal data:

$$\int_{P1}^{P2} \frac{V^E}{RT}\, dP \leq \frac{V^E_{max}}{RT} (P_{max} - P_{min})$$

For isobaric data:

$$\int_{T1}^{T2} \frac{H^E}{RT}\, dT \leq \frac{H^E_{max}}{RT} (T_{max} - T_{min})$$

Using the above approximation the following values were obtained

For n-Hexane + Methylcyclohexane at 70°C:

Excess volume (22) term was approximately

3.979 * 10E-06

For n-Hexane + Toluene at 70°C:

Excess volume (21) term was approximately

1.155 * 10E-06

For Methylcylohexane + Toluene at 760 mm Hg:

Excess enthalpy (23) term was approximately

4.616 * 10E-03

For n-Hexane + Methylcyclohexane at 760 mm Hg:

Excess enthalpy (18) term was approximately

6.13 * 10E-4

For n-Hexane + Toluene at 760 mm Hg:

Excess enthalpy (23) term was approximately

1.198 * 10E-03

In Figure 22, the positive area is approximately 0.125. For the system methylcyclohexane + toluene at 760 mm Hg, the excess enthalpy term is 0.0046, which is the largest among the excess terms for the systems studied. This excess value is approximately 4% of the positive area (2% of the total area) in Figure 22, hence the excess terms were neglegible for this study.

VITA

Amit G. Sura

Candidate for the Degree of

Master of Science

Thesis: DESIGN, CONSTRUCTION AND TESTING OF A NEW APPARATUS FOR VAPOR LIQUID EQUILIBRIUM STUDIES AT LOW PRESSURES

Major Field: Chemical Engineering

Biographical:

Personal Data: Born in Bombay, India, January 19, 1967, the son of Gokuldas O. and Urmila Sura.

Education: Graduated from Sheth Madhavdas Amersey High School, Bombay, in June 1981; received the Bachelor of Engineering degree in Chemical Engineering from University of Bombay, Bombay, India, in June 1988; completed requirements for the Master of Science degree at Oklahoma State University in July, 1991.

Professional Experience: Trainee Engineer, Indian Organic Chemicals Ltd., Khopoli dist. Raigad, Maharashtra 410203, India. Research Assistant at Oklahoma State University, January, 1990, to May, 1991.